From the Research Center Borstel
Leibniz-Center for Medicine and Bioscience

Priority Research Area Asthma and Allergy
Director: Prof. Dr. Susanne Krauss-Etschmann
Division of Biochemical Immunology
Director: Prof. Dr. Frank Petersen

Mouse Chymase mMCP-4 in Experimental Asthma

Dissertation
for Fulfillment of
Requirements
for the Doctoral Degree
of the University of Lübeck

from the Department of Natural Sciences

Submitted by

Marjan Ahmadi
from Tehran

Lübeck 2017

First referee:	Prof. Dr. rer. nat. Frank Petersen
Second referee:	Prof. Dr. rer. nat. Tamás Laskay
Date of oral examination:	25.01.2019
Approved for printing.	Lübeck, 28.01.2019

~This thesis is dedicated to my parents ~

Table of contents

List of Abbreviations

AHR	Airway hyperreactivity
Alum	Aluminum hydroxide
APC	Antigen presenting cell
BAL	Bronchoalveolar lavage
BALB/c	Bagg albino strain c (mouse strain)
BMMC	Bone marrow derived mast cells
bp	Base pair
BSA	Bovine serum albumin
°C	Celsius
CCL	Chemokine (C-C motif) ligand
CD	Cluster of differentiation
c-kit	(CD117) SCF receptor
C57BL/6	C57 black 6 (mouse strain)
CXCL	Chemokine (C-X-C motif) ligand
DC	Dendritic cells
dest	distilled
DNA	Deoxyribonucleic acid
DNase	Desoxyribonuclease
dNTP	Desoxyribonucleosid triphosphat
D-PBS	Dulbecco´s phosphate buffered saline
e. g.	Exempli gratia (for example)
EDTA	Ethylenediaminetetraacetic acid
ELISA	Enzyme-linked Immunosorbent Assay
FACS	Fluorescence activated cell sorting
FC	Flow cytometry
FCS	Fetal calf serum
FcεRI	Fcε-Receptor I; high-affinity IgE-Receptor
Fig.	Figure
FITC	Fluorescein isothiocyanate
fMLP	N-Formylmethionyl-leucyl-Phenylalanine
FSC	Forward scatter
GINA	Global Initiative for Asthma

Abbreviations

GmbH	„ Company with limited liability “
GM-CSF	granulocyte macrophage colony-stimulating factor
h	Hours
HDM	House dust mite
HEPES	(4-(2-hydroxyethyl)-1-piperazineethanesulfonic acid
hLMC	Human lung mast cells
HRP	Horseradish peroxidase
IFN-γ	Interferon-γ
IgE	Immunoglobulin E
IL	Interleukin
i.n.	Intranasal
i.p.	Intraperitoneal
i.t.	intratracheal
ko	knock-out
LTB4	Leukotriene B4
LTC4	Leukotriene C4
MC	Mast cells
MCh	Methachocholine
min	Minutes
ml	Milliliter
mMCP-4	Mouse mast cell protease 4
n	Sample size
newCAST	Computer assisted stereological toolbox
ng	Nanogram
nM	Nanomolar
OVA	Ovalbumin
p	Calculated probability (P value)
PAS	Periodic acid-Schiff
PBS	Phosphate buffered saline
PCR	polymerase chain reaction
PE	Phycoerythrin
PerCp-Cy5.5	Peridinin-Chlorophyll-Protein Complex
PFA	Paraformaldehyde
pg/ml	Picogram per milliliter

Abbreviations

PGD2	Prostaglandin D2
PMN	polymorphonuclear neutrophils
RPMI Medium	Roswell Park Memorial Institute medium
RT	Room temperature
SD	Standard deviation
s.	Seconds
SSC	Side scatter
SST	Serum Separation Tubes
SURS	Systematic uniform random sampling
TAE	Tris-Acetate-EDTA
TGF-β	Transforming growth factor-β
Th	T helper cell
TMB	3,3',5,5'-Tetramethylbenzidine
TNF	Tumor necrosis factor
Tris	Tris (hydroxymethyl)-aminomethane
U	Unit
VCAM	Vascular cell adhesion molecule
VEGF	Vascular-endothelial growth factor
wt	Wildtype
W-sh	C57BL/6-*Kit*$^{W\text{-}sh/W\text{-}sh}$ (MC deficient mouse strain
W/W-v	WBB6F1-*Kit*$^{W/W\text{-}v}$ (MC deficient mouse strain)
µg	Microgram
µl	Microliter
µM	Micromolar

Abstract

Allergic asthma is one of the most common chronic respiratory disease in adults and children worldwide with increasing prevalence. Among the multiple pulmonary pathologies in asthma, airway hyperreactivity (AHR), goblet cell hyperplasia associated with mucus hypersecretion and inflammation of lung tissue are cardinal features of the disease. To date, a curative therapeutic approach of asthma is missing and treatment strategies merely focus on the abatement of symptoms. Therefore, the identification of novel therapeutic targets adjusted to the disease phenotype is a major challenge for a more effective medication in the future. It is commonly accepted that mast cell (MC) and its mediators contribute to the pathogenesis of allergic asthma. Within these mediators, the role of MC chymase and its murine equivalent, mMCP-4, is poorly understood. Although several findings mainly based on experiments performed *in vitro* argue for a proinflammatory function of this enzyme, recently published data derived from an acute asthma model *in vivo* clearly demonstrate a protective role of mMCP-4 in disease. Since the significance of the enzyme under chronic inflammatory conditions is unclear, the aim of this thesis was to determine the function of mMCP-4 and to analyze its effects in the induction of the asthma pathology in an alum-free chronic mouse model of the disease. For this purpose, chronic inflammation was induced in mMCP-4$^{-/-}$ and their corresponding wild type (*wt*) control after sensitization with OVA by repeated challenge with the allergen for 9 weeks. In order to identify MC-specific effects in this model and to discriminate them from mMCP-4-regulated functions, disease was induced in parallel in MC-deficient mice and MC-deficient animals reconstituted with MC either derived from *wt* or mMCP-4$^{-/-}$ mice. In contrast to previous finding in acute asthma models, mMCP-4$^{-/-}$ mice and MC-deficient mice reconstituted with mMCP-4$^{-/-}$ MC were protected from the development of an AHR, indicating a pro-pathogenic role of the enzyme under chronic conditions. A proinflammatory function of chymase was confirmed by *in vitro* experiments demonstrating that purified chymase or chymotryptic activity in activated human lung MC impairs the integrity of lung epithelial cells.

Surprisingly, an AHR significantly surmounting that of *wt* controls was observed in MC-deficient mice, but not MC-deficient mice reconstituted with MC from *wt* animals. These findings argue for a functional switch of MC and mMCP-4 from acute to chronic disease. While in the acute situation MC play a disease promoting role and mMCP-4 protects mice from developing disease, in the latter condition chymase acts proinflammatory whereas MC may have a protective function. These opposing regulatory roles of MC and mMCP-4 appear to be

Abstract

selective for the induction of AHR since mucus production and goblet cell hyperplasia were not different between *wt* controls and experimental groups of mice lacking MC or mMCP-4.

Beside its regulatory role in allergic lung inflammation, a previously unrecognized role of mMCP-4 in the control of cytokines in homeostasis could be identified. Levels of the Th1, Th2, Th9 and Th17/22 cytokines were significantly increased in non-sensitized mice lacking mMCP-4 as compared to *wt* or MC-deficient mice. Increased cytokine expression was not seen in sensitized mMCP-4-deficient mice, indicating a potential function of the protease in the removal or suppression of unwanted cytokines produced in the host under steady-state conditions.

As potential therapeutic targets, MC and their proinflammatory products are under broad investigation. Results from this study provide not only new insights on the role of MC and mMCP-4 in the regulation of chronic experimental asthma but identifies them, depending on the respective disease status or phenotype, as potential future targets in novel treatment strategies. However, further studies are required to substantiate these findings in humans and to elucidate the mechanisms underlying mMCP-4-mediated regulation in health and disease.

Zusammenfassung

Allergisches Asthma ist eine der weltweit häufigsten chronischen Atemwegserkrankungen bei Erwachsenen und Kindern mit einer zunehmenden Prävalenz. Unter den multiplen pulmonalen Pathologien des Asthmas gehören die Atemwegs-Hyperreaktivität (AHR), die mit einer Becherzell-Hyperplasie verbundenen erhöhten Mukusproduktion sowie eine Entzündung des Lungengewebes zu den Kardinalsymptomen dieser Erkrankung. Bis heute existiert kein kurativer therapeutischer Ansatz in der Asthmatherapie und die Behandlungsstrategien fokussieren im Wesentlichen nur auf die Milderung der Symptome. Die Identifikation neuer therapeutischer Zielstrukturen, die an den Phänotyp der Krankheit angepasst sind, stellt daher eine große Herausforderung für eine effektive Behandlung der Erkrankung in der Zukunft dar. Es ist bereits seit Langem bekannt, dass Mastzellen und deren Mediatoren zur Pathogenese von allergischem Asthma beitragen. Die Rolle der Mastzellchymase und ihrem murinen Äquivalent der mMCP-4 ist dagegen in diesem Zusammenhang weitgehend ungeklärt. Obwohl eine Reihe von auf hauptsächlich *in vitro* durchgeführten Experimenten beruhenden Befunden für eine proinflammatorische Funktion dieses Enzyms sprechen, weisen neue auf einem akuten Asthma-Modell *in vivo* basierende Ergebnisse eindeutig auf eine protektive Rolle von mMCP-4 bei dieser Erkrankung hin. Die Funktion von mMCP-4 unter chronisch entzündlichen Bedingungen war zu Beginn dieser Arbeit unklar. Es war daher das Ziel dieser Arbeit, die Funktion und Wirkung dieser Protease bei der Pathogenese des Asthmas in einem Alum-freien chronischen Mausmodell der Erkrankung zu bestimmen. Hierfür wurde eine chronische Entzündung in mMCP-4$^{-/-}$-Mäusen und deren entsprechenden Wildtypkontrollen nach einer Sensibilisierung mit OVA und durch wiederholte Provokation mit dem Allergen über 9 Wochen induziert. Um Mastzell-spezifische Effekte in diesem Modell identifizieren und sie von mMCP-4-regulierten Funktionen zu unterscheiden zu können, wurde die Krankheit parallel in Mastzell-defizienten Mäusen, welche entweder unbehandelt blieben oder mit Mastzellen aus Wildtyp- oder mMCP-4$^{-/-}$-Mäusen rekonstituiert wurden, induziert. Im Gegensatz zu den bisherigen Befunden aus den akuten Asthma-Modellen waren mMCP-4$^{-/-}$-Mäuse und MC-defiziente Mäuse, welche mit mMCP-4$^{-/-}$ -Mastzellen rekonstituiert waren, von der Entstehung einer AHR geschützt. Dieser Befund weist erstmals auf eine propathogene Rolle des Enzyms unter chronischen Bedingungen hin. Eine proinflammatorische Funktion der Chymase wurde auch in einer Reihe von *in vitro* durchgeführten Experimente bestätigt, in denen gezeigt werden konnte, dass sowohl gereinigte Chymase als auch der chymotryptisch aktive Überstand aktivierter humaner Lungenmastzellen die Integrität von Lungenepithelzellen beeinträchtigen kann. In unerwarteten Ergebnissen

zeigte sich, dass Mastzell-defiziente Mäuse eine im Vergleich zu Wildtyp-Kontrollen signifikant erhöhte AHR entwickelten, welche nach Rekonstitution der Tiere mit aus Wildtyp-Tieren stammenden Mastzellen reversibel war. Diese Daten deuten auf eine reziproke Umkehrung der Funktionen von Mastzellen und mMCP-4 im Laufe der Entwicklung von einer akuten zu einer chronischen Erkrankung hin. In der akuten Phase wirken Mastzellen krankheitsfördernd während mMCP-4 einen protektiven Effekt besitzt. In der chronischen Phase hingegen verstärkt die Chymase die AHR und Mastzellen entwickeln anti-entzündliche Eigenschaften. Die einander entgegengesetzten regulatorischen Rollen von Mastzellen und mMCP-4 erscheinen selektiv für die Induktion der AHR, da sich Mukusproduktion und Becherzell-Hyperplasie zwischen Wildtyp-Kontrollen und Mastzell-defizienten bzw. mMCP-4-defizienten Tieren nicht unterschied.

Neben ihrer Rolle bei der allergischen Entzündung konnte eine bisher nicht beschriebene neue Funktion von mMCP-4 in der Regulation von Zytokinen in der Homöostase beobachtet werden. Die Konzentrationen einer Reihe von Th1-, Th2-, Th9- und Th17/22-Zytokinen waren bei nicht-sensibilisierten mMCP-4-defizienten Mäusen im Vergleich zu den Wildtypkontrollen oder Mastzell-defizienten Mäusen signifikant erhöht. Diese erhöhte Zytokin-Expression wurde bei sensibilisierten mMCP-4-defizienten Mäusen nicht beobachtet. Dieser Befund deutet auf eine potentielle Funktion der Protease zur Aufrechterhaltung niedriger Zytokinspiegel im gesunden Organismus hin, welche zu einer Unterdrückung unerwünschter Immunreaktionen beitragen könnte.

Mastzellen und ihre proinflammatorischen Mediatoren sind als potenzielle therapeutische Ziele Gegenstand einer intensiven Forschung. Die Ergebnisse dieser Studie liefern nicht nur neue Erkenntnisse über die mögliche Rolle von Mastzellen und der mMCP-4 bei der Regulation des chronischen Asthmas, sondern identifizieren diese, abhängig vom jeweiligen Krankheitsstatus oder Phänotyp, als potenzielle zukünftige Angriffsstrukturen neuer Behandlungsstrategien. Eine Reihe von weiteren Untersuchungen sind jedoch notwendig, um die Relevanz dieser Befunde für die Erkrankung im Menschen zu prüfen und die der mMCP-4-vermittelten Regulation zugrunde liegenden Mechanismen in Homöostase und Erkrankung zu klären.

1 Introduction

1.1 Allergic Asthma

1.1.1 Epidemiology of allergic asthma

Asthma is a chronic disease of the airways, affecting the life of more than 300 million people of all age groups worldwide, with increasing prevalence [1–3]. A wide number of environmental risk factors linked e.g. to changes in lifestyle in addition to a genetic predisposition, may contribute to the increase of asthma[1–4]. In highly developed countries, such as UK, New Zealand, USA, or Australia, more than 14% of the population suffer from asthma. However, recent epidemiological data from developing countries in Asia, Africa or Latin America show also increasing numbers of asthma patients (Fig.1) [1–4].

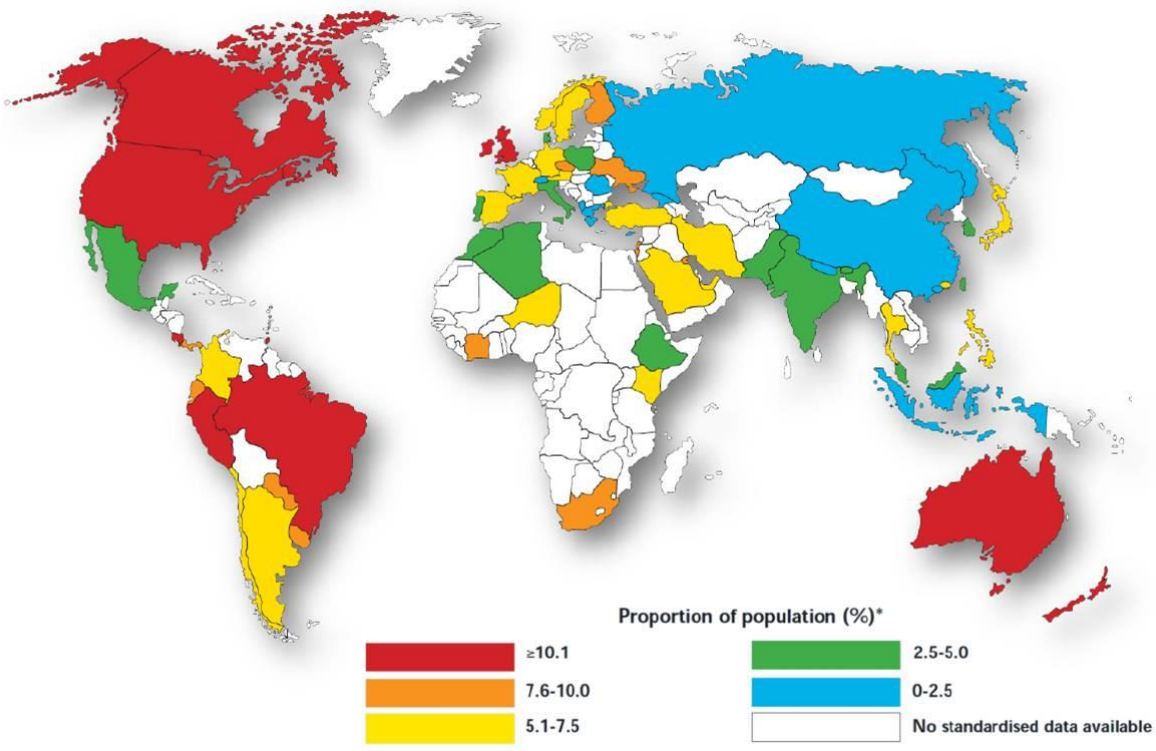

Fig. 1: Worldwide prevalence of Asthma (Masoli *et al.* , 2004)[3]

Asthma-related mortality has decreased in the last decades, mainly due to the control of the disease by the help of new treatment guidelines and the use of preventive anti-inflammatory drugs. But still the worldwide number of deaths caused by asthma is about 180.000 per year,

with differences between ages, economic groups, and countries, affecting mainly populations with low income[1–4]. Access to basic asthma medications or medical care is still a problem for asthmatics in many areas of the world[3]. Direct costs (e.g. medications or hospitalization) and indirect costs (e.g. for temporary or permanent disability, early retirement) are different from country to country. The mean expense of one patient per year run up to 1,900 US$ in Europe and 3,100 US$ in the USA. Approximately 30 million asthmatics live in Europe (age 15 to 64) with a total expense of about 20 billion €[2,5]. The world health organization (WHO) announced in 2004 that the expenses of asthma worldwide probably exceeded those of HIV/AIDS and tuberculosis together[2]. High costs, absence from school in children, or work loss in adults due to disease, have consequences for their future life and results additionally also in psychological burden in asthmatics[2]. Further intense scientific investigations are needed for the better understanding of the pathophysiology of asthma and its treatment.

1.1.2 Pathology of allergic Asthma

Asthma is a complex chronic inflammatory airway disease which is associated with airway hyperreactivity (AHR), tissue inflammation and remodeling. Recurrent episodes of coughing, wheezing, excess of airway mucus production, chest tightness and breathlessness are symptoms of asthma, which may differ depending on the severity of the disease[6–10]. There are two main types of asthma, allergic (atopic or extrinsic) and non-allergic (non-atopic or intrinsic) asthma[11]. Allergic asthma can be induced by specific proteins known as allergens and is characterized by the presence of allergen-specific IgE. By contrast, in non-allergic asthma which can be induced by infections of the airways, cold air, medications or other, allergen-specific IgE is not detected[12]. The more common form of the disease is probably allergic asthma which is classified as a type I hypersensitivity reaction[13–15]. Type I hypersensitivity reaction, which includes allergy, is an over-reaction of the immune system, especially in genetically susceptible individuals towards usually harmless environmental substances (allergens). Allergens can be of different chemical structure (e.g. proteins, carbohydrates) and sources, such as tree pollen, animal dander, house-dust-mite faecal particles (HDM), food (e.g. eggs, nuts), with differences in the sensitization route. The symptoms in response to these allergens can occur seasonally (e.g grass or tree pollen) or during all-seasons (e.g HDM) and can vary from mild to severe reactions or even become life-threathening[16].

Sensitization Phase

The allergic reaction is initiated by the recognition of a harmless substance by the immune system as potentially dangerous. During this process termed sensitization, allergens are taken up predominantly via mucosal tissues by antigen-presenting cells (APC) such as dendritic cells (DC). Some allergens with enzyme activity can enter the tissue by cleavage of the epithelial-cell tight junctions and then being taken up and processed by APC. The APC migrate to lymphoid tissue presenting the processed allergen as peptide on the major histocompatibility complex II (MHC-II-Complex) to the allergen-specific T cell receptor (TCR) on naïve T cells (Th0). Depending on the cytokine milieu, Th0 cells can differentiate in T helper1 (Th1), Th2, Th17 cells or regulatory T cells (Treg)[17]. In presence of IL-12 and IFNγ Th0 cells differentiate into Th1 cells[18,19]. Th2 cells, which are typical for asthma, differentiate from Th0 cells in presence of interleukin 4 (IL-4). Further contact of Th2 cells to B cells in presence of IL-4 and IL-13 result in immunoglobulin E (IgE) producing plasma cells. This allergen-specific IgE binds to the high affinity IgE-receptor FcεRI on the surface of MC and basophils (Fig.2). Sensitization per se does not generate disease symptoms. Disease manifestation requires a further re-exposure and crosslinking of the IgE-receptors via the same antigen, leading to activation and the secretion of different mediators from these cells and recruitment of further immune cells resulting in an amplification of the immune response[17].

Three temporal phases of allergic inflammation have been described. The early-phase reaction, which is the immediate (within second to minutes), late-phase reaction, which is a subsequent (within several hours) immune response after allergen challenge and the chronic phase, which is resulting from repeated allergen exposure (challenge), leading to persistent inflammation and chronification of allergic inflammation[13,17].

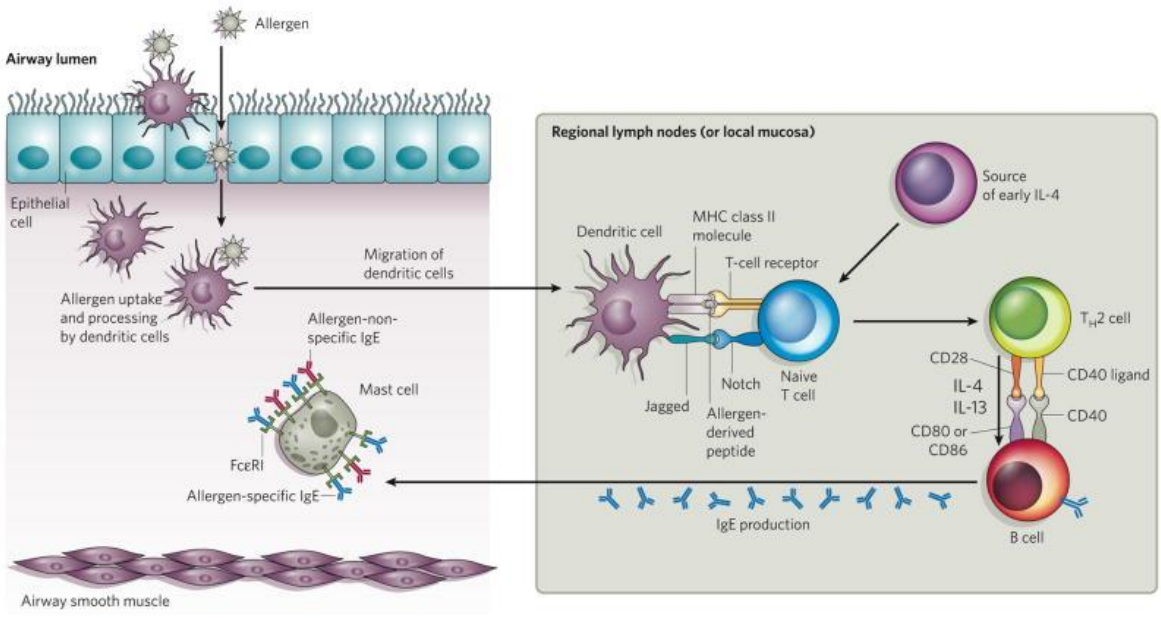

Fig. 2: Allergen sensitization in the Lung (Galli *et al.* , 2008)[17]
Allergens can be up taken and processed by APC such as DC. DC migrate then to regional lymphoid tissue and present the processed allergen to naïve T cells, which differentiate to Th cells depending on cytokine milieu. Th cells, in this case Th2 cells, produce IL-4 and IL-13. Together with these and further co-stimulatory molecules, Th2 cells induce B cell immunoglobulin class switch. The B cells produce allergen specific IgE, which binds to high affinity FcεRI on tissue-resident MCs and leads to their activation**.**

Early-phase reaction

MC, activated within minutes, are the major cells which contribute to the immune response in the early-phase reaction of allergic inflammation. The crosslinking of FcεRI via specific IgE bound to a respective allergen lead to activation of MC and initiates a complex intracellular signaling cascade which results in the degranulation of these cells and the secretion of several mediators from their secretory granules[20]. The occurring symptoms in the lung of sensitized individuals can be for e.g. wheezing by increased secretion of mucus or exacerbating airflow limitations by contraction of bronchial smooth muscles. Some of these mediators initiate the migration and activation of further immune cells to the side of inflammation, augment the immune response and thereby contributing to progress toward the late-phase reaction of allergic inflammation[17,21].

Late-phase reaction

Symptoms occurring few hours after allergen exposure (ca. 2-6 h, with a peak after 6-9 h) belong to the late-phase reaction of an allergic inflammation, which is developed in a subgroup of allergic patients[17]. Beside MC and their mediators, a variety of further cells like T cells, eosinophils, and neutrophils contribute to this disease state. The complex interaction between

tissue resident cells such as epithelial cells and in blood or lymphoid tissue circulating cells such as B and T cells, together with the mediators creates an proinflammatory milieu, which can last for several hours.

Chronic allergic Inflammation

The pathology of chronic allergic asthma is associated with enduring effects of repeated exposure to specific allergens and hence the involvement of many innate and adaptive immune cells which changes the local tissue inflammation leading to chronification of allergic inflammation and tissue damage. This includes also an increase in cytokine and chemokine production, an increase in the deposition of extracellular matrix protein, as well as functional changes in fibroblasts, smooth muscle cells and epithelial cells at the affected sites[17,22]. The long-term interaction between this complex mixture of immune cells and their mediators amplify the asthma hallmarks, AHR, inflammation and tissue remodeling (Fig. 3)[17].

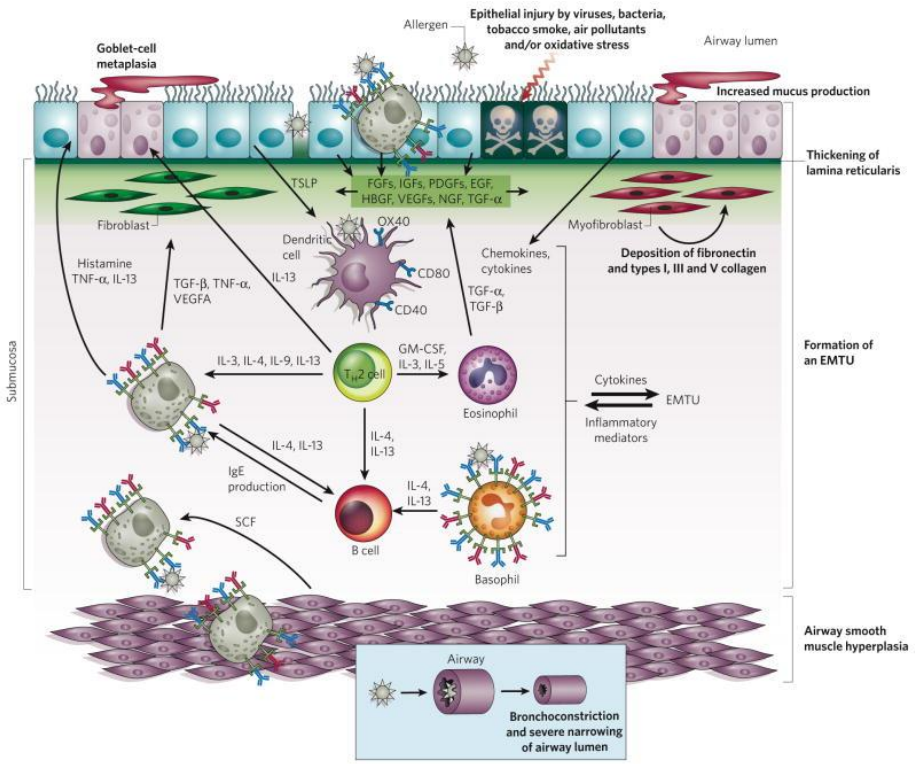

Fig. 3: Chronic phase of allergic inflammation in the Lung (Galli *et al.*, 2008)[17]
The repeated long term exposure to allergens leads to the accumulation of innate immune cells (for e.g. eosinophils, basophils and MCs) as well as adaptive immune cells (e.g. T-cells such as Th2-cells and B-cells) in tissue. Together with epithelial cells, fibroblasts, myofibroblasts, smooth muscle cells, blood and lymphatic vessels and nerves, they recruit and activate each other through their mediators and stay in close interaction, contributing to the chronic allergic inflammation. This chronification of the inflammatory response results in changes of the structure of the affected tissue including substantial

thickening of the epithelium, lamina reticularis, submucosa and smooth muscles and increased deposition of extracellular-matrix proteins fibronectin and collagen. In addition, it leads also to goblet cell hyperplasia and increased mucus production. The repetitive epithelial injury and following airway remodeling can be further exacerbated by contact with pathogens or other environmental substances.

1.2 Mast cells

1.2.1 Mast cell origin and heterogeneity (human vs. mouse)

MCs develop from $CD34^+/CD117^+$ hematopoietic progenitor cells. These cells leave the bone marrow in an immature form, circulate in blood and migrate into peripheral tissues, where they terminally differentiate under the control of different cytokines, and adhesion molecules within the surrounding milieu[23–25]. MCs are long-living cells and in mature state present in nearly all tissues, especially near the boundaries between external environment and the internal milieu. They are found surrounding blood and lymph vessels, neurons, epithelia and glands, smooth muscles and fibroblasts, which are also targets of their mediators[24,26,27]. MC occur in normal lung at low density. However, MC progenitors migrate during inflammatory conditions into the bronchial epithelium and smooth muscle, which is observed in human asthma as well as in asthma mouse models[28,29]. This migration to lung tissue is mediated by vascular cell adhesion molecule 1 (VCAM1) together with integrins (α4β1 and α4β7). The molecules involved in migration of MC progenitors varies depending on their target tissue[30].

Regarding the protease composition in their granules, two subforms of MCs have been described in humans. MCs with tryptase content are named as MC(T) and are prominent in mucosal tissues. Furthermore, MCs containing tryptase, chymase and carboxypeptidase A are termed MC(TC) and are mostly present in serosal environment, respectively in connective tissue. However, both subforms are present in most tissues to different extents[23,31]. Based on their tissue localization, morphology, heparin and protease content, murine MC are distinguished in mucosal MCs (MMCs) and connective tissue MCs (CTMCs). While MMCs predominantly express mouse MC protease-1 and -2, in CTMCs, the prominent MC proteases are mMCP-4, -5, -6 and caboxypeptidase A. Regarding to their localization, MMCs correlate most likely to human MC(T) and CTMC to human MC(TC)[32].

As part of the innate immune system, MC have an optimal position in the body to act as a first line defense against invasive pathogens or toxins[31]. They are highly granulated and own a repertoire of different receptors such as FcεRI or several Toll-like receptors (TLRs). They can be activated by a variety of different stimuli such as activated complement proteins, by direct injury or chemicals substances (opioids, alcohols, antibiotics and other), microbes or

IgE/antigen complexes. Following a complex cascade of cytoplasmic signals, MC granules fuse with the plasma membrane and secrete their content in a process termed degranulation [33,34].

1.2.2 Mast cell mediators in allergic asthma

The crosslinking of FcεRI via specific IgE bound to a respective allergen lead to activation of MC and initiates a complex intracellular signaling cascade which results in the degranulation of these cells and the secretion of several preformed and new synthesized biologically active mediators from their secretory granules into extracellular space[20]. In early-phase reaction, secretion of preformed mediators like vasoactive amines (histamine), neutral proteases (chymases, tryptases and carboxypeptidase A3), proteoglycans (heparin), lipid mediators like prostaglandin D2 (PGD2) and leukotriene B4 (LTB4), growth factors (vascular endothelial growth factor A (VEGFA), GM-CSF) and cytokines (e.g TNFα) lead to acute inflammatory symptoms[21,35,36]. Newly synthesized (lipid-) mediators are prostaglandins (PGD_2), leukotrienes (LTC_4, LTB_4) and a large number of growth factors (TGF-β), cytokines (IL-1, IL-6, IL-10), and chemokines. The ability to differentially release these mediators depends on the respective stimuli, the MC-subtype and the surrounding tissue[21,26,27]. The released mediators have mostly more than one and, sometimes, redundant functions. Histamine and LTC_4 increase vascular permeability and induce mucus secretion. Furthermore, histamine induces smooth muscle contraction[37]. MC serine proteases are the most abundant proteins stored in the granules and have multiple functions in immune response. Chymase and tryptase are involved in inflammation, tissue remodeling and bronchial hyperresponsiveness[28,38]. Carboxypeptidase A is also stored in a complex with heparin and is involved in degradation of vasoconstrictive factor endothelin 1 and snake venom toxins[39]. The lipid mediator PGD_2 is chemotactic for eosinophils, induces bronchoconstriction and vasodilatation in allergic inflammation and can promote polarization and recruitment of Th2 cells through inhibition of Th1 cytokines[40]. Leukotrienes (LTC_4, LTB_4) induce prolonged bronchoconstriction and promote bronchial mucus secretion. LTB_4 (including several other cytokines such as IL-8) has been also shown to recruit neutrophils[17,41]. Activated neutrophils can release several mediators which induce epithelial damage, increased vascular permeability, hypersecretion of mucus, bronchoconstriction and AHR[42].

De novo synthesized cytokines (e.g. IL-1, -6, -8, -10, -13, -16), chemokines (such as CCL2, CCL3), prolong and amplify the allergic inflammation and may contribute more to the late-phase reaction. They are involved in the regulation, recruitment and activation of other immune

cells. The recruitment of eosinophils into the lung is regulated by Th2 cytokines such as IL-5 and IL-13 and chemoattractants such as eotaxin. Eosinophils contribute to mucus hypersecretion, induction of AHR and tissue remodeling by release of their granule content[43]. Beside immune cells also structural cells such as epithelial cells contribute to the allergic inflammation. The release of CC chemokine ligands (e.g. CCL2) can promote recruitment and activation of monocytes and also the recruitment and maturation of DC to take up and process allergens[17,42,44]. Some growth factors are preformed and released rapidly such as VEGF-A while some are new synthesized such as TGF-β. Both are involved in airway remodeling processes[22].

1.3 Experimental asthma

Human allergic asthma involves many cell types and consists of multiple phenotypes. It is associated with persistent airway AHR, airway inflammation and airway remodeling. Airway remodeling includes structural changes in airways such as goblet cell hyperplasia, smooth muscle thickening, increased vascularity and subepithelial and airway wall fibrosis, in response to repeated long-term exposure to a range of different triggers. The mechanisms underlying the asthma pathology are still not fully understood. Required experiments to investigate these mechanisms are for obvious ethical reasons not acceptable in humans[45,46]. For understanding of immunological processes at a certain cellular or molecular level, *in vitro* systems with human materials have been shown to be a useful tool. However, complementary *in vivo* systems are necessary for analyzing the complex interaction of cell types and mediators within the lung and the body under physiological conditions[45]. Among other animal species used in experimental asthma models, mice have been favored for many reasons, such as low cost, a well-characterized immune system and, most important, the availability of a variety of genetically modified mouse strains and the wide array of specific reagents for further analysis. This enables not only the investigation of the disease from different aspects but facilitates also therapeutic approaches[47]. Nevertheless, due to anatomical and functional differences of the lung tissue between mouse and human, a single experimental model cannot resemble all morphological and functional characteristics of the human chronic asthma. Therefore, the outcome of such experiments has to be considered carefully and cannot directly be translated to asthmatic patients. Nonetheless, most findings about the disease process in asthma and the response to allergens, are derived from investigations in animal models and further use of animal models will help to understand the specific features and to puzzle out the disease [46,48].

Allergic airway inflammation in mice is initiated by sensitization of the animal to a non-self protein. Commonly used are ovalbumin derived from chicken egg but also allergens more relevant for humans, such as house dust mite (HDM), cockroach, animal dander or pollen extracts, and several others. Unlike in humans, direct inhalation of the allergens in mice induces frequently tolerance or mild pulmonary inflammation, with an exception of some allergens characterized by an intrinsic enzymatic activity like as HDM. Systemic sensitizations in this species is commonly successful via repeated intraperitoneal injection of the allergen[46]. After injection, the immune system needs several days to initiate a reaction against the allergen. Lung inflammation is induced by repeated local exposure to the allergen by intranasal (i.n), intratracheal (i.t.), oropharyngeal or aerosol. The application features of allergic inflammation, such as AHR, influx of immune cells (e.g. eosinophils), typically reach their peak 24h to 72h after the last allergen exposure[49]. However, there is a wide range of protocols used for sensitization and challenge. The pathogenesis of the disease in all asthma models are affected by various parameters, such as the genetic background of the mice, the use of adjuvant, or the route of allergen administration[46]. As an example, it has been shown that the presence of the adjuvant aluminum hydroxide (alum) in asthma models induces a MC-independent allergic inflammation, where as its absence revealed an important role of MCs in the induction of allergic asthma[50,51]. It is currently hypothesized that one of the reasons for the discrepancy between promising treatment strategies developed in mouse models of asthma and their failure in clinical trials in asthma patients is, that the MC-dependency has not been sufficiently considered in the animal studies. Therefore, additional investigations are necessary to further clarify the role of MCs in different asthma phenotypes[52].

1.3.1 MC-deficient mouse models in experimental asthma

So far, no reagents or drugs exists which can solely and specifically suppress MC functions[53]. Mouse strains deficient in MCs may serve as helpful tools in performing experimental asthma models with regard to MC-dependency in the resulting effects. For this purpose, several constitutive and conditional MC knock-out mouse strains have been developed. The most prominent constitutive MC-deficient mouse strains are the WBB6F1-$Kit^{W/W\text{-}v}$ (W/W-v) and C57BL/6-$Kit^{W\text{-}sh/W\text{-}sh}$ (W-sh). The MC-deficiency in both strains is based on different mutations in the locus coding for KIT, the receptor for *stem cell factor* (SCF), which is the main growth and survival factor for MCs. Kit^{W}, represents a point mutation which results in a truncated KIT and is thereby not expressed on the cell surface. $Kit^{W\text{-}v}$ is a mutation in the c-*kit* tyrosine kinase domain that reduces the kinase activity of the receptor. The WBB6F1-$Kit^{W/W\text{-}v}$ (W/W-v) MC-

deficient strain are also deficient in melanocytes. Furthermore, they are anaemic, sterile and show reduced numbers of neutrophils and basophils. The *Kit*$^{W\text{-}sh}$, is an inversion mutation affecting a segment upstream of the c-*kit* transcription start site on mouse chromosome 5. The C57BL/6-*Kit*$^{W\text{-}sh/W\text{-}sh}$ (W-sh) MC-deficient mice have also a melanocyte-deficiency, but have normal red blood cell count, are fertile, and show in contrast to W/W-v mice an increase in neutrophils and basophils[52,54–56]. A major disadvantage of both mouse models results from the expression of KIT. Since this receptor is not exclusively expressed on MC but on a variety of further cells of the immune system, a central problem is the discrimination between effects and phenotypes associated with the loss of KIT and those related to MC ablation. Currently, the reconstitution of MC-deficient mice with MCs derived from wildtype animals with the same genetic background is the only way to solve this problem. For MC-dependent effects, reconstituted mice should ideally develop a phenotype corresponding to the wildtype control. However, it should be mentioned that further pitfalls may arise from incomplete or irregular reconstitution of MC in the different organs[52].

1.4 Mast cell chymase

Mast cells (MC) store a wide range of proteases in their secretory granules, which can account for up to 35% of the total cellular protein. While proteases such as renin, cathepsin G, matrix metalloprotease 9 (MMP9), active caspase-3, lysosomal cathepsins, granzyme B or neuropsin/Prss19, are expressed by a variety of cells, some proteases are highly specific for MCs. Typical members of the latter group, are chymase, tryptase and MC-carboxypeptidase A (CPA). The majority of these proteases belong to the chymotrypsin-related serine proteases, where MC chymases represent the most relevant subgroup[27,57,58]. Chymases are monomeric enzymes characterized by a cleavage specificity at the COOH-terminus of hydrophobic aromatic amino acid residues such as Phe, Tyr and Trp. Chymases are classified in α- and β-chymases, according the phylogenetic tree[59]. In most investigated mammalian species, a single gene encoding an α-chymase has been identified. In rodents, however, additional genes encoding for β-chymases have been identified[60], While α-chymase (*CMA1*), which is expressed in MCTC subform together with the other specific MC proteases, tryptase and MC-CPA, is the only member of this group in humans[57]. A large family of chymases are described in mice. The β-chymase mouse mast cell protease 4 (mMCP-4/gene name: *Mcpt-4*) and the α-chymase mMCP-5 (*Mcpt-5*), together with tryptases and MC-CPA, are mainly present in the CTMC

subpopulation. For efficient storage in MC secretory granules, these enzymes are complexed with serglycin proteoglycans[57]. Proteoglycans contain highly negative charged sulfate-groups in their carbohydrate side chains which interact with certain basic region of MC proteases[57,61–63]. The β-chymases mMCP-1 and -2 (*Mcpt-1 and -2*) are predominantly expressed in MMC subpopulation. Since only one human chymase is confronted with four corresponding enzymes in mice, comparative studies between both species have been performed to identify the chymase which represents the human equivalent. Mouse chymases mMCP-1 and -2 differ significantly from human α-chymase in their proteoglycan-binding properties, tissue distribution, and substrate preferences. In addition, mMCP-2 does not show chymase activity[64]. Regarding to their similiarties in amino acid sequence, mMCP-5 can be recognized as the closest homologue to human α-chymase. However, mMCP-5 does not show a chymotrypsin-like but more an elastolytic enzymatic activity, which disqualifies it as an appropriate equivalent[27]. In contrast to the chymases described before, mMCP-4 has similar heparin-binding properties, a comparable substrate specificity (e.g. MMP-activation and angiotensin I conversion to II) and tissue distribution as compared to human chymase[65,66]. Taken together, despite to differences on the genetic level, these properties clearly identify mMCP-4 as the functional homologue to the human α-chymase[66].

Therefore, mMCP-4$^{-/-}$ mice may be a suitable tool for investigating the role of chymase and help to clarify functions of human α-chymase[57]. By the use of mMCP-4$^{-/-}$ mice, in animal models of different diseases, several pro- as well as anti-inflammatory properties of mMCP-4 have been described depending on the corresponding inflammatory condition (Table 1). In some autoimmune disease models like rheumatoid arthritis, abdominal aortic aneurysm or bullous pemphigoid mMCP-4 appear to be pro-inflammatory[67–69]. An anti-inflammatory role for mMCP-4 was found in a model of kidney fibrosis, in a model of brain/spinal cord inflammation, and in a model of sepsis [70–73]. mMCP-4 can also enhance host resistance to the toxicity of certain animal venoms[74]. Interestingly, mMCP-4 can contribute to normal tissue homeostasis e.g. by regulation of connective tissue turnover[75].

Table 1: Role of mouse chymase mMCP-4 in disease.

mMCP-4 in disease	**Function**
Proinflammatory:	
Rheumatoid arthritis[67]	by affecting anticollagen II IgG generation and inflammation
Abdominal aortic aneurysm[68]	by affecting angiogenesis, apoptosis and inflammation
Bullous pemphigoid[69]	by activating MMP-9 and cleaving BP180
Anti-inflammatory:	
Kidney fibrosis[70]	anti-fibrotic potential by degrading interstitial deposits of fibronectin
Brain[71]/Spinal cord[72] inflammation	suppression of inflammation by decreasing numbers of immune cells and degradation of inflammatory cytokines such as MCP-1, IL6 and -13
Sepsis[73]	by degradation of TNF
Acute experimental asthma[76,77]	by affecting smooth muscle cells, modulating IL-33 levels and inflammation
Animal venoms[74]	by degradation of venom peptides
Tissue homeostasis:	
Contribution to normal tissue homeostasis[75]	regulation of connective tissue turnover by activation of pro-MMP-2 and -9

Among others, fibronectin and procollagenase (MMP-1) are substrates of the human α-chymase[78,79]. Beside other functions, this enzyme can also convert angiotensin I into the vasoconstrictor hormone angiotensin II, which affects the blood pressure[80,81]. Additionally, it has been shown that human α-chymase can recruit inflammatory cells (*in vivo* and *in vitro*) and impair epithelial permeability. Therefore, it can be expected that chymases may have a more pathogenic role in allergic inflammation and asthma[82,83]. Only a few investigations have been done so far addressing the role of mMCP-4 in asthma. Recent studies where mMCP-4$^{-/-}$ mice were used in an acute model of asthma suggest a potent protective role of this chymase in the disease[76,77]. However, its role in a chronic course of the disease has not been investigated yet. To better understand the pathophysiological function of mMCP-4 in asthma and to assess the potential of chymase as a future therapeutic target, studies in a chronic model of this order are required.

1.5 Hypothesis and aim of work

The interaction of a broad range of inflammatory cells such as mast cells, neutrophils, eosinophils and T-cells including their mediators contributes to the complexity of asthma resulting in heterogenous clinical phenotypes[84]. While the role of MC and many of their mediators in the induction of human allergic asthma is under broad investigation, the specific role of MC chymase is largely illusive.[28,85,86].

According to my hypothesis, chymase could represent an essential modulator of allergic inflammation. The constitutive release of chymase in the chronic course of the disease may lead to permeabilization, damage and remodeling of the epithelial barriers, facilitating allergen uptake, and to further recruitment of inflammatory cells and mediators to the sight of inflamed tissue and thereby contribute to persistence inflammation.

Hypothesis

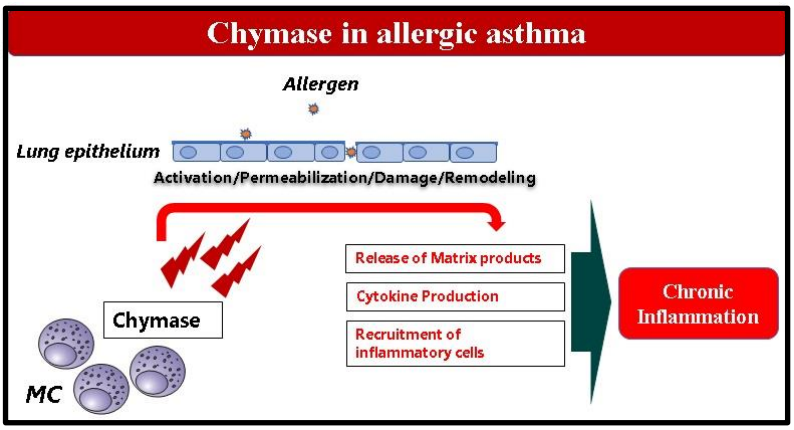

To address this hypothesis, I studied the role of mMCP-4 in an alum-free mouse model of chronic asthma, using MC-deficient C57BL/6-Kit$^{Wsh/Wsh}$ and mMCP-4$^{-/-}$-mice.

This work will focus on the following questions:

1 Does chymase exert proinflammatory properties *in vitro*?
2 Do mast cells and/or mouse chymase mMCP-4 contribute to the pathogenesis of chronic sthma?
3 Which pathophysiological processes of asthma are regulated by mast cells and mouse chymase mMCP-4?
4 By which regulatory mechanism do mast cells and mouse chymase mMCP-4 affect the allergic inflammation in the lung?

2 Materials and Methods

2.1 Materials

2.1.1 Laboratory supplies

Supplies	**Manufacturer**
5 ml-Polystyrene FACS-tubes with lid	BD Falcon, Franklin Lakes, NJ, USA
1,4 ml FACS-tubes	MP32022, Micronic, NL
15-50 mL tubes	Sarstedt, G -Nümbrecht
(0,5 ml, 1,5 ml, 2,0 ml) tubes	Sarstedt, G -Nümbrecht
Stainless-Steel Embedding Cassettes Tissue-Tek®	Sakura Finetek, G -Staufen
Embedding cassettes (Histosette)	Labonord, G -Mönchengladbach
FEATHER® disposable microtome blades A35 und C35	Pfm medical, G -Cologne
NUNC F96 Maxisorp™Surface	Thermo Scientific, G-Langenselbold
Microtiter plate round-bottom 96-well	Greiner Bio-One GmbH, G-Frieckenhausen
Cell culture cluster plate, Costar, flat-bottom, (6well, 24well, 96well)	Corning Incorporated, Corning, NY, USA
Cell culture flask	Sarstedt, USA
superfrost®plus Microscope slides	R. Langenbrinck, G-Emmendingen
serum-separating BD Microtainer SST™ Tubes	BD Pharmingen
Polycarbonate filter membrane (3µm-Pore, 25x80mm, PVP-surface treatment)	Neuro Probe Inc., Gaithersburg, MD USA
pre-separation filter (30µm meshed filter)	Miltenyi Biotec GmBH, G-Bergisch Gladbach

2.1.2 Chemicals and laboratory reagents

Products	**Manufacturer**
Acetyl-ß-methylcholine (methacholine)	Sigma Aldrich
Agar-agar	Merck, G-Darmstadt
Agarose	peqLab, G-Erlangen
Aqua dest	B. Braun, G-Melsungen
BSA, low endotoxin	PAN-Biochtech, G-Aidenbach
$CaCl_2$	Merck, G-Darmstadt
Casyton	Innovatis AG, G-Reutlingen
Human chymase, recombinant	Sigma Aldrich, G-Steinheim
Human chymase, purified from skin	ENZO Life Science Inc., G-Lörrach
Chymopapaine	Sigma Aldrich, G-Steinheim
Chymostatin	Sigma Aldrich, G-Steinheim
Ciprofloxacinhydrochlorid	Fluka Biochemica

Products	**Manufacturer**
Collagenase D	Roche
Collagenase Type I	Worthington Biochemical Cooperation, NJ, USA
Desoxynukleotide (dNTPs)	Roth, G-Karlsruhe
Dispase II	Roche, G-Mannheim
DMEM	Biochrom AG, G-Berlin
DNase	Sigma Aldrich, D25
100bp DNA standard	Thermo Scientific, D-Langenselbold
Dream Taq-DNA polymerase	Thermo Scientific, D-Langenselbold
EDTA	Merck, G-Darmstadt
Entellan	Merck, G-Darmstadt
Elastase	Worthington Biochemical Cooperation, NJ, USA
Ethanol, absolut	Sigma-Aldrich, G-Steinheim
FCS	PAN-Biochtech, G-Aidenbach
fMLP	Sigma Aldrich, G-Steinheim
Gelatine	Fluka Biochemica
Gel-loading buffer (6x)	Roth, G-Karlsruhe
L-Glutamin	PAA, A-Pausching
Murine GM-CSF	PeproTech, G-Hamburg
Heparin	Rotexmedica, G-Trittau
HEPES	Merck, G-Darmstadt
Hexa-decyl-tri-methyl-ammonium-bromide	Sigma Aldrich, G-Steinheim
Hexosamindase substrate	Sigma Aldrich, G-Steinheim
Histomount	Merck, G-Darmstadt
Murine IL-3	PeproTech, G-Hamburg
Iscove's modified Dulbecco medium (IMDM)	PAA
Ketamindor (Ketamine)100 mg/ml	WDT, G-Garbsen
$MgCl_2$	Merck, G-Darmstadt
ß-Mercaptoethanol	PAN-Biochtech, G-Aidenbach
NaCl	B-Braun, G-Melsungen
Nonessential amino acids	Invitrogen, G-Darmstadt
Ovalbumin (OVA)	Sigma Aldrich, G-Steinheim
Pancoll	PAN-Biochtech, G-Aidenbach
Pancuronium bromide	Sigma Aldrich, G-Steinheim
Paraplast Plus (paraffin)	Roth, G-Karlsruhe
Penicillin/Streptomycin-solution	PAN-Biochtech, G-Aidenbach
Percoll	Sigma Aldrich, G-Steinheim
Periodic acid	Roth, G-Karlsruhe
Phosphate buffer (Na_2HPO_4)	Merck, G-Darmstadt
Protease inhibitor cocktail (1x complete™ Mini)	Roche, G-Mannheim
Polyvinyl alcohol (PVA)	Merck, G-Darmstadt
Roti®Histofix 4% (paraformaldehyde, 4%)	Roth, G-Karlsruhe
Roti® Histokit II	Roth, G-Karlsruhe
Roti®-Safe GelStain	Roth, G-Karlsruhe
Roticlear	Roth, G-Karlsruhe
RPMI 1640 with 10mM HEPES	Biochrom AG, G-Berlin
RPMI 1640, Ø Phenolred	Biochrom AG, G-Berlin

Products	**Manufacturer**
Schiffs Reagent	Roth, G-Karlsruhe
Human SCF	Invitrogen, G-Darmstadt
Murine SCF	PeproTech, G-Hamburg
Sevoflurane	Abbott, UK
Sodium citrate	Sigma Aldrich, G-Steinheim
Sodium pyruvate	PAN-Biochtech, G-Aidenbach
Stem Pro-34 SFM	Invitrogen, G-Darmstadt
Suc-Ala-Ala-Pro-Phe-p-NA (chymase substrate)	Sigma Aldrich, G-Steinheim
Sulfric acid (1 M H_2SO_4)	Merck, G-Darmstadt
Supplement (StemPro-nutrientsupplement)	Gibco by life technologie
Toluidine blue	Sigma Aldrich, G-Steinheim
Trypan blue	Chroma-gesellschaft schmidt&Co, G-Stuttgart
TAE-Buffer, 50x	Roth, G-Karlsruhe
Tetramethylbenzidine (TMB)	Sigma-Aldrich, G-Steinheim
Triton X-100	Sigma-Aldrich, G-Steinheim
Vitamin solution	Invitrogen, G-Darmstadt
Xylavet (Xylazine), 20mg/ml	CP-pharma, G-Burgdorf

2.1.3 Antibodies

Specifity	**Clon**	**Isotype**	**Labeling**	**Manufacturer**	**Purpose**
Live/Dead (UV)	-	-	-	Invitrogen	FC
TruStain Fc-block (anti-Maus CD16/32)	93	IgG2a, κ	-	BioLegend	FC
FcεRIα	MAR-1	IgG	Percp/Cy5.5	Biolegend	FC
T1/ST2 (IL-33 receptor)	DJ8	IgG1	FITC	Biolegend	FC
CD117 (c-kit)	2B8	IgG2b	PE	Biolegend	FC
Human IgE	-	-	-	Calbiochem	MCS
Goat anti human IgE	-	-	-	Invitrogen	MCS
Mouse anti human CD-117 (microbeads)	AC126	IgG1	-	Miltenyi Biotec GmBH, G-Bergisch Gladbach	MCI
Mouse anti human CD203c-PE (microbeads)	FR3-16A11	IgG1	PE	Miltenyi Biotec GmBH, G-Bergisch Gladbach	MCI
Mouse anti-PE (microbeads)	n.m.	-	-	Miltenyi Biotec GmBH, G-Bergisch Gladbach	MCI

Specifity	Clon	Isotype	Labeling	Manufacturer	Purpose
Human FcR-Blocking-reagent	-	IgG	-	Miltenyi Biotec GmbH, G-Bergisch Gladbach	MCI

PerCp-Cy5.5= Peridinin-Chlorophyll-Protein Complex, FITC= Fluorescein isothiocyanate, PE= Phycoerythrin, Beads= superparamagnetic particles, n.m.= not mentioned, FC=Flowcytometry, MCS=Mast cell stimulation, MCI= Mast cell isolation

2.1.4 Oligonucleotides (Primers)

Primers were synthetized by manufacturer metabion international AG (D-Martinsried)

Primer	Nucleotide sequence
200_Neo Rvs	5`-GGG CCA GCT CAT TCC TCC CAC TCA TGA TCT-´3
201_Wt ex2 Rvs	5`-GGT GAT CTC CAG ATG GGC CAT GTA AGG GCG-´3
202_New Wt+Neo Fwd	5`-CAA GGT CCA ACT AAC TCC CTT TGT GCT CC-´3

2.1.5 Ready-to-use Kits

Kit	Manufacturer
LEGENDplex™ assay kit (Mouse Th Cytokine Panel, 13-plex)	BioLegend, CA, USA
Mouse OVA specific IgE ELISA Kit LEGEND MAX™	BioLegend, CA, USA
May Grünwald Giemsa Staining	Sigma-Aldrich, G-Steinheim
Diff Quick® set (staining)	Medion Grifols Diagnostics AG CH-Düdingen
Dneasy 96 Blood & Tissue Kit	Qiagen, G-Hilden
Dream Taq DNA Polymerase kit, Fermentas	Thermo Scientific, G-St. Leon-Rot
Roti Histokit II	Roth, G-Karlsruhe

2.1.6 Equipment (Instruments/Devices/software)

Equipment	Manufacturer
Autotechnicon *Microm STP 120*	Thermo Scientific, G-Langenselbold
ELISA Reader Tecan Sunrise (Chemotaxis assay, OVA-specific IgE ELISA, Hexosamindase assay)	Tecan, G-Crailsheim
ELISA Reader Tecan Spectra (Chymotryptic enzyme activity)	Tecan, G-Crailsheim
FinePointe	Buxco Research Systems
FinePointe-Buxco software	Buxco Research Systems

Equipment	**Manufacturer**
Incubator, 37°C, CO_2; *Hera Cell*	Thermo Scientific, G-Langenselbold
Incubator, 60 °C	Memmert, G-Schwabach
Light microscope (Diff. BAL cell count)	Zeiss, G-Göttingen
Light microscope Primostar (Neutrophil isolation)	Zeiss, G-Göttingen
Light microscope Olympus BX41 (Camera: Nikon DS-Ri1) (Images for Histology)	Olympus, G-Hamburg
Light microscope Olympus BX61, Camera Olympus DP72 (newCAST streological analysis)	Olympus, G-Hamburg
LSRII – flow cytometer	BD Bioscience
newCAST-Software	Visiopharm, Hoersholm, DK
Paraffin-Microtom *SM 2000R*	Leica, G-Nussloch
Water bath*Typ 12B*	Julabo, G-Seelbach
Balance	Kern, G-Balingen
Hotplate	Dargatz
Centrifuge (0,2-2,0 ml Tube; DNA-Isolation) *Mikro 200*	Hettich, G -Tuttlingen
Centrifuge (0,2-2,0 ml Tube; serum and BAL) *Mikro 22R*	Hettich, G -Tuttlingen
Centrifuge (15-50 ml Tube; hLMC, BMMC, restimulation assay) *Rotixa 50RS*	Hettich, G -Tuttlingen
Centrifuge (15-50 ml Tube; PMN-Isolation) *Rotina 420*	Hettich, G-Tuttlingen
Centrifuge (96-well Plate; FACSstaining) *Rotina 420R*	Hettich, G-Tuttlingen
Cytospincentrifuge	Shandon
Thermocycler (Labcycler)	Sensoquest, G-Göttingen
Vacuum pump *ME2*	Vacuubrand GmbH, G-Wertheim
xCELLigence® RTCA DP	ACEA Bioscience Inc., CA, USA
RTCA software *for xCELLigence® RTCA*	ACEA Bioscience Inc., CA, USA
E-plate 96well for xCELLigence® RTCA	ACEA Bioscience Inc., CA, USA
Casy (Cell counter)	Innovatis AG, G-Reutlingen
Boyden-Chamber *AP48* (48-well)	Neuro Probe Inc., Gaithersburg, MD USA
Roll mixer RS-TR05	Phoenix instruments, G-Garbsen
autoMACS®Pro Separator	Miltenyi Biotec GmBH, G-Bergisch Gladbach
autoMACS® separation columns	Miltenyi Biotec GmBH, G-Bergisch Gladbach

2.2 Methods

2.2.1 Cell isolation and culture

2.2.1.1 Human neutrophils

Neutrophil polymorphonuclear granulocytes (PMN) were isolated from whole blood donated from healthy volunteers. Approval for these studies was obtained from the Institutional Review board at the University of Lübeck (Lübeck, Germany; Az. 12-202A) according to the Declaration of Helsinki. All volunteers gave written informed consent.

To prevent coagulation of blood, 4 ml heparin was mixed with each ml blood sample (25000 IE per 5 ml). For separation of PMNs from other blood cells, a combination of sedimentation and density gradient separation method was performed[87]. First, blood samples were mixed 1:3 with PVA (1% in NaCl). After sedimentation of red blood cells for 20 min at RT, aliquots of erythrocyte-free SN (30 ml) were carefully layered on top of 8 ml isotonic pancoll solution and centrifuged for 24 min at 850 x g at RT. After removal of the SN, neutrophil-containing pellets were resuspended in 5 ml ice-cold aqua dest. for 45 sec. to lyze remaining erythrocytes. The reaction was terminated by addition of a respective volume of 2-fold concentrated D-PBS, followed by centrifugation for 10 min at 200 x g at 4°C. After a repeated washing step with D-PBS/0,5 % BSA, cells were counted in an electronic cell counter. Cells were resuspended finally in D-PBS/0,5% BSA (2 x 10^6 cells/ml) and stored on ice before use.

Purity of PMN cell suspensions were additionally determined on cytospin preparations after Diff Quick staining (s. section 2.1.5).

2.2.1.2 Human lung mast cells (hLMC)

For isolation of hLMC, tumor-free lung tissue obtained from patients with bronchial carcinoma undergoing lobectomy was provided by the Division of clinical and experimental pathology (Research Center Borstel). Approval for these studies was obtained from the Institutional Review board at the University of Lübeck (Lübeck, Germany; Az. 12-202A) according to the Declaration of Helsinki. All volunteers gave written informed consent. Preparation of hLMC was performed according to Schiemann *et al.* with minor modifications[88]. Briefly, lung tissue was weighted, chopped into small pieces, washed and incubated in mast cell (MC)-buffer (s. appendix) overnight at 8°C under agitation. Tissue suspensions were processed through a close-meshed tissue strainer. To obtain single cell suspensions, homogenates were digested with 1 ml/g tissue of a protease cocktail consisting of dispase II (1,5 mg/g), chymopapain (1 U/g),

collagenase Typ I (0,5 mg/ml), elastase (4 U/g) including 1% gelatin in MC-buffer. Tissue suspensions were incubated 4h at 37°C in the protease cocktail (1ml/1g lung tissue) under continuous agitation using a roll mixer. Resulting single cell suspensions were washed twice in MC-buffer for 10 min at 300 x at RT and further separated by Percoll density gradient centrifugation. For this purpose, Percoll solutions of 80%, 60% and 50% were prepared in MC-buffer and layered in 50 ml tubes (Fig. 1). Subsequently, cell suspensions (5 ml) combined with 60 % Percoll (5 ml) solution were layered carefully on the top. Finally, MC-buffer was administered on top and samples were centrifuged for 20 min at 400g.

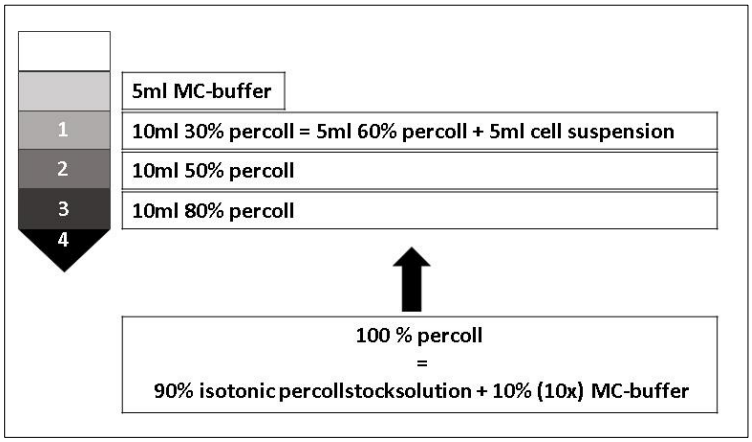

Purification of hLMCs by density percoll gradient separation. Cell suspensions were carefully layered together with MC-buffer and different Percoll concentrations for a density gradient separation. Fractions were numbered from 1 to 4.

MC numbers and viability were determined from boundary layers of fraction 1/2 (30%/50%) and 2/3 (50%/80%) separately, after percoll-centrifugation. Cell suspensions were first washed in 10 ml MC-buffer for 10 min at 300 x g at RT, pellets were resuspended in 10 ml ice-cold, degassed D-PBS/0,5 % BSA and counted after combined staining with trypan blue and toluidine blue dye. Cell suspensions containing more than 4% MCs were pooled and washed for 10 min at 300 x g at 4°C and finally resuspended in 600 µl ice-cold, degassed D-PBS/0,5 % BSA. Further purification of MCs was performed by automated magnetic bead separation using antibodies directed against CD117 and CD203c-PE coated to paramagnetic microparticles. Briefly, pooled cell suspensions were incubated with 200 µl FcR-Blocking reagent and 100 µl CD203c-PE (1:9) for 15 min (4°C) and further incubated with 200 µl CD117 (1:5) for additional 15 min (4°C). Samples were diluted with 30 ml D-PBS/0,5% BSA and centrifuged for 10 min at 300 x g at 4°C. Cell pellets were resuspended in 800 µl D-PBS/0,5%BSA, combined with 200 µl anti PE beads (1:5) and incubated for further 15 min at 4°C. After incubation, samples

were diluted with 20 ml D-PBS/0,5% BSA and washed repeatedly in D-PBS/0,5% BSA for 10 min at 300 x g at 4°C. Finally, cell pellets were resuspended in 10 ml D-PBS/0,5% BSA and filtered through a pre-separation filter (30µm meshed filter, Miltenyi Biotec). Labeled MCs were separated from whole cell suspension by autoMACS® separation columns and the resulting eluate containing MCs was washed in 30 ml D-PBS/0,5% BSA for 10 min at 300 x g at RT and pellet was resuspended in human MC medium (s. appendix) and cultured at a density of $0{,}5x10^6$ cells/ml at 37°C and 5% CO_2. Medium was changed weekly and experiments were performed earliest 2 weeks after isolation.

2.2.1.3 Mouse bone marrow derived mast cells (BMMC)

MCs can be generated under certain culture conditions from bone marrow cells. The protocol used for mouse BMMC generation here followed a method described by Orinska *et al* with minor differences[89]. Bone marrow cells were isolated from 6-8 weeks old C57BL/6- and mMCP-$4^{-/-}$-mice. Mice were euthanized by CO_2 inhalation and animal surfaces were disinfected with 70% ethanol. Skin and muscles of the lower extremities were removed to expose the bones. Bones were than taken out and cleaned from the surrounding tissue with gauze compress (Gazin, Lohmann und Rauscher, Neuwied, D).

Femurs were opened at both ends and bone marrow was flushed by injecting 10 ml D-PBS with a canule (0,4x19 mm, BD) and tissue material was transferred to a 50 ml tube. The cell suspension was centrifuged for 10 min at 340 x g. To lyze the erythrocytes, cells of each mouse were incubated for 15 min at RT in 3 ml lysis buffer (s. appendix), lysis was then stopped by adding 10 ml BMMC-medium (s. appendix) to the cell suspension. After a second centrifugation step, cells were transferred to BMMC-medium supplemented with 10 ng/ml SCF and 5 ng/ml murine IL-3 and cultured at 37°C and 7.5% CO_2 for up to 5 weeks. In the first two weeks, 10 µg/ml Ciprofloxacin hydrochloride as an antibiotic was added to the BMMC-culture. Medium was changed every week.

2.2.1.4 Preparation, culture and restimulation of lung cells

After BAL collection, mouse lungs were explanted and right and left lung lobes were separated by employing a knot in primary bronchus. Left lung lobes were processed for histologicalanalysis (2.2.7). Separated right lung lobes were chopped into small pieces and collected in MC-buffer (s. appendix) and further processed for isolation and restimulation of lung cells. Expression of different cytokines were analyzed in SN of the restimulated lung cells.Lung tissue samples were enzymatically digested in 5 ml of digestion buffer (s. appendix) containing Collagenase D (0,5mg/ml) and incubated for 45 min at 37°C. Tissues were passed through a cell strainer, rinsed and washed in 2 ml washing buffer (s. appendix). Cell suspensions were centrifuged for 10 min at 350 x g at RT and resuspended in 10 ml washing buffer. The centrifugation step was repeated and cell pellets were resuspended and incubated in 2 ml lysis buffer (s. appendix) for 3 min at RT with agitation, in order to eliminate erythrocytes. Cell suspensions were then washed with 20 ml D-PBS Ø CaMg/0,1%BSA and cell numbers as well as cell viability was determined.

Cell suspensions of each mouse were adjusted to $1,7x10^6$ cells/ml with lung cell culture medium (s. appendix) and cultured in aliquots of 1 ml in 24-well culture plates supplemented with 44.5 µg/ml OVA (1 µM) for restimulation at 37°C and 5% CO_2. After 3 days of culture, cell suspensions were harvested, centrifuged for 5 min at 350 x g at RT and cell-free SN were stored at -20°C for further analysis.

2.2.1.5 Human lung epithelial cell line

The 16HBE14o− cell line was used to investigate effects of human chymase and SN of hLMC on the epithelial cell integrity. 16HBE14o cells were developed from human bronchial epithelium by transfection of primary cultured epithelial cells with the pSVori- plasmid. This cell line represent differentiated epithelial cells with regard to morphology and functions and provides a valuable resource for studying different aspects of human airway cell biology[90]. 16HBE14o cells were cultured at a density of 7,5 x 10^4 cells/cm^2 in DMEM medium (high glucose, 2mM Glutamine) with addition of 10% FCS.

2.2.2 Cell activation *in vitro*

2.2.2.1 Chemotaxis assay

PMN chemotaxis was determined in a 48-well micro chemotaxis chamber (Boyden-Chamber, s. equipment) according to the method of Ludwig *et al*[91]. In this assay, neutrophils migrate from the upper compartment of the chamber through a polycarbonate filter membrane with defined pore size towards the lower compartment, which contains the chemotactic stimulus. Polycarbonate filter membranes used in this assay had a smooth hindering adhesion and a rough side which facilitated cells to adhere to the filter. Filter membranes were incubated first in 96% ethanol for 10 min, followed by a second incubation in 1 M ethanolic NaOH solution for 10 min. Filter membranes were then washed 3 times with distilled water (each time for 10 min), equilibrated to 0,1M chemotaxis-phosphate buffer (s. appendix) and dried on air. Micro chambers were blocked for 1h at 37°C with chemotaxis blocking buffer (s. appendix) and dried in an incubator for 20 min at 60°C. To avoid stimulus evaporation in the wells, chambers were then placed on ice before use. Increasing concentrations of human chymase (0.46 U/ml, 0.17 U/ml, 0,056 U/ml, 0,018 U/ml, 0,006 U/ml; Enzo life science) were put in the lower wells. Positive controls received fMLP (3nM) instead of chymase while negative controls contained only PBS. Parallel samples were supplemented with 10 µM chymostatin in addition to the stimuli. Chambers were sealed by the filter membrane with the smooth side toward stimuli, mounted to the upper chambers and incubated for 30 min at 37°C in humidified atmosphere. PMNs ($2x10^6$ cells/ml) were preincubated for 10 min at 37°C. Subsequently, $CaCl_2$ and $MgCl_2$ were added to the PMN cell suspension to a final concentration of 0,132 mg/ml and 0,1 mg/ml, respectively. PMN cell suspension (50 µl/well) was pipetted in to the upper wells following incubation for 1h at 37°C in humidified atmosphere. After incubation, cells migrated into the lower chamber (25 µl) were transferred to a microtiter plate and lyzed with 25 µl of 0,2% Hexa-decyl-tri-methyl-ammonium-bromide. Lysates were serially diluted and myeloperoxidase enzyme activity was visualized by addition of 50 µl/well TMB substrate solution. The enzymatic reaction was stopped after 10 min by adding 50 µl/well of 1 M H_2SO_4 to the samples and absorption was determined in an automated spectrophotometer (lambda= 405 nm; s. equipment). Numbers of migrated cells were calculated by means of a standard of lyzed cells run in parallel.

2.2.2.2 Activation of human lung mast cells

Human LMC were activated by crosslinking of FcεRI-bound IgE. Therefore, cells were incubated with 0,5 µg/ml human IgE for 18 h at 37°C and 5% CO_2. After removal of unbound IgE by centrifugation (10 min, 300 x g, RT), cells were resuspended in MC-stimulation medium ($3x10^6$ cells/ml) and activated by the addition of 3 µg/ml anti-IgE for 30-45 min at 37°C and 5% CO_2. Subsequently, cell suspensions were centrifuged for 10 min at 450 x g and SN were collected and stored at -20°C for further experiments.

MC degranulation

Degranulation of MC was assessed by determination of chymotryptic enzyme activity released into the cell free SN. For measurement of the chymotryptic activity, 50 µl hLMC SN or human chymase (1 U/ml) as a control, were combined with 50 µl chromogenic chymase substrate solution (Suc-Ala-Ala-Pro-Phe-p-NA, 20mM, sigma) and time kinetics were performed over 15 min. Absorbance was recorded at 410 nm every minute by an automated spectrophotometer. MC stimulation medium served as a negative control. Enzyme activity of the same samples was tested in parallel in presence of 10 µM (f.c.) chymase inhibitor chymostatin. Chymotryptic substrate turn-over in U/ml was calculated from the resulting mean absorbance in OD according the Lambert Beer principle using following formula:

$$c = A/\varepsilon \times b$$

$$c = A/\varepsilon \times b * (\text{reaction volume/sample volume}) = \text{U(µmol/min)/100µl}$$

$$c = A/\varepsilon \times b * (\text{reaction volume/sample volume}) *10 = \text{U(µmol/min)/ml}$$

c → substrate turnover U(µmol/min)
A → delta OD (absorbance/min)
ε → molar attenuation coefficient
b → path length
reaction volume → 0,1ml
sample volume → 0,025ml

2.2.2.3 Determination of the epithelial cell integrity

Epithelial cell integrity in response to different stimuli was analyzed by real time electrical impedance monitoring using the xCELLigence system. Microtiter plates with microelectrodes at the bottom of the wells (E-plates) detect an intact monolayer of cells as a constant high cell index (CI). Any changes affecting the intact cell monolayer like alteration of the morphology or detachment from the plate are recorded as a decrease of CI.

The 16HBE14o− cell line was used to investigate effects of human chymase and hLMC SN on the epithelial cell integrity. Cells were seeded (100 µl, 0.56 x10^6 cells/ml in 16HBE14o culture medium) on a 96-well E-plate and placed in the xCELLigence system for 24 h at 37°C/5% CO_2 to form a monolayer with a corresponding constant high CI. Culture medium was then aspirated and replaced by 100 µl MC stimulation medium containing 1 U/ml human chymase or hLMC SN in the presence or absence of 10 µM chymase inhibitor chymostatin. MC stimulation medium alone served as a negative control. Incubation was continued for 20 h at 37°C/5% CO_2 and CI were recorded real time. Data were processed by the RTCA software and results were exported to Microsoft Office Excel 2007 followed by analysis in GraphPad prism 5.0. To discriminate between morphological changes and cell loss by detachment, cell numbers were determined by their content of ß-hexosaminidase. For this purpose, SN were aspirated and remaining adherent cells in E-plates were washed twice with 150 µl/Well D-PBS with CaMg and lyzed in 75 µl 0.1% Triton X-100 for 30 min at 37°C under agitation and cleared by centrifugation for 10 min at 450 x g at RT. SN (50 µl) from each well were transferred to a new microtiter plate and combined with 50 µl ß-hexosaminidase substrate solution (s. appendix). After 40 min of incubation at 37°C in a humidified chamber, reaction was terminated by addition of 50 µl/well basic stop solution. Absorption was determined in an automated spectrophotometer at a wavelength of 405 nm. Numbers of adherent cells were calculated by means of a standard of lyzed cells run in parallel.

2.2.3 Animals

2.2.3.1 Mice origin and keeping

Three different mouse strains, were used to analyze the role of MCs and chymase mMCP-4. Female mice were kept in individually ventilated cages under specific pathogen free conditions

and used at ages of 6-12 weeks. All animal experiments in this study were approved by the Animal Ethics Board of the Ministry of Environment, Kiel, Germany (Az. 99-8/14).

C57BL/6-mice and MC-deficient C57BL/6-*kit*$^{W\text{-}sh/W\text{-}sh}$ -mice were bred in the animal facility of research center Borstel, Germany. mMCP-4$^{-/-}$(*Mcpt-4*$^{-/-}$) -mice are on a C57BL/6 genetic background and deficient in chymase mMCP-4. Breeding pairs of these mice were kindly provided by our collaboration partner, Prof. Simon P. Hogan (Cincinnati Children´s Hospital, Cincinnati USA) and were bred and kept in the animal facility of research center Borstel, Germany.

2.2.3.2 Mice genotyping

C57BL/6-*kit*$^{W\text{-}sh/W\text{-}sh}$ -mice were characterized by the Animal Facility of Research Center Borstel. For genotyping of mMCP-4$^{-/-}$-mice, DNA was obtained from ear-biopsies of mice. DNA was extracted and prepared from tissues by using commercially available kit (Dneasy 96 Blood & Tissue Kit, Qiagen) following the recommendations of the manufacturer. Amplification of isolated DNA was performed using primer 200 and primer 202 for mMCP-4$^{-/-}$ (440 bp) and primer 201 and primer 202 for mMCP-4$^{+/+}$ littermates (850 bp). For the PCR reaction, a mastermix was prepared as followed using Dream Taq DNA-Polymerase-Kit (s. ready to use kits):

Mastermix:

0,2 µl	primer 200 (20 µM)
0,2 µl	primer 202 (20 µM)
1,25µl	Dream Taq Puffer (incl. $MgCl_2$) (10 x)
1,25µl	dNTPs (2 mM)
7,5 µl	H2O
0,5 µl	DNA

The PCR amplification reactions were run according the following program:

PCR Program:

		94°C – 5 min
50x	{	94°C – 45 sec
		57°C – 45 sec
		72°C – 45 sec
		72°C – 5 min
		4°C – ∞

Agarose gel electrophoresis

The PCR products were supplemented with DNA gel-loading buffer (6x) and 5 µl of 100 bp DNA-standard were loaded on 4% agarose gels. Electrophoresis were run for 40 min 100 V and fragments were visualized in stained gels (10µl Roti®-Safe GelStain) under UV light.

2.2.4 Experimental asthma

2.2.4.1 Immunization protocol

The role of MC and MC-chymase mMCP-4 was investigated in an alum-free chronic model of asthma according to a method described by Yu *et al*[92], with changes. Mice were sensitized by three intraperitoneal (i.p.) injections of 50 µg OVA in 100 µl D-PBS on days 1, 4, and 7, while control mice received PBS alone. At day 12, all mice were challenged oropharyngeally with 50µl of 1,5% OVA (in D-PBS). During challenge, mice were anesthetized by inhalation of sevofluran. Challenge was repeated weekly for 9 weeks (Fig. 4) and 24h after the last exposition lung function measurment for the assessment of AHR was performed. Mice were then scarified and BAL, sera and lung tissue were collected for analysis of airway inflammation, mucus production and cytokine production.

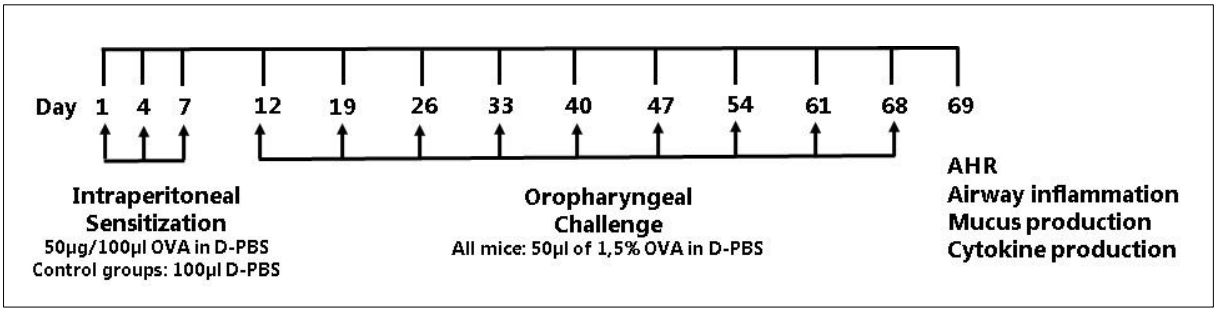

Fig.: 4 Chronic asthma model. Sensitization was induced by three times i.p. injection of OVA, Control mice received only D-PBS. Challenge started at day 12 and was repeated weekly for 9 weeks. At day 69, AHR was assessed and BAL, blood and lung tissue was collected for further analysis.

2.2.4.2 Engraftment of MCs in mast cell deficient mice

C57BL/6-*kit*$^{W\text{-}sh/W\text{-}sh}$ -mice have a phenotype of MC-deficiency together with other anomalies effecting other cell types. To discriminate the outcome of the experiment in MC-dependent and -independent effects, it was necessary to reconstitute MC in this mouse strain in some experimental groups.

In order to engraft MCs in lung tissue of MC-deficient C57BL/6-*kit*$^{W\text{-}sh/W\text{-}sh}$ -mice, BMMCs were generated from bone marrow cells of C57BL/6- and mMCP-4$^{-/-}$-mice as described in section 2.2.1.3 above. Each MC-deficient animal received an injection of 2x10^6 BMMCs in a volume of 100 µl D-PBS intraperitoneally as well as 5x10^6 BMMCs in a volume of 200 µl D-PBS intravenously into the tail vein. MC-deficient mice were engrafted either with BMMCs derived from C57BL/6- or mMCP-4$^{-/-}$-mice. Reconstituted mice were used 9 weeks after BMMC injection for further experiments.

2.2.4.3 Lung function measurement

AHR is an essential feature of asthma. AHR is defined as an inadequately increased response of the airway smooth muscle to bronchoconstricting stimuli, which leads to limitation of air flow. Stimuli inducing bronchoconstriction can be of natural or pharmacological origin and act either indirect (e.g. allergens) or direct (e.g. histamine and methacholine) on airway smooth muscle cells. The latter group of stimuli is also used for clinical diagnosis. In animal models, the most frequently used bronchoconstrictor is methacholine. It acts directly on muscarinic receptors (type M3) on the smooth muscle cell membrane[93]. In this study, AHR in response to methacholine was assessed by invasive measurement of lung function using the FinePointe-Buxco system. Mice were anesthetized by intraperitoneal injection of a solution made out of 100 mg/kg Ketamin (100 mg/ml) and 20 mg/kg Xylasin/Rompun (20 mg/ml) per 100 g body weight. Animals were tracheotomized with a small canule linked via an adaptor to the mechanical ventilation system. Body temperature of mice was kept to 37°C throughout the process. Subsequently, an i.p. injection of 50 µl Pancuronium bromide (10 mg/ml) as a muscle relaxant was employed to the mice. Mechanical ventilation was run continuously throughout the measurement. Lung function measurement was started with nebulized D-PBS to set a baseline for the resulting lung resistance, followed by stepwise increased doses of nebulized methacholine (MCh) from 0,78125 mg/ml → 1,5625 → 3,125 → 6,25 → 12,5→ 25 → 50 to 100 mg/ml. Airflow and transpulmonary pressure in response to MCh inhalation were recorded and analyzed with the FinePointe Review software 2.3.1.0 continuously up to 45 minutes and pulmonary resistance (R_L, cm H_2O/ml/s) was calculated.

2.2.4.4 Bronchoalveolar lavage (BAL)

BAL was collected for the analysis of cell infiltrates and proteins from lung lumen. After lung function measurement, the mouse lung was lavaged. PBS supplemented with proteinase inhibitors (1 ml, cold; 1x complete^{TM} Mini, Roche) was applied into the lung through the canule placed in the trachea and BAL was collected in 2 ml tubes. Total numbers of BAL cells were determined in a neubauer chamber by trypan blue exclusion. BAL cells were then centrifuged for 5 min at 500 x g at 8°C and SN were collected and stored at -20°C for further analysis. Cell pellets were resuspended at a density of $0{,}5x10^6$ cells/ml in D-PBS with 30% FCS.

2.2.4.5 Differential BAL cell count of leukocytes

For cytospin preparations,150 µl cell suspension derived from BAL were centrifuged on a slide with a cytospin-centrifuge for 7 min at 700g at RT. Determination of cell types and cell numbers were performed after polychromatic May-Grünwald-Giemsa-staining. Cell populations were evaluated according to their color and cellular morphology. For this purpose, slides were incubated for 6 min in May-Grünwald staining solution and subsequently rinsed in distilled water. Thereafter, slides were counterstained for 20 min in Giemsa-solution (1:15 diluted in distilled water) and rinsed twice for 10 s with distilled water and dried on air. For differential BAL cell count of leukocytes, 300 cells per slide were evaluated by bright field microscopy.

2.2.4.6 Collection and preparation of blood samples

For preparation of serum, blood samples were collected from abdominal aorta of each mouse, transferred to serum-separating tubes (SST) and incubated for 30 min at RT to allow coagulation. Subsequently, SST-Tubes were centrifuged for 3 min at 14000 x g at 8°C. Cleared SN were transferred to new tubes and stored at -20°C for further analysis.

2.2.5 Analysis of BMMC by flow cytometry

Flow cytometry or fluorescence-activated cell sorting (FACS) is a frequently used technique in research laboratories as well as clinical medicine and biology. This tool facilitates the analysis of certain cell populations by measurement of the physical properties of single cells in a stream of fluid, such as size (provided by forward scatter channel (FSC)) and internal complexity (provided by side scatter channel (SSC)) with help of their optical and fluorescence

characteristics. Additionally, different cell populations can be characterized and purified by analyzing specific antigens or proteins on their cell membranes or inside the cells using conjugated antibodies to fluorescent dyes. Lasers excite the fluorescent molecules on labeled cells to a higher energy state. After the electrons return to their ground state, fluorochrome molecules emit light energy at higher wavelengths, that is recorded by the instrument software as events. Single cells sharing same characteristics are then visualized together and can be purified as a cell population. Single cell populations are useful in experimental studies, therefor FACS can be a suitable procedure to purify cell populations of known phenotype[94].

BMMC were stained with three different fluorescent-labeled antibodies directed against CD117 (c-kit, PE), T1/ST2 (IL-33 receptor, FITC), and FcεRIα (Percp/Cy5.5). Cell suspensions ($5x10^5$ cells/200 µl) in D-PBS/0,1% BSA were centrifuged for 3 min at 1600 x g at 4°C. Pellets were incubated for 10 min at 4°C in Fc-Block TruStain fcX (1:1000, anti-mouse CD16/32), to reduce unspecific binding, and in LIVE/DEAD Blue (1:1000), to exclude death cells. After washing in 100 µl/well FACS-staining buffer (s. appendix) and centrifugation for 3 min at 1600 x g at 4°C, each sample received a combination of all three antibodies diluted in FACS-staining buffer, to a final concentration of 5 µg/ml for each antibody. In parallel, unstained cells and Fluorescence-minus-one (FMO) served as control. For FMO controls, samples were stained only with two of the respective antibodies to calculate unspecific fluorescent signal spillover for the third color. After 10 min incubation at 4°C in the dark, again samples were washed as described above. FACS-fixation buffer (100 µl/well; s. appendix) was added and samples were incubated for further 10 min in the dark at RT. After a final washing step, pellets were resuspended in 200 µl/well FACS-staining buffer, transferred in small FACS-tubes and stored at 8°C in the dark before measurement in flow cytometer LSRII.

Flow cytometry data analysis

Fluorescence intensities as well as forward and side scatter intensities were quantified by BD LSR II Flow Cytometer and recorded by FACSDiva software. Data (FCS files, 3.0 version) were further analyzed by FlowJo software (version V10.2). The gates were set by including Fluorescence-minus-one (FMO) controls for all fluorescence channels. Spectral overlap (spillover) between the emission spectra of three fluorochromes was reduced by fluorescence compensation.

2.2.6 Immunochemical methods

2.2.6.1 OVA-specific IgE ELISA

Immunoglobulin E (IgE) is produced by plasma cells and directed against a specific antigen or allergen. Allergen specific IgE levels can be measured in sera to determine an efficient sensitization by *enzyme-linked Immunosorbent Assay* (ELISA). Here, a mouse OVA-specific IgE ELISA kit (LEGEND MAX™; s. ready to use kits) was used, according the manufacturer's instructions. Briefly, sera were incubated in an OVA pre-coated plate to capture OVA-specific IgE. By adding a biotinylated detection antibody directed against murine IgE a „*sandwich complex*" was built. Finally, an avidin-horseradish peroxidase solution (avidin-HRP D) followed by incubation with a chromogenic substrate was used for quantitative determination of OVA-specific IgE and absorption was determined in an automated spectrophotometer at a wavelength of 450 nm. A serial dilution of an IgE solution with defined concentrations run in parallel, was used as a standard for calculation of IgE levels in the samples.

2.2.6.2 Determination of cytokines in SN of lung cells

Analysis of cytokines in SN of restimulated lung cells was performed by using the 13-plex LEGENDplex™ assay kit, according to the instructions of the manufacturer. This multiplex consists of an assay panel of fluorescence–encoded beads which can be detected by flow cytometry. It allows the simultaneous quantification of 13 different mouse cytokines, including IL-2, 4, 5, 6, 9, 10, 13, 17A, 17F, 21, 22, IFN-γ and TNF-α. Similar to a sandwich ELISA, each bead set used in this assay was conjugated with a specific antibody on its surface for capturing a specific cytokine. Cytokine-specific beads were identified in the flow cytometer according to their size and an intrinsic fluorescence signal. SN derived from lung cell cultures were incubated with a mixture of capture beads for 2 h at RT under agitation. After a washing step, a cocktail of cytokine specific antibodies was added to each sample. Bound antibodies were visualized by addition of Streptavidin-phycoerythrin (SA-PE). Samples were measured in a LSRII flow cytometer. Cytokines-specific beads were distinguished by forward - (FSC) and side scatter (SSC) and further by the PE fluorescent signal intensity. Concentrations of individual cytokines were calculated according to respective standard samples running in parallel using a software provided by Biolegend. Further analysis of data was made by Microsoft office excel version 2007 and GraphPad prism version 5.0.

2.2.7 Histological methods

2.2.7.1 Preparation of paraffin lung sections for histology

Left lung lobes were continuously filled with 4% paraformaldehyde solution in PBS (PFA) for 20 min. Lung tissues were then placed in a bottle with 4% PFA for 24 h for further fixation. Thereafter, lung tissues were further processed for histological analysis. First, lung tissues were placed horizontally in a 2% agar-agar solution, facing with the dorsal site upward and stored for 4h at 4°C. Next, lung tissues were sliced in parallel cuts of 2 mm, according to the *systematic uniform random sampling* (SURS) method[95,96]. The slicing direction was organized randomly using a randomization table. This method enables a statistically uniformed analysis and quantification of all parts of the lung tissue with the same probability. All slices were placed with the same orientation in an embedding cassette in 4% PFA solution. Samples were dehydrated in an automatically controlled process of ascending ethanol series and subsequently embedded in paraffin. Paraffin embedded lung sections were further cut with a microtome in slices of 2 µm thickness, placed on a slide and dried on a hot plate for a minimum of 30 min at 37°C before staining. Slices made by randomized cutting were collected together on one slide for each mouse respective.

2.2.7.2 PAS staining of lung sections

For quantification of mucus and mucus containing goblet cells, paraffin embedded lung sections were stained with Periodic acid-Schiff and counterstained with hematoxylin II solution according Gill (1:5 diluted in distilled water). Periodic acid oxidizes carbohydrate macromolecules found in mucus to aldehydes. These aldehydes then react with the Schiff reagent and mucus appears in a purple-magenta color. In a first step, specimens were deparaffinized using Roticlear solution (2x for 10 min) and rehydrated in a descending ethanol series (100 %, 96 % and 70 % ethanol) for 1 min in each solution. Next, sections were incubated in 0,5% periodic acid for 10 min, floated with tap water for 3 min and afterwards rinsed with distilled water. Subsequently, lung sections were incubated in Schiff reagent for 15 min, floated with tap water and afterwards rinsed with distilled water. Thereafter, lung sections were counterstained in hematoxylin II solution for 1 min, rinsed with tap water and dehydrated in an ascending ethanol series (70%, 96% and 100% ethanol) for 1 min in each solution. After incubation for 15 min with Roti-clear, slides were covered with histomount mounting medium and mounted with cover slip. Mucus, mucus containing goblet cells and inflammatory cells

were quantified in PAS stained lung sections using Olympus Bx61 light microscope (Camera Olympus Dp72) and *computer assisted stereological toolbox* software (newCAST).

2.2.7.3 Computer-based stereological analysis

Mucus, mucus containing goblet cells, and inflammatory cells were quantified in PAS stained lung sections using light microscope connected to a camera and controlled by newCAST software. The newCAST software enables stereological quantification of lung sections. The respective cell populations were counted on captured images with help of defined points, lines and counting frames. Images were framed and a percentage of the framed area which had to be analyzed was defined in the software. Subsequently, the software selected randomly different area and these captured images were shown to the viewer for the counting[95,96]. The viewer could then count the points emerged on mucus (P_{muc}), bronchial epithelium (P_{bep}) and inflammatory cells (P_{Inf}). The number of points on each object is proportional to the volume. Line were counted by intersections with goblet cells (I_{gc}) or PAS-negative bronchial epithelium (I_{bep}). The resulting values of the counting could then be used in different formulae to calculate the following parameters:

Unit area goblet cells per total epithelium in percentage:

$$\frac{I_{gc}}{I_{gc}+I_{bep}} \ (\%)$$

I_{gc} → Lines counted by intersections with goblet cells (I_{gc})

I_{bep} → Lines counted by intersections PAS-negative bronchial epithelium (I_{bep})

Mucus per unit area of basal lamina in $\mu m^3/\mu m^2$

$$\frac{1}{P} \times \frac{\Sigma P_{muc}}{2x \Sigma (I_{gc}+I_{bep})} \ (\mu m^3/\mu m^2)$$

$\sum P_{muc}$ → The sum of all points emerged on mucus (P_{muc})

$\sum I_{gc}$ → The sum of all lines counted by intersections with goblet cells (I_{gc})

$\sum I_{bep}$ → The sum of all lines counted by intersections PAS-negative bronchial epithelium (I_{bep})

l/P → Line lengh (depending on the magnification)

Inflammatory cells per unit area of basal lamina in cells/µm^2

$$\frac{1}{P} \times \frac{\Sigma P_{ez}}{2x \Sigma (I_{gc} + I_{bep})} (\mu m^3/\mu m^2)$$

$\sum P_{ez} \rightarrow$ The sum of all points emerged on inflammatory cells (P_{Inf})

2.2.7.4 Toluidine blue staining of lung sections

Toluidine blue staining was performed for the detection of MCs in lung sections. Toluidine blue is a basic metachromatic dye with high affinity to acidic tissue components. The blue dye attaches glycosaminoglycan (heparin) and stains MCs in purple metachromatic color[97]. Paraffin lung sections were first deparaffinated by incubation in 100% xylol (3x 10min) and 100% ethanol (2x 3 min) followed by 3 min incubation in decreasing concentrations of ethanol (96%, 80%, 70%, 50%). Next, lung sections were stained for 1h at RT with freshly prepared toluidine blue staining solution (1,6 g toluidine, 15,36 g Citric acid and 800 ml 50% ethanol). After incubation, slides were shortly incubated two times in 100% ethanol followed by 3 incubation steps in 100% xylol for 10 min each. Subsequently, slides were mounted in Roti Histokit II with cover-slip and dired on air. Stained lung tissue slides were analyzed in a bright field microscope (Olympus BX41) and images were taken with an associated Nikon camera (Nikon DS-Ril).

2.2.8 Statistical analysis

Statistical analysis was performed with GraphPad Prism 5.0. using either unpaired two-tailed student t test (Mann-Whitney Test) or Two-way ANOVA. Statistical tests including significance level (p value), sample size (n) and percentile of boxplots are described in detail for each analysis in the chapter “results”.

3 Results

The aim of this study was to investigate the role and function of chymase in chronic experimental asthma. The idea behind this work was based on the hypothesis that chymases released from activated mast cells have regulatory functions and affect the allergic inflammation by recruitment of neutrophils, but also by damage and remodeling of the lung epithelium. For this purpose, as a first step the role of chymase in neutrophil chemotaxis and its effects on epithelial cell integrity was examined *in vitro*. Complementary to the *in vitro* studies, a chronic asthma model was performed to analyze the role of chymase in the pathophysiology of allergic asthma *in vivo*.

3.1 Effect of chymase on neutrophil chemotaxis

Neutrophils have been shown to play an essential role in models of allergic asthma. Since mast cell chymase has been considered as pro-inflammatory in many pathological situations, in a first approach the capacity of the protease to activate neutrophils directly was investigated. The role of chymase in recruitment of neutrophils was analyzed in a neutrophil chemotaxis assay. For this purpose, neutrophils were isolated from whole blood of healthy volunteers (n=5) and neutrophil chemotaxis was then determined in micro-chemotaxis chambers according to the method of Ludwig et al[91]. Neutrophils were placed in the upper compartment and exposed to increasing concentrations of human chymase placed in the lower wells. fMLP (3nM) served as positive control while the negative control received PBS. In addition, stimuli and control were tested in presence of 10 µM chymase inhibitor chymostatin. After 1h incubation at 37°C, migrated cells in the lower chamber were determined by their content of endogenous myeloperoxidase enzyme. Enzymatic activity of human chymase and its sensitivity to chymostatin was confirmed in a chymotryptic activity assay (data not shown). As compared to fMLP which induced the migration of approximately 30% of total cells, chemotaxis induced by chymase appeared to be rather weak with a maximum of 7 % migrated cells at 0.46 U/ml enzyme activity (Fig. 5). Although the amount of chymostatin used in the experiment was sufficient for a complete inhibition of the enzyme activity (data not shown), only a partial reduction of chymase-induced chemotaxis was observed.

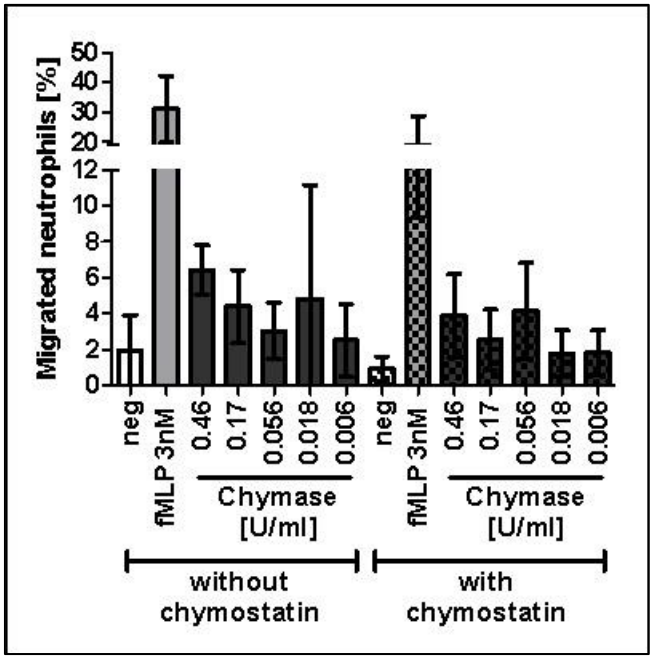

Fig. 5: Effect of chymase on neutrophil chemotaxis. Neutrophils were isolated from human blood samples. Neutrophil chemotaxis was analyzed in presence of increasing concentrations of human chymase. PBS served as negative control (neg) whereas fMLP (3nM) was used as positive control. Data are presented as mean ± SD of 5 independent experiments.

3.2 Effect of chymase and mast cell supernatants on epithelial cell integrity

Beside the direct activation of effector cells, chymase may drive inflammatory processes also by affecting the function of barrier cells. Groschwitz *et al.* have shown that human chymase can regulate intestinal epithelial barrier homeostasis by increasing epithelial permeability and decreasing the expression of tight junction proteins[83]. In this study effects of human chymase and supernatants of activated human lung mast cells (hLMC) on lung epithelial cell integrity was analyzed by real time electrical impedance measurement using the xCELLigence system. An intact monolayer of epithelial cells is detected by the xCELLigence system as low impedance which is expressed as a constant high cell index. A decrease of the CI can be induced by alteration of the cells such as morphological changes or detachment from the plate.

In a first experiment, it was analyzed whether chymotryptic activity is present in SN of hLMC. The enzymatic activity of 4 different hLMC SN was determined in a chymotryptic activity assay with human chymase as positive control. hLMC stimulation medium (s. appendix) served as negative control. In addition, same conditions were analyzed in presence of chymase inhibitor chymostatin. Chymotryptic activity was present in SN of stimulated hLMC and could be completely inhibited in presence of chymostatin (Fig. 6).

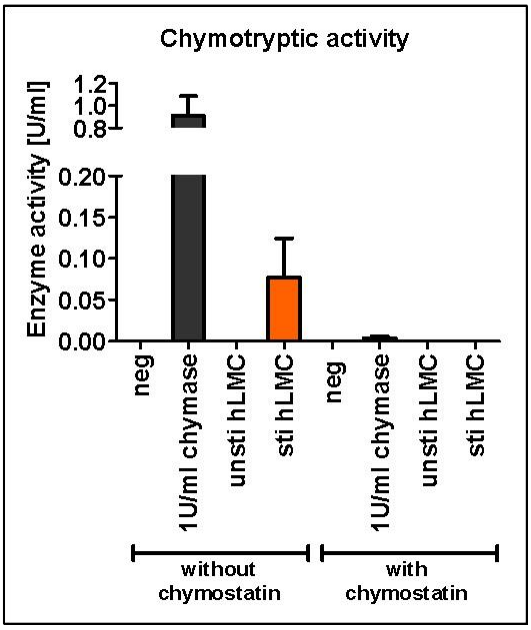

Fig. 6: Supernatants of activated human lung mast cells show chymotryptic activity. hLMC ($3x10^6$ cells/ml) received 0,5 µg/ml human IgE and 3µg/ml anti-IgE for stimulation. Enzymatic activity was determined in SN derived from stimulated and unstimulated hLMC. Human chymase (1U/ml) was used as positive control whereas hLMC stimulation served as negative control. Chymotryptic substrate turn-over was recorded in time kinetics over 15 min. Data are presented as mean ± SD of results obtained with 4 different hLMC cultures.

After confirmation of a relevant chymotryptic activity in activated hLMC, human epithelial cells (16HBE14o− cell line) were cultured with SN of activated hLMC (Fig. 7A) or 1 U/ml human chymase (Fig. 7C) in presence and absence of 10 µM chymase inhibitor chymostatin. SN of unstimulated hLMC and medium served as negative controls. Activated hLMC decreased the barrier integrity of epithelial cells after 3h up to 10% which remained stable at this level (Fig. 7A). Human chymase showed a stronger effect starting directly after incubation, where the CI was continuously decreasing reaching 15% after 3h and 30% after 7h of incubation (Fig. 7C). These effects were completely reversed in presence of chymostatin to the levels of the negative controls. To discriminate between morphological changes and cell loss by detachment, cell numbers were determined by their content of ß-hexosaminidase at the end of the experiment. For this purpose, remaining adherent cells were lyzed and numbers of adherent cells were calculated by their content of endogenous ß-hexosaminidase (Fig. 7B/D). After 24h epithelial cells showed ~10% fewer adherent cells after incubation with SN of activated hLMC compared to negative controls which was recovered in presence of chymostatin. Human chymase decreased the number of adherent cells up to 52% which could be reversed to 65% in presence of chymostatin. According to the obtained results human chymase from activated

hLMC can impair the epithelial integrity and induces detachment of cells depended on chymase doses.

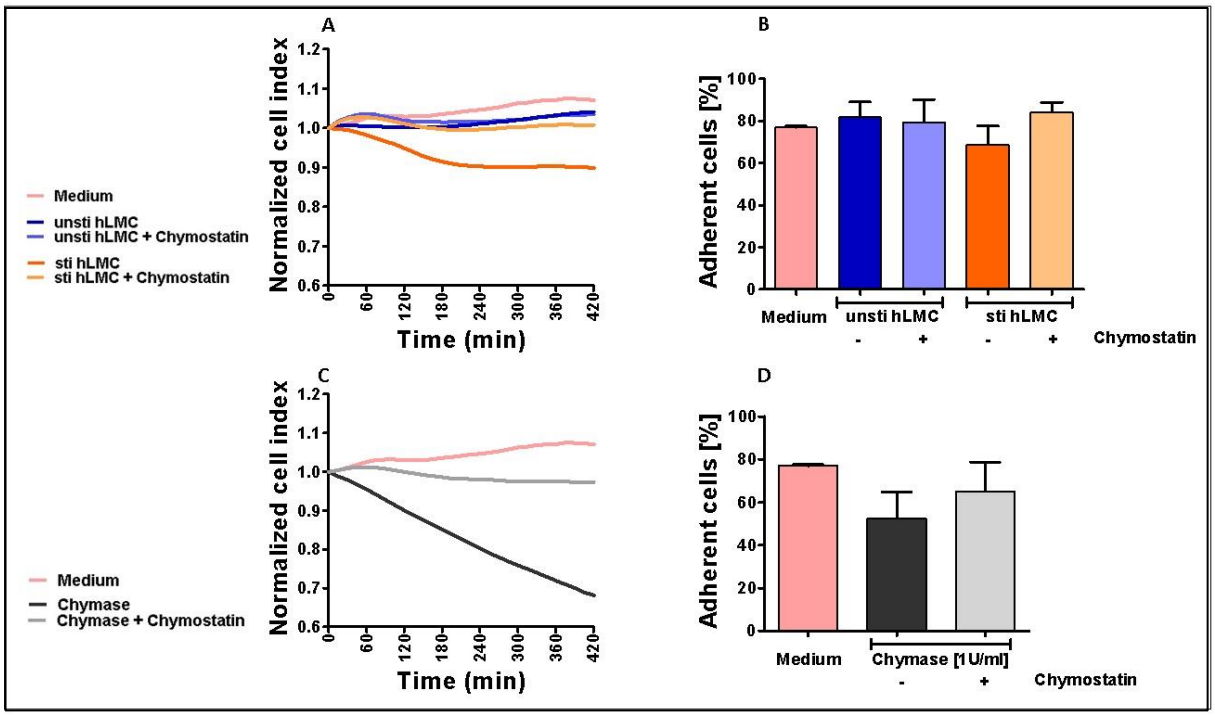

Fig. 7: Supernatants of activated mast cells and chymase impair epithelial cell barrier integrity. Human lung epithelial cells (16HBE14o− cell line; 0.56 x10^6 cells/ml, 100µl per well) were incubated with supernatants of unstimulated hLMC (containing no detectable chymase activity) or stimulated hLMC (containing 0.06 U/ml chymotryptic activity) (A). Alternatively, epithelial cells were treated with 1 U/ml chymase (C). All experiments were performed either in the absence or presence of 10 µM chymostatin. Effects on barrier cells were determined by impedance measurement (A, C), normalized to a starting point by constant high CI after incubation with compounds. Data are shown as CI mean of 4 different hLMC cultures (A) or chymase (C) treated epithelial cells in time per min. Cell detachment was determined after 24h of incubation with hLMC-SN (B) or chymase (D) and expressed as residual adherent cells. Data are presented as mean ± SD of 4 different hLMC cultures (B) or chymase (D) treated epithelial cells.

3.3 The role of chymase mMCP-4 in chronic experimental asthma

Although chymase is generally seen as a pathogenic driver in many inflammatory processes[67–69,82,83], Wearn *et al.* described a protective function of chymase mMCP-4 in experimental asthma using mMCP-4 ko mice[76,77]. However, results in this study were derived from an acute model of the disease, in which potential effects of the enzyme on long term regulatory processes like chronic inflammation and tissue remodeling were not taken into consideration. Therefore, here the role of chymase mMCP-4 was investigated by using mMCP-4-deficient mice in a chronic model of asthma, originally described by Yu et al[92]. Since in conventional ko-strains

the protein of interest is absent in all cells and tissues during the entire lifespan of the animal, it may be difficult to address the role of this molecule in a specific cell type or to an observed disease phenotype. For example, the outcome of a phenotype in a disease model may be not due to a direct participation of the molecule in the disorder but could be a consequence of disturbed embryogenesis which would affect many regulatory processes. In order to circumvent this problem, additional experiments using MC-deficient C57BL/6-*kit*$^{W\text{-}sh/W\text{-}sh}$-mice (W-sh) reconstituted either with wild type C57BL/6 (W-sh + *wt* MC) BMMC or BMMC derived from mMCP-4$^{-/-}$ (W-sh + ko MC) animals were performed.

Mice groups		**Sensitization**	**Challenge**
C57BL/6(*wt*)	**control**	**PBS**	**OVA**
C57BL/6 (*wt*)		**OVA**	
mMCP-4$^{-/-}$(ko)	**control**	**PBS**	
mMCP-4$^{-/-}$ (ko)		**OVA**	
C57BL/6-*kit*$^{W\text{-}sh/W\text{-}sh}$	**control**	**PBS**	
C57BL/6-*kit*$^{W\text{-}sh/W\text{-}sh}$		**OVA**	
C57BL/6-*kit*$^{W\text{-}sh/W\text{-}sh}$ +wt MC	**control**	**PBS**	
C57BL/6-*kit*$^{W\text{-}sh/W\text{-}sh}$ +wt MC		**OVA**	
C57BL/6-*kit*$^{W\text{-}sh/W\text{-}sh}$ +ko MC	**control**	**PBS**	
C57BL/6-*kit*$^{W\text{-}sh/W\text{-}sh}$ +ko MC		**OVA**	

The experimental setting chosen here does not only allow the investigation on the role of mMCP-4 in chronic experimental asthma in general but enables the specific determination of the function of mMCP-4 in MC and its discrimination from other MC-related effects.

In the performed chronic model mice were sensitized by three intraperitoneal (i.p.) injections of OVA on days 1, 4 and 7, while control mice received PBS alone. At day 12, all mice were challenged oropharyngeally with OVA. Challenge was repeated weekly for 9 weeks and 24h after the last challenge lung function measurment for the assessment of AHR was performed. Mice were then sacrificed and BAL, sera and lung tissue were collected for analysis of airway inflammation, mucus production and cytokine production.

3.3.1 Generation of BMMC

BMMC for the reconstitution of MC-deficient mice were generated from bone marrow cells of C57BL/6 (*wt*) as well as mMCP-4$^{-/-}$ mice (ko) and cultured in presence of 10 ng/ml mSCF and 5 ng/ml mIL-3. After 5 weeks of culture, cell suspensions were analyzed for purity by the expression of Mc-specific cell surface receptors c-kit, FcεRIα and IL-33r. Therefore, cells were stained with fluorescent-labeled antibodies directed against CD117 (c-kit, PE), T1/ST2 (IL-33 receptor, FITC) and FcεRIα (Percp/Cy5.5) and analyzed by flow cytometry. Compensation was set up with help of FMO control. First, a cell population containing all intact cells was identified and selected based on size and internal complexity depicted in the forward-side scatter diagram. Cell debris and dead cells which appeared as distinct population in the lower left quadrant were excluded from further analysis (Fig. 8A/D). Cell populations were further selected based on T1/ST2- and FcεRIα-expressing cells (Fig. 8B/E). Finally, MC were identified by gating on CD117-expressing cells (Fig. 8C/F). BMMC cultures were all positive for the characteristic cell surface receptors and contained over 95% pure MC (*wt*: 95,7%, ko: 97,5%).

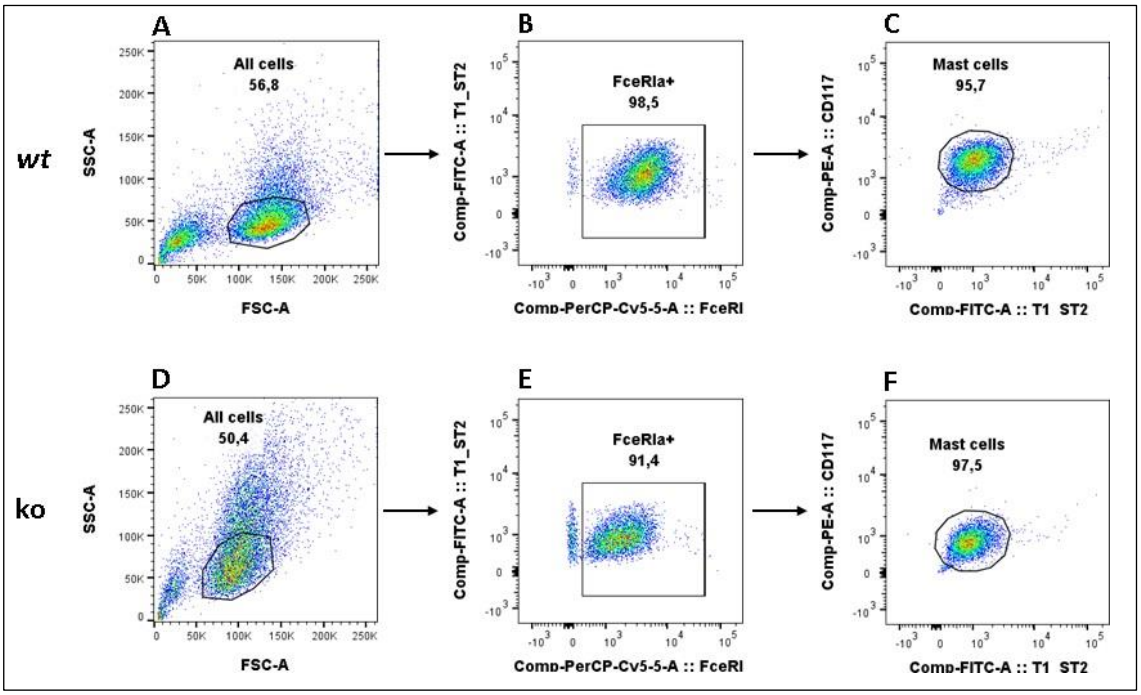

Fig. 8: Generation of BMMC from bone marrow of C57BL/6 (wt) and mMCP-4-/- (ko) mice.
Bone marrow cells derived from wt or ko mice were cultured in presence of mIL-3 and mSCF for generation of BMMC. After 5 weeks of culture, cells were stained with three different fluorescent-labeled antibodies directed against CD117 (c-kit, PE), T1/ST2 (IL-33 receptor, FITC) and FcεRIα (Percp/Cy5.5) and were analyzed for pure MC populations by FACS. Fluorescence minus one (FMO) was used for each fluorescent-labeled Ab, to exclude unspecific fluorescent signal spillover. First gates were set up for all living cells by forward and side scatter intensities (A, D). Finally, gates were set up

for pure BMMC populations by FcεRIα, T1/ST2 and CD117 intensities (B, C, E, F). Data from one representative experiment out of 3-6 are shown.

3.3.2 Reconstitution of MC in MC-deficient mice

In some experimental groups, MC-deficient C57BL/6-*kit*$^{W\text{-}sh/W\text{-}sh}$ (W-sh) mice were reconstituted with BMMC derived from C57BL/6 (*wt*) or mMCP-4$^{-/-}$ (ko) mice before their use in the chronic asthma model. For this purpose, MC generated from bone marrow cells were injected twice, intraperitoneally as well as intravenously into each. Reconstituted mice were used 9 weeks after BMMC injection for chronic asthma model. The efficiency of the reconstitution was analyzed on paraffin sections of lung tissue according to the *systematic uniform random sampling* (SURS) method. After toluidine staining, MC in lung tissues were visualized in dark blue color. Qualitative analysis of stained lung tissues was performed using a light microscope. Successful reconstitution of MC in lung tissue could be observed in all mice independently of the presence or absence of mMCP-4 or allergen treatment (Fig. 9B/C). While no MC were detectable in W-sh mice which were not reconstituted (Fig. 9A), these cells were visible in samples of W-sh mice reconstituted either with *wt* (Fig. 9B) or mMCP-4$^{-/-}$ MC (Fig. 9C) as well as in samples of C57BL/6 *wt* and mMCP-4$^{-/-}$ mice used as positive controls (Fig. 9 D/E).

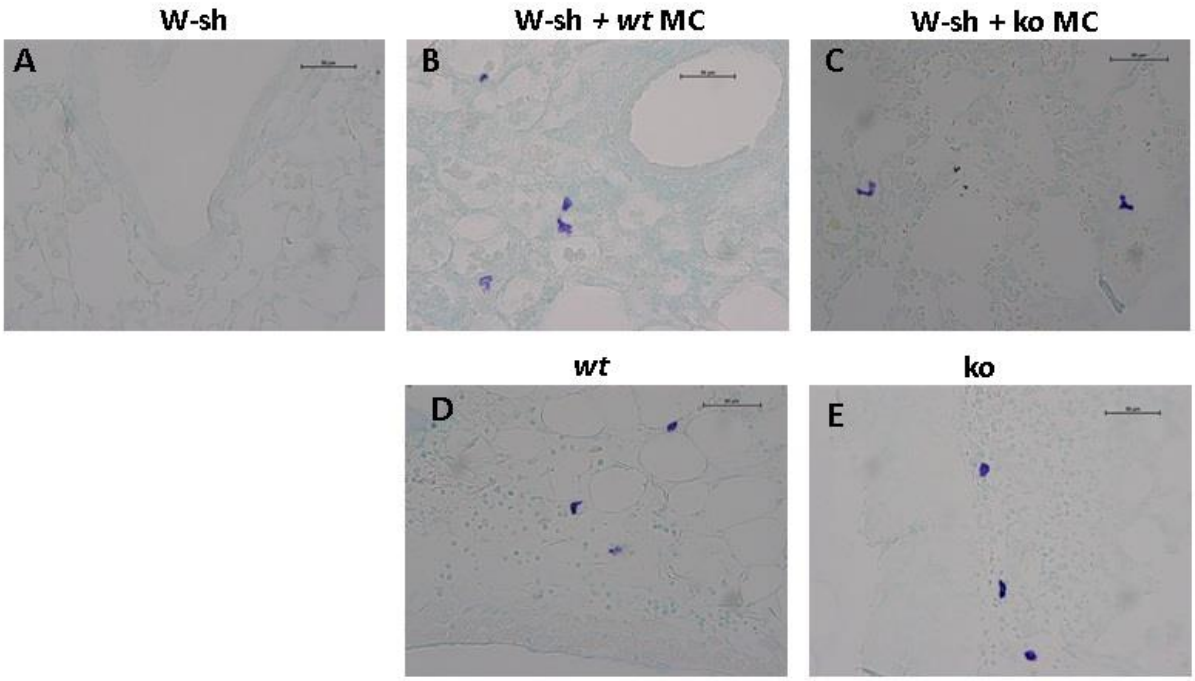

Fig. 9: Successful engraftment of MC in lung tissues of MC-deficient mice. Lung tissues of MC-deficient C57BL/6-*kit*$^{W\text{-}sh/W\text{-}sh}$ (W-sh) (A), MC-deficient -mice reconstituted either with *wt* BMMC (W-sh + *wt* MC) (B) or with mMCP-4$^{-/-}$ BMMC (W-sh + ko MC) (C), C57BL/6-mice (*wt*) (D) and mMCP-4$^{-/-}$ (ko) (E) were screened for MC in paraffin embedded lung sections stained with toluidine blue. MC-deficient W-sh, *wt* and ko mice served as controls. Images were taken with 40x magnification and bars indicate 50 µm. One representative experiment out of 6-19 per group is shown.

3.3.3 IgE-titers in sensitized mice

Sera of mice were analyzed for OVA-specific IgE titers by ELISA to determine the efficiency of the sensitization. The repeated injection of OVA induced the production of OVA-specific IgE, and elevated titers of IgE were observed all sensitized groups compared to PBS-treated controls (Fig. 10A-C). Although in nearly all non-sensitized mice scored negative for OVA-specific IgE, a few animals within these groups showed a spontaneous IgE production. The reason for this is unclear. However, results obtained by further analysis were always carefully re-evaluated in these mice. Medians of measured IgE in OVA-sensitized groups after 9 weeks of OVA-challenge ranged between 1,7 ng/ml and 7 ng/ml.

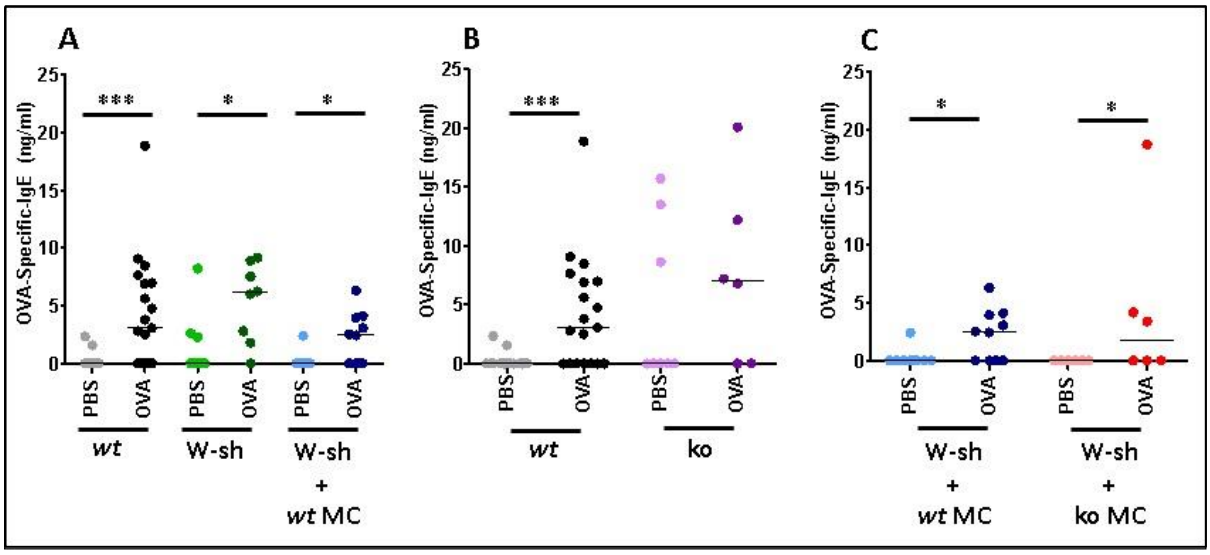

Fig. 10: OVA-specific IgE in sera of sensitized and non-sensitized mice. Mice (n=6-19 per group) were sensitized i.p. three-times with 50 µg Ovalbumin (OVA) while control groups received PBS. One day after the 9th OVA challenge sera were prepared from blood samples of each mouse and analyzed for IgE specifically against OVA. Data are presented as median and dots represent individual results obtained from each animal. Statistics were calculated using Mann-Whitney-test (t-test). Significant differences are indicated as asterisks (***, P<0,001; *, P<0,05). W-sh = MC-deficient C57BL/6-*kit*$^{W\text{-}sh/W\text{-}sh}$, W-sh + *wt* MC= MC-deficient C57BL/6-*kit*$^{W\text{-}sh/W\text{-}sh}$ reconstituted with *wt* MC, W-sh + ko MC = MC-deficient C57BL/6-*kit*$^{W\text{-}sh/W\text{-}sh}$ reconstituted with mMCP-4$^{-/-}$ MC, *wt* = C57BL/6, ko = mMCP-4$^{-/-}$.

3.3.4 Induction of AHR

The determination of AHR is one the most important clinical criteria in the diagnosis of allergic asthma. For analyzing the role of MC and chymase mMCP-4 in chronic experimental asthma, AHR was assessed on anesthetized mice in an invasive method of lung function measurement using methacholine as stimuli. Lung function measurement was performed 24h after the 9th exposure to OVA (day 69) using FinePoint-Buxco-system. Anesthetized mice were exposed to stepwise increased doses of nebulized methacholine (0 mg/ml-100 mg/ml) and airway resistance in response to methacholine was continuously recorded. Since the different mouse strains used varied significantly in their body size, data were normalized to a base value of 100%, to allow a proper comparability between the data sets obtained from individual groups.

3.3.4.1 Elevated AHR in MC-deficient mice

In order to discriminate between the role of MC and mMCP-4 in experimental asthma, in a first approach the relevance of MC in the induction of AHR was investigated. Therefore, airway resistance was determined in *wt*, MC-deficient W-sh mice and W-sh mice reconstituted with *wt* MC and expressed in response to methacholine doses. All PBS-sensitized and OVA challenged

control groups showed an increase in airway resistance dose-dependent on the methacholine concentration. At 100 mg/ml methacholine a low airway resistance between 236% and 264% was observed in all non-sensitized control groups (Fig. 11). By contrast, sensitization of *wt* animals provoked a moderate AHR by significant increase reaching 312% at the highest methacholine concentration (*wt* PBS < OVA ***). Surprisingly, airway resistance was found to be further elevated in sensitized MC-deficient W-sh mice (W-sh PBS < OVA***), reaching with 418% at 100 mg/ml methacholine the strongest AHR of all experimental groups. This effect could be reversed to the level of airway resistance seen in *wt* control when W-sh mice were reconstituted with *wt* MC prior to sensitization, with significant difference to PBS control (W-sh + *wt* MC PBS < OVA*). Taken together, these data show that MC-deficiency is associated with an increased AHR and suggest that MC have a protective function in chronic experimental asthma by reducing an AHR reaction.

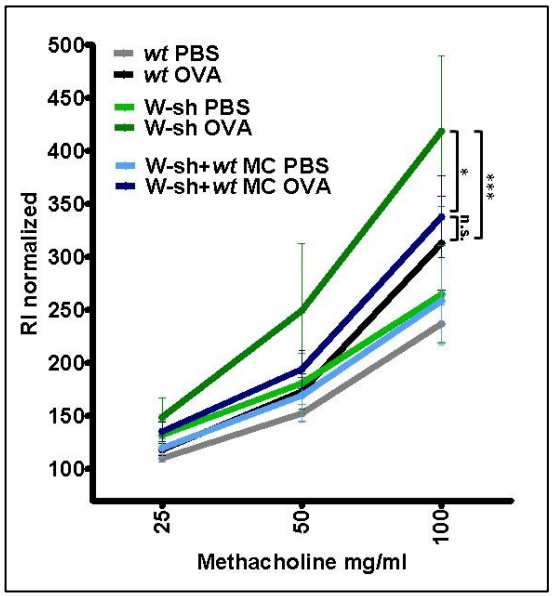

Fig. 11: AHR in MC-deficient W-sh and C57BL/6 mice. C57BL/6- (*wt*), MC-deficient C57BL/6-*kit*$^{W\text{-}sh/W\text{-}sh}$ - (W-sh) mice, and W-sh mice reconstituted with *wt* BMMC (W-sh + *wt* MC) were sensitized with OVA while control mice received PBS (n=6-19 per group). All mice were repeatedly challenged with OVA for 9 weeks and AHR in response to increasing doses of methacholine was assessed. Data were normalized to starting base line values of 100% and given as mean ± standard deviation. Statistics were calculated for differences in airway resistance at 100 mg/ml methacholine by using Two-way ANOVA. Significant differences are indicated as ***(P<0,001) and *(P<0,05).

3.3.4.2 Deficiency in mMCP-4 is associated with a reduction of AHR

In the next step, the role of mMCP-4 in AHR of chronic experimental asthma was investigated. For this purpose, the disease was induced in C57BL/6- (*wt*), mMCP-4$^{-/-}$ - (ko) and MC-deficient W-sh mice reconstituted either with *wt* BMMC (W-sh + *wt* MC) or mMCP-4$^{-/-}$ BMMC (W-sh + ko MC). While a significantly increased AHR could be observed in sensitized *wt* mice reaching 312% at 100 mg/ml methacholine concentration compared to PBS control (*wt* PBS < OVA ***), mMCP-4$^{-/-}$ (ko) mice were found to be resistant to an induction of AHR with 186% showing no significant difference between sensitized and non-sensitized experimental group (Fig 12A). These findings were confirmed in MC-reconstituted W-sh mice. AHR was significantly increased with 337% at the highest methacholine doses in sensitized W-sh + *wt* MC mice compared to PBS control (W-sh + *wt* MC PBS < OVA*), while sensitized W-sh + ko MC mice did not develop AHR with 206% showing no significant difference to non-sensitized control (Fig. 12B). These data show that mMCP-4-deficiency is associated with a reduction of AHR and suggest a proinflammatory function of mMCP-4 in chronic experimental asthma by induction of AHR.

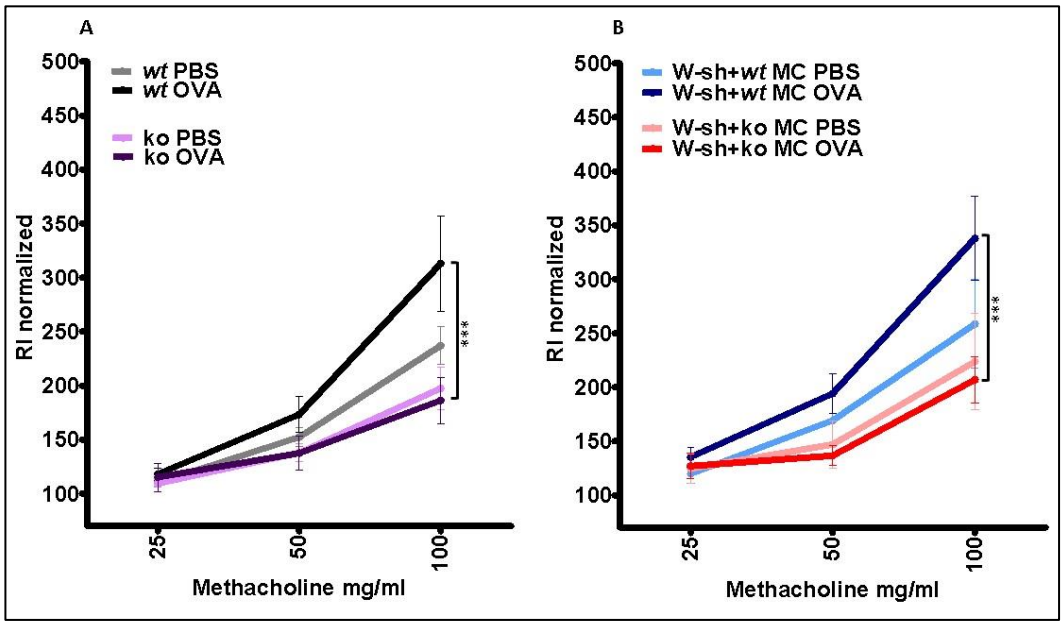

Fig. 12: Reduced AHR in sensitized mice lacking mMCP-4. C57BL/6- (*wt*) (A), mMCP-4$^{-/-}$ (ko) (A) and MC-deficient -mice reconstituted either with *wt* BMMC (W-sh + *wt* MC) or mMCP-4$^{-/-}$ BMMC (W-sh + ko MC) (B) were sensitized with OVA while control mice received PBS (n=6-19 per group). All mice were exposed to OVA for 9 weeks and AHR in response to increased doses of methacholine was assessed as airway resistance. Data were normalized to starting base value of 100% and given as mean ± standard deviation. Statistics were calculated for differences in airway resistance at 100 mg/ml methacholine by using Two-way ANOVA. Significant differences are indicated as ***(P<0,001).

3.3.5 Cellularity of the BAL

Inflammation in the lung associated with increased numbers of inflammatory cells is a characteristic feature of allergic asthma. Subsequently, after lung function measurement, mice lungs derived from all experimental groups were lavaged with PBS supplemented with proteinase inhibitor in order to investigate inflammatory cell infiltrates in the lung lumen. Cytospins of BAL cell suspensions were prepared and stained with May-Grünwald-Giemsa-solution. Inflammatory cells were analyzed based on their color and cellular morphology using light microscopy. In order to obtain further information about the extent of lung inflammation, cell numbers of eosinophils, macrophages, lymphocytes and neutrophils including total cell numbers per ml BAL were determined for each mouse.

3.3.5.1 Increased inflammatory cells in non-sensitized and sensitized mice

To determine the role of MC and mMCP-4 on the cellularity of the BAL, samples of all experimental groups were analyzed for the presence of inflammatory cells (Fig. 13). PBS-treated and OVA-sensitized groups did not show significant differences in cellular infiltration arguing against a dependency on the status of sensitization (Fig. 13B-Q). In this chronic model, mice were sensitized either with OVA or received PBS but all mice were challenged with OVA. Repeated OVA challenge over 9 weeks in PBS control mice could possibly induce moderate lung inflammation. Indeed, naive C57BL/6 (*wt*) mice used as a further negative control did not show an increase in inflammatory cells in the BAL (Fig. 13A).

However, OVA sensitized MC-deficient W-sh mice showed significant increase in total cell - (Fig. 13B) and macrophage numbers (Fig. 13C) compared to OVA sensitized *wt* controls. This effect could not be reversed by repopulation of W-sh mice with *wt* MC, indicating that this effect may be strain but not MC-related. Also, a significant increase of eosinophils could be detected in sensitized W-sh mice reconstituted with mMCP-4$^{-/-}$ MC as compared to W-sh mice repopulated with *wt* MC, but not to PBS control (Fig. 13N). In summary, these data show that in this animal model the inflammatory status as determined by the infiltration of inflammatory cells into the lung appeared to be largely independent from sensitization of the animals, from the presence of MC as well as from chymase mMCP-4.

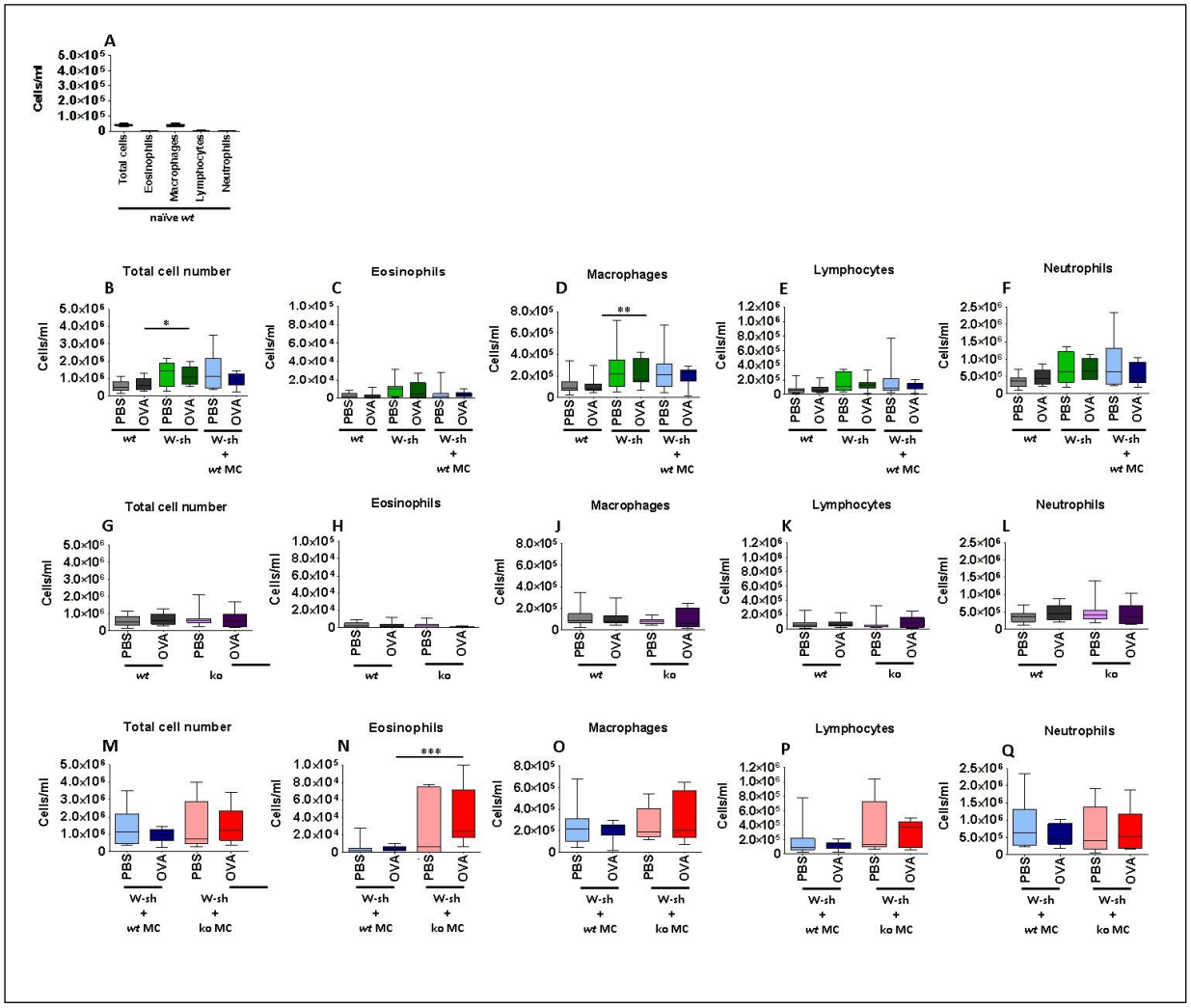

Fig. 13: Cellularity of the BAL in non-sensitized and sensitized mice. C57BL/6-mice (*wt*), MC-deficient C57BL/6-*kit*$^{W\text{-}sh/W\text{-}sh}$ (W-sh), and MC-deficient mice reconstituted with *wt* BMMC (W-sh + *wt* MC) or with mMCP-4$^{-/-}$ BMMC (W-sh + ko MC) were sensitized with OVA while control mice received PBS. All mice were challenged with OVA (n=6-19 per group). BAL was collect at day 69, 24h after of the last challenge. Naive C57BL/6 served as additional negative control (A). Inflammatory cell count was performed to analyze different leukocyte population of May-Grünwald-Giemsa stained BAL cytospins. Numbers of counted cells per ml BAL for total cells (A, B, G, M), eosinophils (A, C, H, N), macrophages (A, D, J, O), lymphocytes (A, E, K, P) and neutrophils (A, F, L, Q) are presented as Box and Whiskers (min to max). Statistics were performed using Mann-Whitney test and Significant differences are indicated as asterisks (***, P<0,001; **, P<0,01; *, P<0,05).

3.3.6 Histopathology of chronic inflamed lung tissue

Goblet cell hyperplasia associated with increased mucus production and inflammatory cell infiltrations in lung tissue are further parameters of allergic asthma. Subsequently after lung function measurement and collection of BAL, lung tissues were processed for paraffin sections according to the *systematic uniform random sampling* (SURS) method to investigate the effect of MC and chymase mMCP-4 in the induction of the mentioned parameters. After periodic acid schiff-staining, goblet cells and mucus in lung tissues were visualized in purple and additional counterstaining with hematoxylin II solution stained inflammatory cells in dark blue. Qualitative analysis of stained lung tissues was performed using a light microscope. Computer assisted stereological toolbox (newCAST) was used for quantitative analysis of lung inflammation. For this purpose, unit area of goblet cells in total epithelium (%) and mucus ($\mu m^3/\mu m^2$) as well as inflammatory cells (cells/µm2) per unit area of basal lamina were determined.

3.3.6.1 Deficiency in MC does not affect goblet cell hyperplasia or mucus production

Since MC and mMCP-4 differentially regulate AHR in experimental asthma, the question arose whether other clinical symptoms of the disease could also be affected by these parameters. Therefore, the role of MC and mMCP-4 in lung inflammation were further analyzed in histological lung tissue sections. In a first step, the function of MC on the airway epithelium was analyzed. Lung sections of C57BL/6 *wt* and MC-deficient W-sh mice as well as W-sh mice reconstituted with MC from *wt* animals derived from the experiment described in section 3.3.4.1 were prepared. Furthermore, to estimate the potential effect induced by the repeated challenge alone in non-sensitized mice, sections derived from naive mice were analyzed as an additional negative control. As compared to naive mice (Fig. 14A), animals of all none-sensitized but challenged groups developed only a mild mucus production (Fig. 14B-D). By contrast, sensitized and challenged mice were characterized by increased mucus production, goblet cell hyperplasia, and signs of connective tissue remodeling (thickening of connective tissue), especially observed in MC-deficient W-sh mice. (Fig. 14E-G). These findings were confirmed by quantitative stereological analysis using newCAST software. While in naïve mice goblet cells and mucus were virtually absent (<2.5% Goblet cell, <0.13 $\mu m^3/\mu m^2$ mucus volume, Fig. 14H/J), a slight increase was seen in all non-sensitized but challenged groups (<28,3% Goblet cell, <1.69 $\mu m^3/\mu m^2$ mucus volume, Fig. 14K/L). However, lung epithelium of OVA sensitized mice contained significantly increased goblet cells (<60%, Fig. 14K) and most of them had also

significantly increased mucus production (<3.02 µm^3/µm^2, Fig. 14L) as compared to PBS controls.

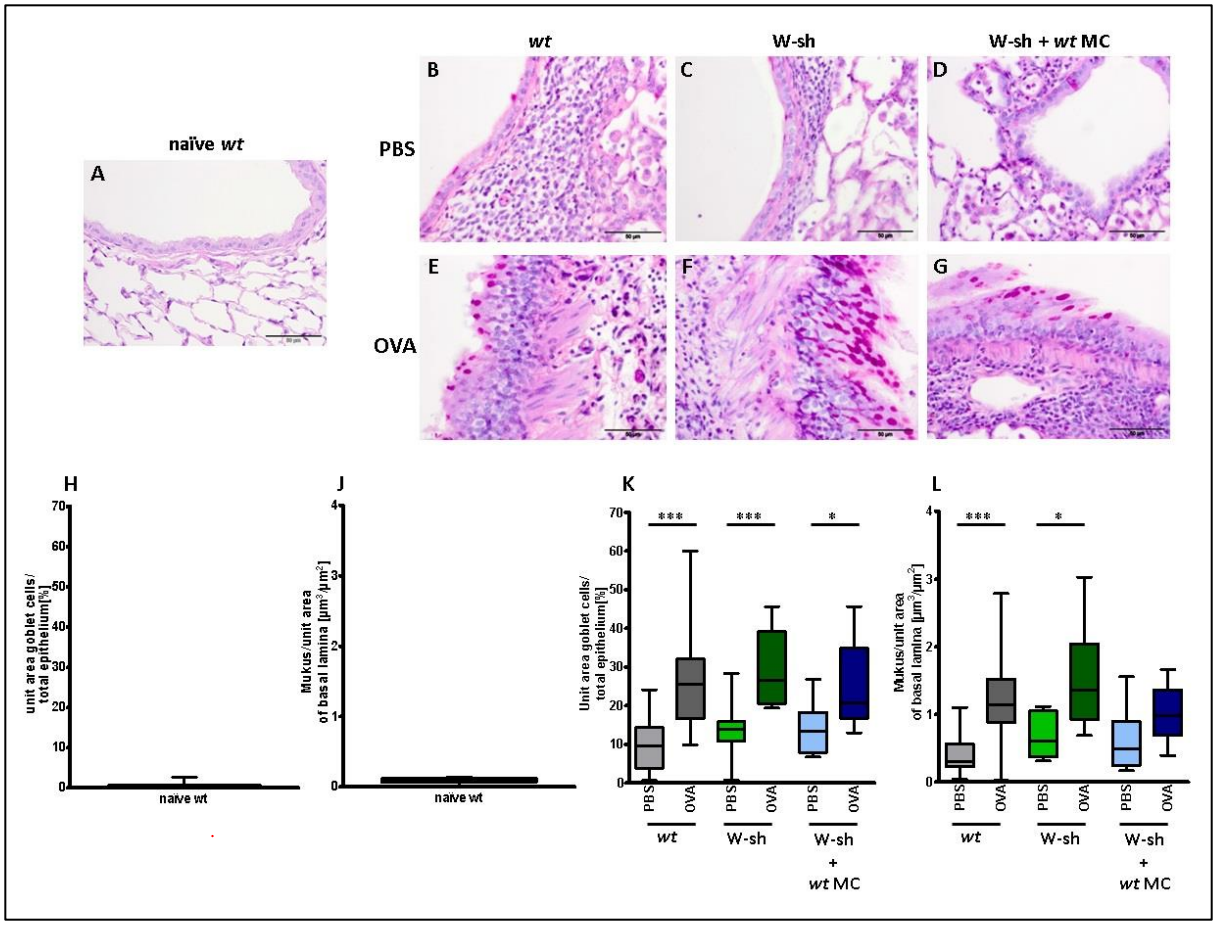

Fig. 14: MC-deficiency does not affect goblet cell hyperplasia or mucus production in experimental asthma. C57BL/6-mice (*wt*) (B, E, K, L), MC-deficient C57BL/6-*kit*$^{W\text{-}sh/W\text{-}sh}$ (W-sh) (C, F, K, L) and MC-deficient mice reconstituted with *wt* BMMC (W-sh + *wt*) (D, G, K, L) were sensitized with OVA while control mice received PBS. All mice were challenged with OVA Untouched C57BL/6 served as additional control (A, H, J). Paraffin embedded lung sections were stained with PAS and counterstained with hematoxylin. Images were taken with 40x magnification and bars represent 50 µm lengths. Unit area of goblet cells in total epithelium (H, K) and mucus per unit area of basal lamina (J, L) were determined in all samples from each group and quantified by stereological analysis with help of the newCAST software. Representative micrographs of each group (n=6-19 per group) are given as Box and Whiskers (min to max). Statistics were calculated using Mann-Whitney test and Significant differences are indicated as asterisks (***, P<0,001; *, P<0,05).

3.3.6.2 Goblet cell hyperplasia and mucus production are not affected by mMCP-4

In the next step, the role of mMCP-4 on changes of the epithelium was analyzed in lung tissue sections derived from mMCP-4$^{-/-}$ mice (ko) and W-sh mice reconstituted with mMCP-4 deficient MC (W-sh + ko MC) while C57BL/6 *wt* and W-sh mice reconstituted with *wt* MC served as control (Fig. 15A-M). As compared to PBS treated controls (Fig. 15A-D/J-M), OVA

sensitized mice showed increased mucus production and goblet cell hyperplasia (Fig. 15E-H/J-M). Neither qualitative nor quantitative differences were observed between *wt*, mMCP-4-deficient, or MC-reconstituted animals. However, it should be mentioned that, thickening of connective tissue were absent in mice lacking mMCP-4 (Fig. 15F/H), while this was present in *wt* and W-sh + *wt* MC (Fig. 15E/G). Taken together, the data obtained show that in this chronic asthma model the inflammatory status as determined by goblet cell hyperplasia and mucus hypersecretion in lung tissue appears to be largely independent from MC as well as from chymase mMCP-4.

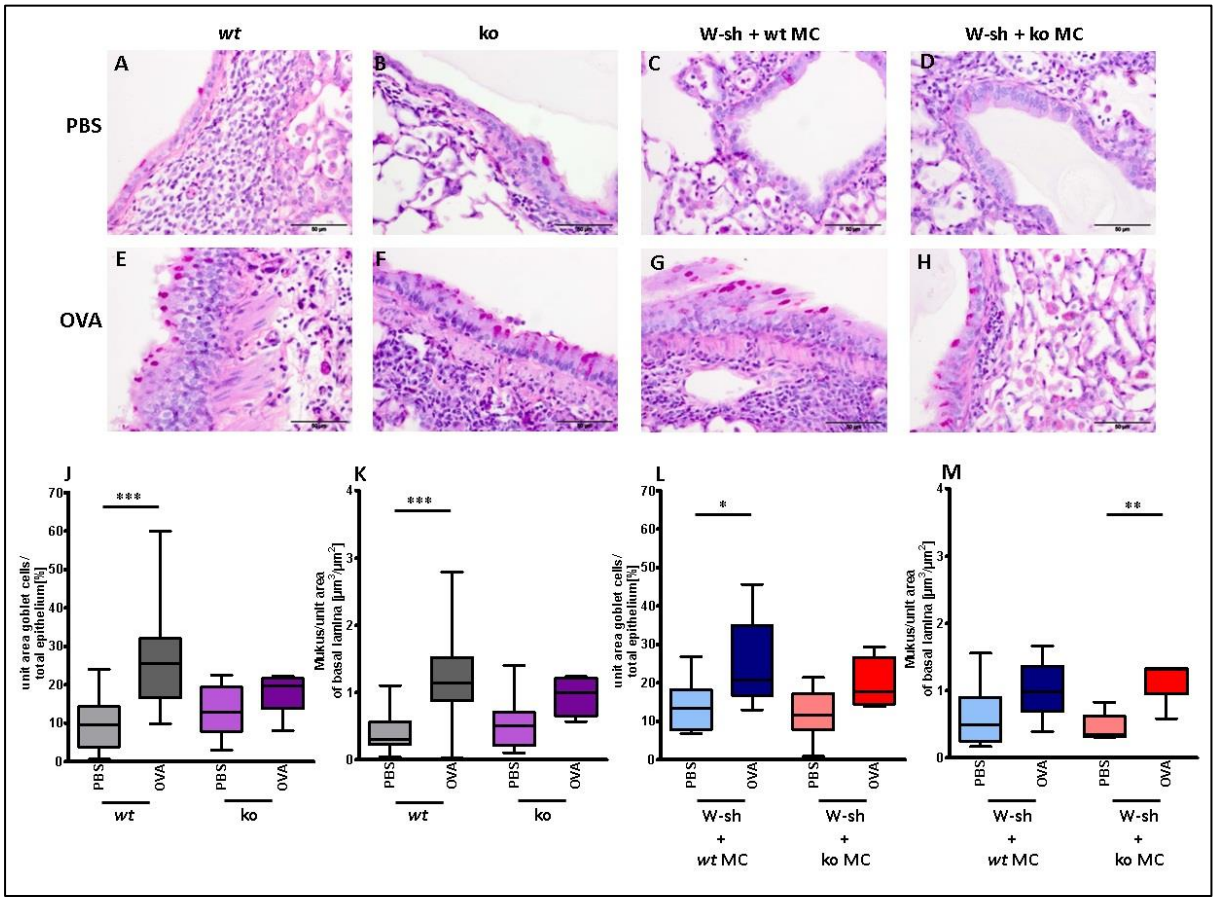

Fig. 15: mMCP-4 deficiency does not affect goblet cell hyperplasia or mucus production in experimental asthma. C57BL/6-mice (*wt*; A, E, J, K), mMCP-4$^{-/-}$ (ko; B, F, K, L) and MC-deficient mice reconstituted with *wt* BMMC (W-sh + *wt* MC; C, G, L, M) or with mMCP-4$^{-/-}$ BMMC (W-sh + ko MC; D, H, L, M) were sensitized with OVA while control mice received PBS. All mice were challenged with OVA. Paraffin embedded lung sections were stained with PAS and counterstained with hematoxylin. Images were taken with 40x magnification and bars represent 50 µm lengths. Unit area of goblet cells in total epithelium (J, L) and mucus per unit area of basal lamina (K, M) were determined in all samples from each group and quantified by stereological analysis with help of newCAST software. Representative micrographs of each group (n=6-19 per group) are given as Box and Whiskers (min to max). Statistics were calculated using Mann-Whitney test and significant difference are indicated as asterisks (***, P<0,001; **, P<0,01; *, P<0,05)

3.3.6.3 Infiltration of inflammatory cells into the lungs in chronic experimental asthma

Inflammation in general is characterized by the immigration of immune cells into the affected tissue. However, based on the representative micrographs shown in Fig. 16B and C, no obvious differences were visible between the individual groups. Quantitative analysis of sections derived from naive mice revealed almost no inflammatory cells in lungs of these mice (<0,13 cells/µm^2, Fig. 16A). However, irrespective of whether mice were sensitized or not and independently of their MC or mMCP-4 status, all mice involved in the chronic model developed inflammatory infiltrates in their lungs (Fig. 16B-C) reaching levels 16-22 fold higher than those observed in naive mice. These findings confirm the data obtained in analysis of inflammatory cells in BAL and provide evidence that repeated challenges with OVA over 9 weeks already induced a limited inflammatory reaction in the lung.

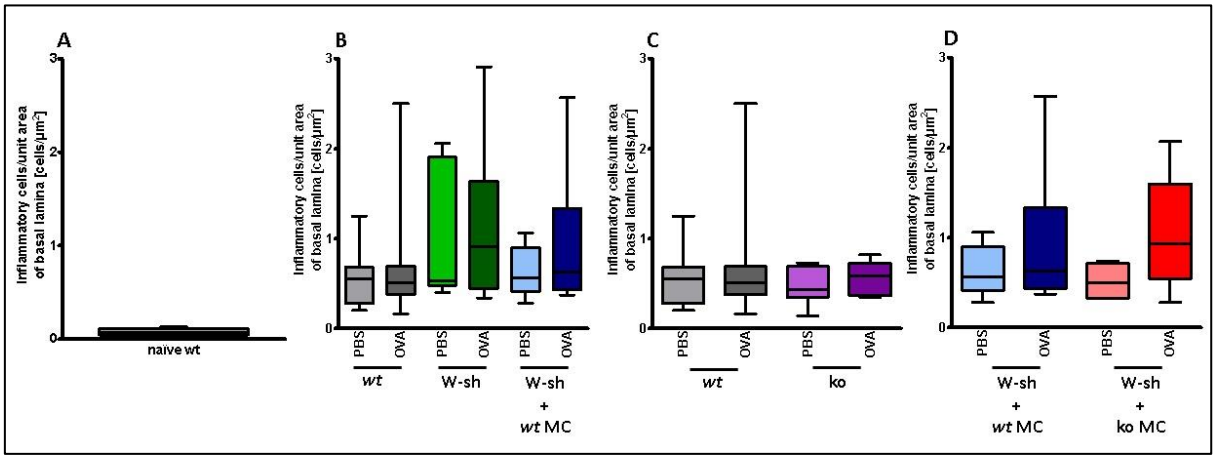

Fig. 16: Comparable increase of inflammatory cells in lung tissue of all mouse groups after repeated OVA challenge. C57BL/6-mice (*wt*; B, C), MC-deficient C57BL/6-*kit*$^{W\text{-}sh/W\text{-}sh}$ (W-sh; B) mMCP-4$^{-/-}$ (ko; C) and MC-deficient mice reconstituted with *wt* BMMC (W-sh + *wt* MC; B, D) or with mMCP-4$^{-/-}$ BMMC (W-sh + ko MC; D) were sensitized with OVA while control mice received PBS. All mice were challenged with OVA. Untouched C57BL/6 *wt* served as additional control (A). Paraffin embedded lung sections were stained with PAS and counterstained with hematoxylin. Inflammatory cells (cells/µm^2) per unit area of basal lamina were determined in all samples from each group and quantified by stereological analysis with help of newCAST software. Representative micrographs of each group (n=6-19 per group) are given as Box and Whiskers (min to max). Statistics were calculated using Mann-Whitney test, with no significant difference in treatment or mouse strains.

3.3.7 Regulation of cytokines in chronic experimental asthma

The analysis of a cytokine profile in an inflammatory event can provide relevant information about the type of inflammation (e.g. TH1, TH2), the participating cell types and tissues, and on the potential outcome of a disease. Furthermore, such a profile may provide first insights in the

mechanisms underlying a specific disease phenotype observed under specific experimental conditions. In order to define the role of MC and mMCP-4 in chronically inflamed lung tissue, determination of cytokines in addition to the analysis of inflammatory cells was performed. For this purpose, lungs were homogenized and the obtained cell suspensions were cultured and restimulated in presence of OVA for 3 days. Subsequently, levels of IL 2, 4, 5, 6, 9, 10, 13, 17A and F, 21, 22, INFg and TNFα were determined in supernatants using a multiplex system which allows simultaneous quantification of several different mouse cytokines in only one sample. According to their dependency on the regulation by disease status, MC and mMCP-4, results obtained for the individual cytokines were categorized into 5 different groups:

- Cytokines *not* regulated in *wt* mice and *not* regulated by MC
- Cytokines regulated in *wt* mice but *not* regulated by MC
- Cytokines *not* regulated in *wt* mice *but* regulated by mMCP-4
- Cytokines regulated in *wt* mice *and* regulated by mMCP-4
- Cytokines *not* regulated by mMCP-4

Due to the ordering used here, each cytokine analyzed appears in two categories.

Cytokines *not* regulated in *wt* mice and *not* regulated by MC

Within this group of cytokines, the secretion was neither affected by sensitization nor was their production different in W-sh, irrespective whether these mice have been reconstituted with MC or not. Members of this group are IL-10, IL-17A/F, IL-22, and TNF-α (Fig. 17B-F). It should be noted that a common feature of these cytokine is their role in the regulation of the innate immune response. Results derived from the analysis of IFN-γ are not clear since this cytokine appears to be elevated in MC-deficient mice, independent from sensitization (Fig. 17A). However, this increase was significant only when sensitized *wt* were compared to sensitized W-sh groups. Based on these data, a regulation of this cytokine by MC cannot be excluded. Moreover, the cytokines IL-2, IL-13, and IL-21 were, beside a few and inconsistent exceptions, not detectable in all supernatants of mice lungs (Fig. 17G-J).

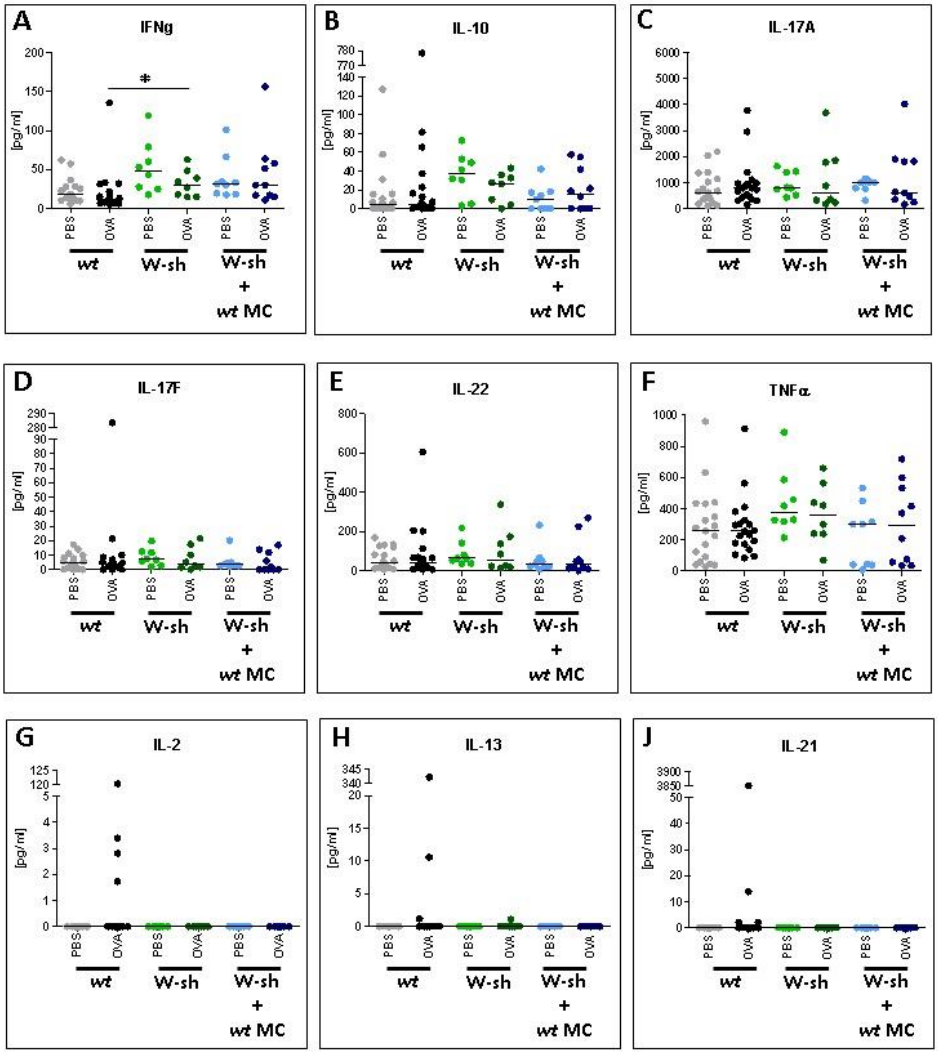

Fig. 17: Cytokines not regulated in *wt* mice or by MC. C57BL/6-mice (*wt*), MC-deficient C57BL/6-*kit*$^{W\text{-}sh/W\text{-}sh}$ - (W-sh) and MC-deficient -mice reconstituted with *wt* BMMC (W-sh + *wt* MC) were sensitized with OVA while control mice received PBS. All mice were challenged with OVA (n=6-19 per group). Lung homogenates were prepared at day 69 after 24h of the last challenge. Lung cell suspensions were cultured and restimulated with OVA for 3 days. Cytokine concentrations were analyzed in SN of restimulated lung cells using legend multiplex system and measured by FACS analysis. Data were further processed in LEGENDplex™ Data Analysis Software and representative micrographs of each group are given as Box and Whiskers (min to max). Statistics were calculated using Mann-Whitney test, significant difference are indicated by asterisks (*, P<0,05).

Cytokines regulated in *wt* mice but *not* regulated by MC

The second group of cytokines consists of the Th2 cytokines IL-4, IL-5, and IL-9 as well as of the pro-inflammatory cytokine IL-6 (Fig. 18A-D). Within this group, an increased expression of the cytokine was seen in sensitized *wt* mice as compared to the PBS-treated control. For IL-4, IL-6, and IL-9 this effect is also observed in W-sh or W-sh mice reconstituted with MC, indicating that MC were not involved in their regulation in asthma. Levels of IL-5 in sensitized

W-sh mice were nearly significant elevated compared to sensitized *wt* controls. However, this effect could not be reversed by reconstitution with *wt* MC, identifying this phenomenon as mouse strain-associated but not as MC-specific.

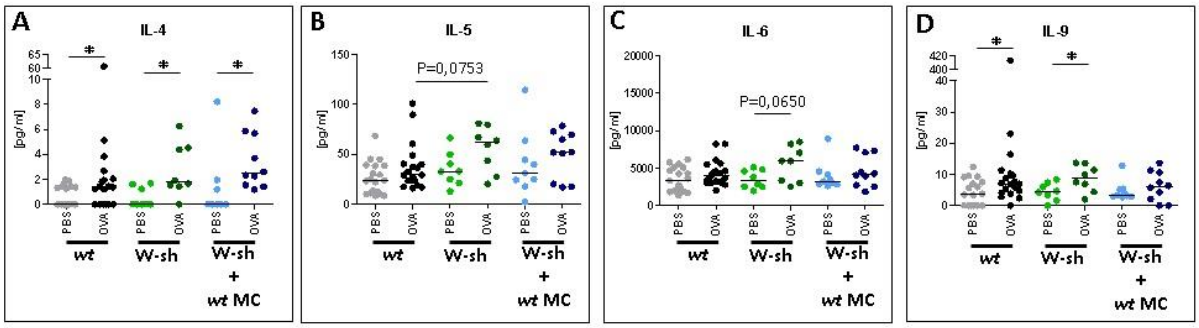

Fig. 18: Cytokines regulated in wt mice but not regulated by MC. C57BL/6-mice (*wt*), MC-deficient C57BL/6-*kit*$^{W\text{-}sh/W\text{-}sh}$ (W-sh) and MC-deficient mice reconstituted with *wt* BMMC (W-sh + *wt* MC) were sensitized with OVA while control mice received PBS. All mice were challenged with OVA (n=6-19 per group). Lung homogenates were prepared at day 69, 24h after the last challenge. Lung cell suspensions were cultured and restimulated with OVA for 3 days. Cytokine concentrations were analyzed in SN of restimulated lung cells using legend multiplex system and measured by FACS analysis. Data were further processed in LEGENDplex™ Data Analysis Software and representative micrographs of each group are given as Box and Whiskers (min to max). Statistics were calculated using Mann-Whitney test, significant difference are indicated by asterisks (*, P<0.05)

Cytokines *not* regulated in *wt* mice *but* regulated by mMCP-4

Analysis of the cytokines of the following two groups revealed an unexpected and complex regulated pattern. Corresponding to results shown for the first group above, several cytokines like the T cell cytokine IL-2, the Th2-cytokines IL-10 and IL-13, the Th1- cytokine IFNγ, or the pro-inflammatory cytokines IL-17A/F, IL-21, and IL-22 were not regulated in chronic experimental asthma in *wt* mice or W-sh mice reconstituted with MC derived from *wt* mice (Fig. 19). However, as compared to these controls, significantly increased concentrations of these cytokines were observed in most non-sensitized mMCP-4$^{-/-}$ mice, which could be reproduced in W-sh mice reconstituted with MC lacking mMCP-4. Unexpectedly, these elevated cytokine levels were not observed in the latter two groups when mice were sensitized before challenge with OVA indicating that induction of disease may revert this effect.

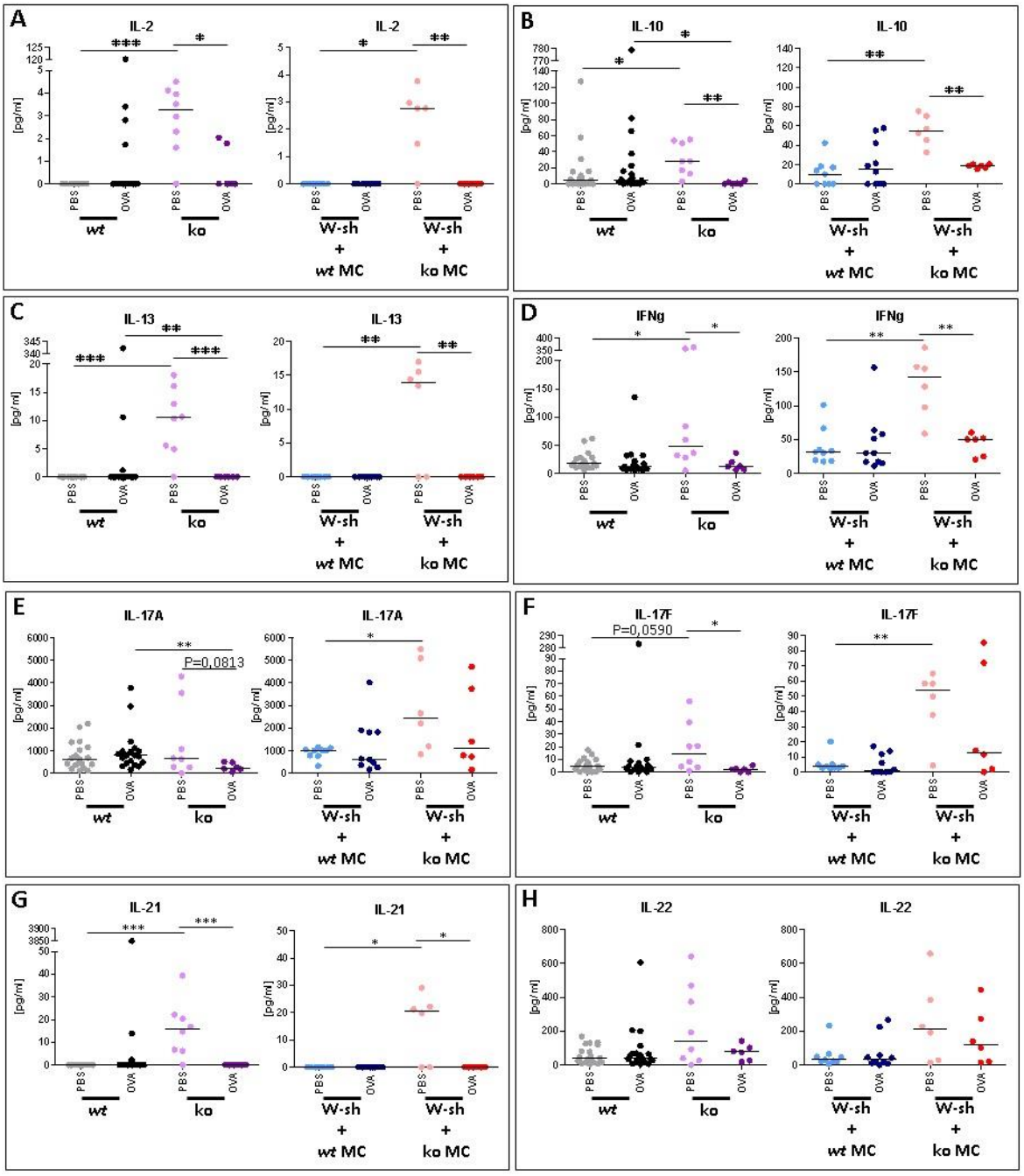

Fig. 19: Cytokines not regulated wt but regulated by mMCP-4. C57BL/6-mice (*wt*), mMCP-4$^{-/-}$ (ko), and MC-deficient -mice reconstituted with *wt* BMMC (W-sh + *wt* MC) or with mMCP-4$^{-/-}$ BMMC (W-sh + ko MC) were sensitized with OVA while control mice received PBS. All mice were challenged with OVA (n=6-19 per group). Lung homogenates were prepared at day 69, 24h after the last challenge. Lung cell suspensions were cultured and restimulated with OVA for 3 days. Cytokine concentrations were analyzed in SN of restimulated lung cells using legend multiplex system and measured by FACS analysis. Data were further processed in LEGENDplex^{TM} Data Analysis Software and representative micrographs of each group are given as Box and Whiskers (min to max). Statistics were calculated using Mann-Whitney test, significant difference are indicated by asterisks (***, P<0,001; **, P<0,01 and *, P<0,05).

Cytokines regulated in *wt* mice *and* regulated by mMCP-4

In the second group shown above, the cytokines IL-4, IL-6, and IL-9 were identified to be upregulated in disease but unaffected by MC in *wt* mice or W-sh mice reconstituted with MC derived from *wt* mice (Fig. 18). However, similar to the effect observed in the third group (Fig. 19), high cytokine levels were detected in supernatants from non-sensitized mMCP-4$^{-/-}$ mice and W-sh mice reconstituted with MC derived from mMCP-4-deficient animals. Most intriguingly, cytokine concentrations in the latter two groups did not only surmount those of non-sensitized *wt* mice or *wt*-reconstituted W-sh but also those observed in diseased mice of these strains. As seen in the third group, levels of cytokines were comparable to those in the corresponding control groups when mMCP-4$^{-/-}$ mice and W-sh mice reconstituted with mMCP-4$^{-/-}$ MC were sensitized before challenge (Fig. 20).

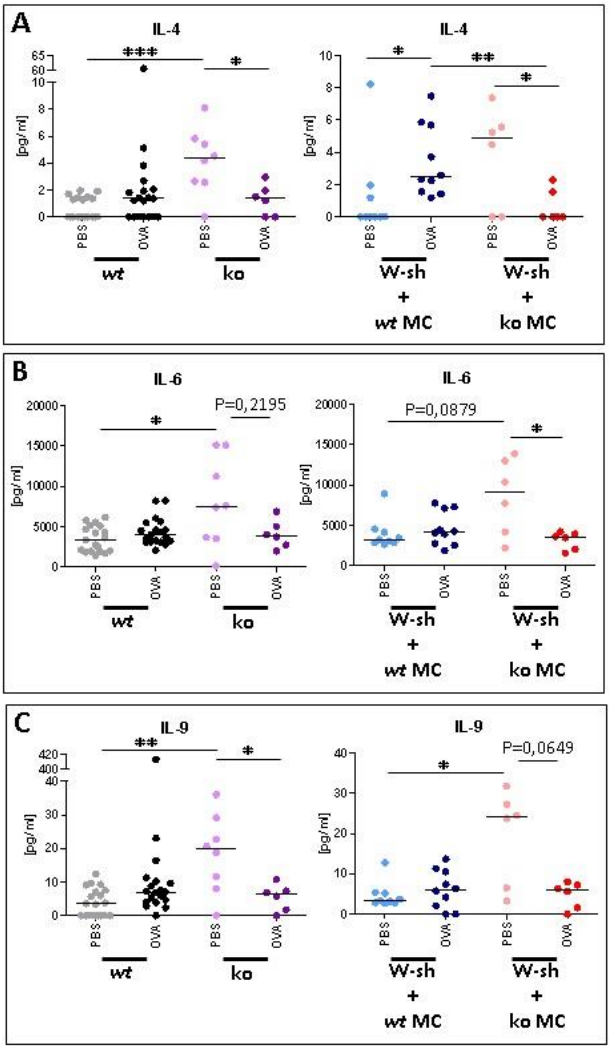

Fig. 20: Cytokines regulated in wt mice and regulated by mMCP-4. C57BL/6-mice (*wt*), mMCP-4$^{-/-}$ (ko), and MC-deficient mice reconstituted with *wt* BMMC (W-sh + *wt* MC) or with mMCP-4$^{-/-}$ BMMC

(W-sh + ko MC) were sensitized with OVA while control mice received PBS. All mice were challenged with OVA (n=6-19 per group). Lung homogenates were prepared at day 69 after 24h of the last challenge. Lung cell suspensions were cultured and restimulated with OVA for 3 days. Cytokine concentrations were analyzed in SN of restimulated lung cells using legend multiplex system and measured by FACS analysis. Data were further processed in LEGENDplex™ Data Analysis Software and representative micrographs of each group are given as Box and Whiskers (min to max). Statistics were calculated using Mann-Whitney test, significant difference are indicated by asterisks (***, P<0,001; **, P<0,01 and *, P<0,05).

Cytokines *not* regulated by mMCP-4

Interestingly, only two members of the rather broad group of cytokines which has been investigated in this study gave no conclusive result but appeared not to be regulated by mMCP-4. The pro-inflammatory cytokine TNF-α remained unchanged between *wt* and mMCP-4$^{-/-}$, irrespective whether animals were sensitized or not (Fig. 21A). However, an increase independent from sensitization was observed in W-sh mice reconstituted with mMCP-4$^{-/-}$ MC as compared to those reconstituted with *wt* MC (Fig. 21A). The Th2 cytokine IL-5 was slightly elevated in OVA sensitized *wt*, mMCP-4$^{-/-}$, W-sh, and W-sh mice reconstituted with *wt* MC (Fig. 18B and 21B). However, no such effect could be detected in W-sh mice reconstituted with mMCP-4$^{-/-}$ MC (Fig. 21B).

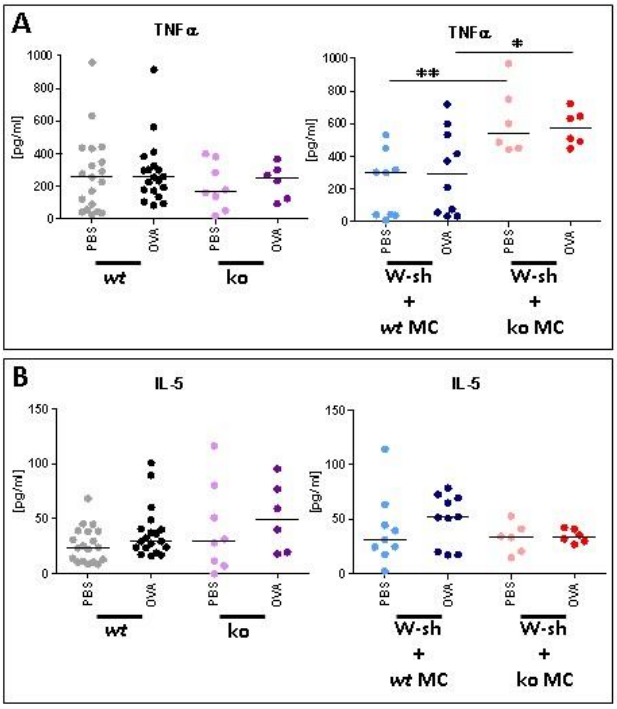

Fig. 21: Cytokines not regulated by mMCP-4. C57BL/6-mice (*wt*), mMCP-4$^{-/-}$ (ko), and MC-deficient mice reconstituted with *wt* BMMC (W-sh + *wt* MC) or with mMCP-4$^{-/-}$ BMMC (W-sh + ko MC) were sensitized with OVA while control mice received PBS. All mice were challenged with OVA (n=6-19

per group). Lung homogenates were prepared at day 69, 24h after of the last challenge. Lung cell suspensions were cultured and restimulated with OVA for 3 days. Cytokine concentrations were analyzed in SN of restimulated lung cells using legend multiplex system and measured by FACS analysis. Data were further processed in LEGENDplex™ Data Analysis Software and representative micrographs of each group are given as Box and Whiskers (min to max). Statistics were calculated using Mann-Whitney test, significant difference are indicated by asterisks (***, P<0,001; **, P<0,01 and *, P<0,05).

Taken together, most of the cytokines which were found to be regulated in the model of chronic asthma could be allocated into two groups. The first group is regulated in *wt* mice independent of MC (IL-4, -5, -6, and -9) while the second group is regulated by mMCP-4 (IFN-γ, IL-2, -4, -6, -9, 10, -13, -17A/F, -21, and -22). The regulation in both groups appears to be remarkably different. While in the first group induction of disease mediated an upregulation of the mediators, in the second group cytokine levels were increased in the absence of mMCP-4 in non-sensitized animals. These finding indicate that mMCP-4 has a previously unrecognized role in the regulation of cytokines in homeostasis.

4 Discussion

Allergic asthma is a complex heterogeneous disease of the airways with symptoms like chronic airway inflammation and remodeling, airflow obstruction and AHR, which result from the complex interaction of different pattern of immune cells including MC and their mediators in response to usually harmless substances [9,84]. According to recent reports, MC contribute to mild or severe asthma dependent on the MC subtypes involved which differ in their expression pattern of serine proteases[98]. Analysis of endobronchial biopsies and epithelial brushing showed a corticosteroid-insensitive increase of chymase positive MCTC in the airway submucosa and the epithelium of severe asthmatics as compared to milder disease forms or healthy subjects[99,100]. Furthermore, it has been shown that human chymase increases intestinal epithelial permeability *in vitro*, decreases the expression of tight junction proteins *in vitro* and represents a potent chemoattractant for neutrophils and some other inflammatory cells *in vitro* and *in vivo*[82,83,101]. In contrast to the described proinflammatory functions of human chymase, a protective role has been suggested for the murine counterpart, mouse chymase mMCP-4, in an acute model asthma described by Waern et al[76,102]. However, the role of mMCP-4 in the chronic course of the disease has not been investigated so far. For this purpose, the aim of this study was to investigate the role of the human chymase counterpart in a chronic model of asthma.

In a first step, a proinflammatory potential of chymase *in vitro* could be observed indicating that chymase may drive inflammatory processes by affecting the function of barrier cells. This effect was further verified in an adjuvant-free chronic model of asthma. After efficient sensitization and repeated OVA challenge, the OVA-induced AHR was selectively regulated by MC and mMCP-4, whereas other parameters of allergic asthma like goblet cell hyperplasia associated with mucus hypersecretion and influx of inflammatory cells into the lung were induced independent of MC or mMCP-4. However, OVA-sensitized MC-deficient W-sh mice revealed the highest level of AHR among the analyzed mice whereas mice lacking chymase mMCP-4 were fully protected against development of AHR, indicating a complex self-antagonizing regulatory function of MC in AHR. This consists of mMCP-4 as a proinflammatory player and a currently unknown protective principle which dominates the overall MC function in the regulation of AHR. Further hallmarks of asthma like lung inflammation or mucus production appeared to be largely independent from MC or mMCP-4. By analyzing the cytokine profiles of MC- and mMCP-4-deficient mice under conditions of health and disease, an unexpected regulatory function of mMCP-4 was uncovered. While regulation of cytokines in diseased mice appeared to be independent of MC, several cytokines

were significantly elevated in non-sensitized mice lacking mMCP-4. These findings indicate a previously unrecognized role of mMCP-4 in the regulation of cytokines in homeostasis.

Regulatory role of mMCP-4 in homeostasis

Chronic inflammations such as allergic asthma are controlled by a broad spectrum of different cytokines which are released by immune and non-immune cells. Typical members are Th1-cytokines such as IL-2, INFγ and TNFα as well as Th2-cytokines such as IL-4, -5, -6, -10, -13 and the Th17-cytokine IL-17A and -F, which can either boost (e.g. IL-4, -5, -17, INFγ) or suppress (IL-10) the allergic reaction[103–109].

Analysis of cytokine levels which was performed here in SN of lung cells restimulated with OVA, could confirm a moderate upregulation of members typical for allergic inflammation like IL-4, IL-5, IL-6, or IL-9 in *wt* mice. However, other cytokines characteristic for asthma like IL-13 were not regulated in this experimental setting. A reason for this could be the lack of alum as a Th2-promoting adjuvant or the use of C57BL/6-mice whose genetic background is biased to Th1-responses[110–112]. Regulation of these cytokines was similar in *wt* and in MC-deficient W-sh mice, indicating that MC were not involved in the regulation of these mediators under inflammatory conditions. Similar to these findings, using the same experimental protocol and allergen but performance of i.n. challenge, Yu *et al.* observed increased levels of IL-4 and IFNγ which were regulated independent of MC[113].

Addressing the role of chymase in the regulation of cytokines uncovered an unexpected phenomenon. Nearly all cytokines analyzed here revealed the same complex regulation pattern, which was concordantly in mMCP-4$^{-/-}$ and mMCP-4$^{-/-}$ MC reconstituted animals. Levels of the Th1- cytokine IFNγ, the T cell cytokine IL-2, the Th2-cytokines IL-4, -6, -10 and -13, the Th-9 cytokine IL-9, and the Th17/Th22 cytokines IL-17A/F, IL-21, and IL-22 were significantly increased in non-sensitized mice lacking mMCP-4 as compared to *wt* or *wt* reconstituted W-sh mice, irrespective whether the latter were sensitized or not. Furthermore, such increase was not observed when mMCP-4-deficient mice were sensitized previous to allergen challenge, indicating a function of chymase in the control of cytokine levels in homeostasis. This phenomenon could be explained by two different mechanisms, by proteolytic degradation of cytokines or by direct regulation of immune cell functions by the chymase (Fig. 22). In previous studies, it was shown that mMCP-4 and human α-chymase are able to cleave and in some cases to activate a variety of cytokines, chemokine and other mediators such as TNFα, IL1β, IL-18,

IL-33, SCF [65,73,77,114–120]. These results were confirmed and extended by a most recent study by Fu *et al.* demonstrating that human chymase can cleave IL-6, -15, -18, -33 and to a lower extend INFγ, IL-3, -4, -11, -13 and several chemokines[121]. Here, IL-4, -6, -13 and INFγ were increased in absence of mMCP-4 in non-sensitized animals compared to non-sensitized controls in the performed chronic model, which may be accumulated in absence of mMCP-4 and, therefore, confirm these findings also for murine chymase mMCP-4. However, the cytokines IL-2, -9, -17A/F, -21 and -22 were also increased in mice lacking mMCP-4 but were not shown to be cleaved by human chymase in the study by Fu *et al*. One explanation for this may be the differences between species in cytokine structure, as differences on the accessibility of potential extended target (hidden sites) sites on these cytokines which could affect the cleavage specificity of the protease[121]. Thus, mMCP-4 may have a broader spectrum of cytokines serving as potential substrates than human chymase. However, a second explanation could be a direct inhibitory effect of mMCP-4 on immune cells. It should be noted, that all cytokines regulated by mMCP-4 in non-sensitized mice can be secreted by T cells. Investigations have shown that human chymase inhibits T cell adhesion to airway smooth muscle (ASM) cells and reduced epidermal growth factor-induced smooth muscle proliferation, which suggest that the local release of chymase may have profound effects on ASM cell function and airway remodeling[122]. Interestingly, the Th2 cytokine IL-5 appeared not to be regulated by mMCP-4. It should be mentioned, that IL-5 is produced by Th2-lymphocytes but also by several other cells like MC and eosinophils and plays also a key role in eosinophilia and mucus hypersecretion in asthma[103,123–125]. These data may indicate, that the source of IL-5 in my experimental approach did not originate from Th2 cells.

However, both mechanisms, degradation of cytokines and regulation of T cells by the enzyme do not explain why cytokine levels were not elevated in sensitized mice in the absence of mMCP-4 or were not elevated in MC-deficient W-sh mice. The reasons for this remain unclear. It is possible that a total lack of MC induces a compensatory mechanism replacing the regulatory function of mMCP-4 in homeostasis. Such mechanism could be provided e.g. by neutrophils, which are elevated in W-sh mice[52,54,126] and also contain several proteases capable in cleaving cytokines[121,127,128]. Furthermore, under inflammatory conditions, multiple proteases secreted e.g. from neutrophils, eosinophils, or macrophages may take over the degradation of T cell cytokines and prevent a hyperactivation of the immune system.

In summary, these results provide evidence for a previously unrecognized role of chymase in the regulation of T cell cytokines in homeostasis.

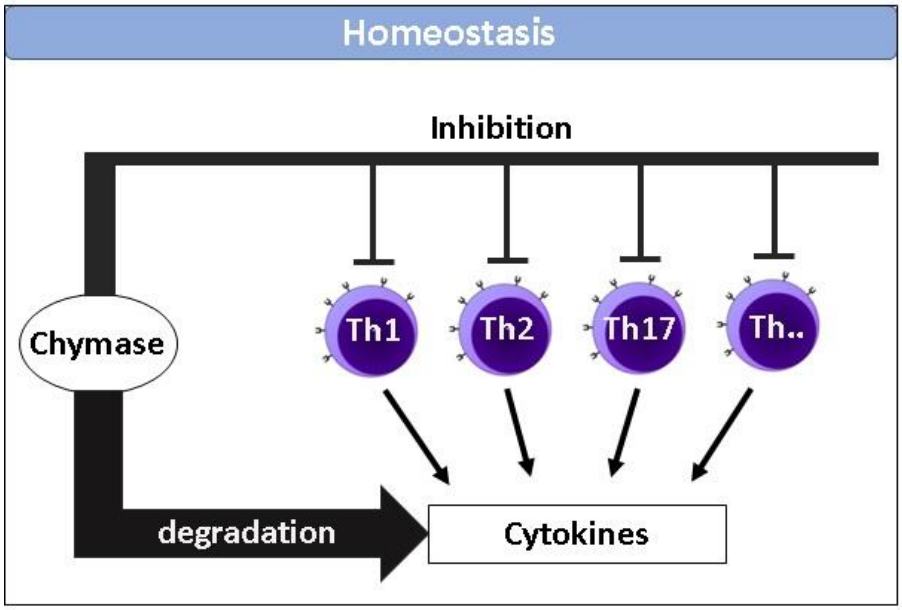

Fig. 22: Model of the regulatory function of chymase in the control of cytokine levels in homeostasis. Control of cytokine levels in homeostasis can be mediated by two different mechanisms: proteolytic degradation of cytokines by chymase or direct regulation of immune cell functions by the enzyme.

Chronic experimental asthma

In the field of asthma research, a variety of animal models are performed to elucidate asthma pathology, with differences in the sensitization protocol, the applied mouse strain as well as the used allergen. The majority of these asthma models are focusing on the acute inflammatory process. In acute models of asthma, sensitization is typically performed with two or 3 intraperitoneal injections, followed by allergen challenge one or two weeks later[49]. Symptoms induced by acute protocols represent many features observed in clinical asthma such as airway inflammation, goblet cell hyperplasia, AHR or elevated levels of allergen specific IgE and help to better understand the interaction of cells and inflammatory mediators and how they drive the acute airway inflammation in the lung. Nevertheless, in humans asthma is typically of chronic nature with features of chronic inflammation and airway remodeling, which cannot be investigated in acute asthma models[46]. Consequently, in this study an alum-free chronic model described by Yu et al[92] was performed to investigate the role of MC and chymase mMCP-4 in

experimental asthma. Different to acute models, the number of challenges was increased and the effector phase was extended. In this experimental setting, many hallmarks of human asthma, including AHR, airway wall remodeling with goblet cell hyperplasia and epithelial hypertrophy could be mimicked. The adjuvant aluminum hydroxide (alum), which is frequently used in the allergen sensitization process of acute as well as chronic models to boost the development of a Th2- driven allergic immune response[129–132], was not applied. Alum is known to promote a strong Th2 response, which may interfere with regulatory signals present in or required for the disease development under more physiological conditions[130,133]. The resulting allergic immune response in presence of alum has been shown to be independent of MC and other innate immune cells, where as its absence revealed an important role of MC in the induction of allergic asthma[50,51,134,135].

Airway hyperreactivity, mucus production, and lung inflammation - three independently regulated events in asthma?

AHR is an essential parameter in asthma diagnostic, which is defined by increased sensitivity to unspecific triggers resulting in bronchoconstriction. For the assessment of AHR, provocation by stimuli like methacholine or histamine are used to determine lung restistance[136]. In this study, AHR could be successfully induced after OVA sensitization and repeated OVA challenge in response to methacholine in *wt* C57BL/6 mice (Fig. 11, 12A). In sharp contrast to previous findings in acute models of asthma described by Waern et al[76,102], who described a strong increase of AHR in mMCP-4-deficient mice, in chronic experimental asthma these mice were protected from developing AHR (Fig. 12A). Moreover, AHR in OVA sensitized MC-deficient C57BL/6-*kit*$^{W\text{-}sh/W\text{-}sh}$ -mice reconstituted with MC derived from mMCP-4$^{-/-}$ mice was also significantly reduced compared to *wt* reconstituted animals, which confirmed the results seen in OVA sensitized mMCP-4$^{-/-}$ mice (Fig. 12B). My data indicate fundamental different roles of chymase in the acute and chronic course of the disease. While mMCP-4 acts protective in the initial phase of an allergic lung inflammation it turned out to be proinflammatory at later stages of the disorder. While the protective function of mMCP-4 is difficult to explain, many previous studies help to explicate its pathogenic role. Investigations have shown that human chymase has inflammatory effects on epithelial cells. Incubation of intestinal epithelial cells with human chymase increased epithelial permeability and decreased expression of tight junction proteins[83].

Furthermore, human chymase has been shown to be a potent stimulus of mucin secretion from bronchial epithelial cells[137]. In accordance to these findings, I could show a protease-mediated impairment of epithelial cell integrity by supernatants (SN) of activated human lung mast cells (hLMC). The observed effect was dependent on chymase, since it could be completely abolished by chymase inhibitor chymostatin. Incubation of epithelial cells with human chymase in the same setting approved this effect. Impairment of lung epithelium through repeated release of chymase in the chronic course of asthma may facilitate allergen uptake and infiltration of inflammatory cells and may also lead to excessive tissue turnover and remodeling process of lung epithelium. Beside a direct effect on tissue damage, mMCP-4 may also act indirectly by the activation of further immune cells. Increased numbers of neutrophils have been observed in lung tissue and sputum of patients with chronic and severe asthma[138–140]. As the accumulation of granulocytes is one of the hallmarks of allergic inflammation, investigators have studied the role of human chymase in recruitment of neutrophils and they have described that human chymase is a potent chemoattractant for neutrophils *in vitro* and intraperitoneal injection of human chymase in BALB/c mice induced the accumulation of neutrophils[82,101]. However, data from *in vitro* neutrophil chemotaxis assays performed in this study indicated only a weak chemotactic activity of chymase. Therefore, it appears more likely that chymase induces neutrophil chemotaxis indirectly, e.g. by proteolytic activation of chemokines. This was shown elegantly in a report of Schiemann *et al.* who could demonstrate the proteolytical processing of an inactive precursor of CXCL7 to its active, neutrophil-activating form[141].

Despite the clear proinflammatory function of mMCP-4, an opposing role for MC in general was identified here. OVA-sensitized MC-deficient C57BL/6-*kit*$^{W\text{-}sh/W\text{-}sh}$-mice developed significant increased AHR as compared to the wild type strain, indicating a protective function of MC in AHR in this experimental setting (Fig. 11). This effect could be reverted by the reconstitution of W-sh mice with MC derived from wild type animals. These findings are in contrast to results published by Yu *et al.* where AHR was decreased in OVA sensitized MC-deficient C57BL/6-*kit*$^{W\text{-}sh/W\text{-}sh}$ -mice in comparison to *wt* controls. Since the protocols for sensitization were identical and MC-reconstitution was successful in both studies, a possible explanation for the conflicting data could be the different route and dose of OVA challenge. In this study, all mice were challenged with 50 µl of 1,5% OVA oropharyngeally (= 750 µg OVA/challenge) while Yu et al applied 30 µl of 20 µg OVA intranasally for provocation.

Therefore, it appears likely that under conditions of high-dose allergen challenge, MC functions change from a disease-promoting towards a protective role in disease. Such protective effect could be mediated e.g. by the release of anti-inflammatory cytokines like TGF-β. Further

studies are required to define the conditions where this turning point in MC function becomes relevant for the pathogenesis of the disease. As summarized in Fig. 23, the differential effect of MC and mMCP-4 on the regulation of AHR in my asthma model could be explained when the presence of two antagonistic regulatory principles in MC are assumed. A currently unknown protective principle dominates the proinflammatory function of mMCP-4, leading to an attenuated AHR observed in *wt* mice. The loss of both regulatory pathways as seen in W-sh mice, results in increased AHR since the dominating protective function is missing now too. Finally, the lack of mMCP-4 shifts the balance completely toward protection and disables the development of AHR.

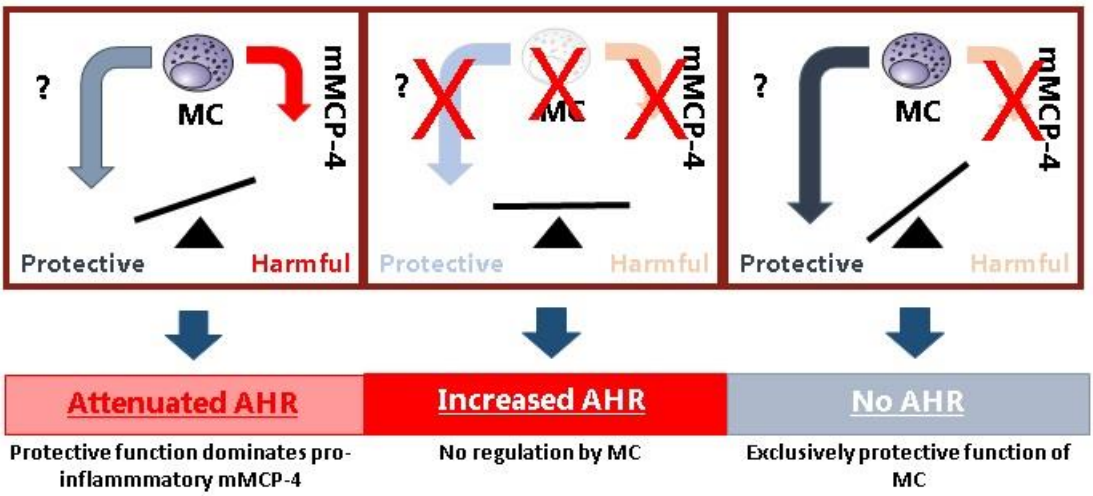

Fig. 23: Different regulation by MC and chymase mMCP-4 in the induction of AHR. MC harbor protective as well as proinflammatory functions. The MC mediator mMCP-4 represents a proinflammatory function in chronic asthma. Attenuated AHR results from the presence of both regulatory principles in which the protective pathway dominates the proinflammatory function of mMCP-4. In the absence of both regulatory principles in MC-deficient mice AHR increases. When selectively the proinflammatory mMCP-4 is lacking, the protective function of MC is fully developed and AHR is suppressed.

Goblet cell hyperplasia is a characteristic feature of airway remodeling in asthma. Goblet cells are major mucus-producing cells and airway mucus hypersecretion contributes to airflow limitation and airway obstruction[142,143]. Goblet cell hyperplasia and mucus hypersecretion have been induced in many adjuvant-free experimental asthma models [46,135,144–147]. Evidence for this characteristic feature was also observed in the performed adjuvant-free chronic model of asthma in this study. All non-sensitized control mice showed a slight increase in goblet cells and mucus volume when compared to naïve *wt* mice (Fig. 14H, J and Fig. 14 K, L). However, a further dramatic increase in goblet cells accompanied with increased mucus production was observed

in OVA sensitized mice as compared to PBS controls (Fig. 14K, L and Fig. 15J- M). Despite to the findings for AHR, no differences could be observed between wild types, MC-deficient mice or MC-deficient mice reconstituted either with wild type MC or mMCP-4$^{-/-}$ MC. Conclusively, allergen induced goblet cell hyperplasia and mucus production in lung tissue of sensitized mice appeared to be regulated independently of MC or chymase mMCP-4. In contrast, data obtained by Yu et. al and other adjuvant-free acute models of asthma using MC-deficient W-sh or W/W-v mice showed MC dependent induction of goblet cell hyperplasia and mucus hypersecretion[92,113,148–150]. Consistent with the data obtained in my study, Wearn *et al.* did also see a no differences in the degree of goblet cell hyperplasia in allergen-treated wt and mMCP-4$^{-/-}$ mice. This is surprising, since chymases have been shown to contribute to extra cellular matrix (ECM) remodeling in a direct way through activation of matrix metalloproteinases (MMPs) or indirect through cleavage of non-helical collagens and fibronectin[35,75,151,152].

Asthma is a disease of airway inflammation and a variety of inflammatory cell types including lymphocytes and macrophages, especially neutrophils and eosinophils, have been noted in lung tissue and bronchoalveolar lavage (BAL) of asthmatic patients as well as in experimental asthma and therefore been implicated as potential effector cells in asthma[86,92,113,135,138,139,153–162]. However, results of the chronic model used did not provide conclusive data concerning the inflammatory status of the diseased lung. Analysis of inflammatory cells in BAL and lung tissue revealed an increase of inflammatory cells as compared to naïve mice (Fig 13A and Fig. 16A). However, this effect was seen without difference in all experimental groups irrespective whether animals were sensitized or not. Therefore, it is possible that repeated challenge with high dosages of OVA over a period of 9 weeks induced marked increase of inflammatory cells in BAL also in non-sensitized animals (Fig. 13B-Q), indicating a critical limitation of this model. A MC-dependent regulation in macrophages could be assumed since sensitized MC-deficient mice showed significantly increased numbers of macrophages compared to sensitized *wt* mice (Fig. 13D). Nevertheless, this presumption is weakened by the fact that first, total cell numbers in MC-deficient W-sh mice were increased compared to *wt* mice (Fig. 13B) and second, MC-deficient mice reconstituted with *wt* (Fig. 13C-F) as well as with mMCP-4$^{-/-}$ (ko) MC (Fig. 13M-Q) show similarly tendency of increased inflammatory cells. A significant increase in eosinophil numbers was observed in OVA-sensitized MC-deficient W-sh mice reconstituted with mMCP-4$^{-/-}$ (ko) MC compared to *wt* counterpart (Fig. 13N), but this could not be confirmed in the obtained data of sensitized mMCP-4$^{-/-}$ mice (Fig. 13 H). The overall

increase of inflammatory cells in MC-deficient mice independent of reconstitution appear to be strain specific. Nonetheless, it should be noted that although an infiltration of inflammatory cells was seen in all groups, clinical symptoms in terms of AHR and mucus production were different between the individual experimental categories.

For a long time, the three cardinal symptoms of asthma, AHR, mucus production, and lung inflammation were seen as commonly regulated pathomechanisms. This idea was doubted already in earlier studies of Kearley *et al.*[163], who could show that AHR and goblet cell hyperplasia could persist in the absence of further inflammatory signs. The results of this study enable a further breakdown of the processes in asthma by segregating AHR as regulated by MC and mMCP-4 from goblet cell hyperplasia and mucus production. Further investigations have to address the question by which cellular and molecular mechanisms MC and mMCP-4 drive AHR in allergic asthma.

Conclusions and outlook

The current study delineates the role of MC and the MC chymase mMCP-4 in the pathogenesis of chronic experimental asthma. Furthermore, it uncovers a previous unrecognized role of mMCP-4 in the regulation of T cell cytokines under homeostatic conditions.

Due to their prominent role in allergic inflammation, since a long-time MC and their proinflammatory products have been identified as attractive potential targets for the treatment of such diseases. While this was successful for some MC-derived mediators like histamine or certain prostaglandins, stabilization of MC in humans was not effective so far[164–168]. This may be caused by the fact that MC as well as their mediators have diverse and partially antagonizing functions under different inflammatory conditions. In acute models of asthma, MC play a disease promoting role while mMCP-4 protects mice from developing disease. According to the results of this study, at least under high dosage antigen challenge, a reciprocal conversion of the function of both players in the modulation of AHR was observed. While the lack of MC led to an increase of AHR, a deficiency of mMCP-4 abolished this reaction. The discrepancy on the function of mMCP-4 in acute and chronic models of asthma may be at least partially explained by its function in homeostasis. In non-sensitized mice lacking mMCP-4, a dramatic elevation of a broad spectrum of different T cell cytokines was observed, indicating that mMCP-4 is involved in the removal or suppression of unwanted cytokines produced in the

body. This could protect the host from inadequate immune reactions and a lack of chymase may promote inflammation as seen in the acute model of asthma. However, in chronic inflammation this function is lost or replaced by other control mechanism and mMCP-4 exposes a second face of the enzyme. While MC in general have a protective effect on the induction of AHR, mMCP-4 clearly promotes this disease symptom. Noteworthy, that neither MC nor mMCP-4 are required for an induction of goblet cell hyperplasia or mucus production, indicating that the regulation of the latter events is clearly separated from that of AHR.

Based on these findings, first future directions on the use of MC and chymase as therapeutic targets can be identified. While approaches addressing directly MC and their functions may be most promising in the early manifestation of the disease or during an acute allergic attack, inhibition or deletion of these cells at later or chronic stages of the disease may be critical due to their potential protective role in this phase. Vice versa, targeting chymase during early or even unclear disease could lead to unwanted exacerbation which may be caused by a deletion of its protective regulatory function during this period. However, with regard to its pathogenic role on AHR at more chronic stages, selective inhibition of chymase could represent a future therapeutic option.

It is clear, that the current study shed only a first light on the significance of chymase on the development of human asthma. Several future studies are required to substantiate these findings and to address the mechanisms underlying its regulatory role in homeostasis as well as acute and chronic disease. In the next step, a critical comparison between human chymase and mMCP-4 in target specificity and regulatory functions should be addressed which will provide more evidence of my findings for the disease in humans.

References

1. Becker, A. B. & Abrams, E. M. Asthma guidelines: The Global Initiative for Asthma in relation to national guidelines. *Curr. Opin. Allergy Clin. Immunol.* (2017). doi:10.1097/ACI.0000000000000346
2. Nunes, C., Pereira, A. M. & Morais-Almeida, M. Asthma costs and social impact. *Asthma Res. Pract.* **3,** (2017).
3. Masoli, M., Fabian, D., Holt, S., Beasley, R. & Global Initiative for Asthma (GINA) Program. The global burden of asthma: executive summary of the GINA Dissemination Committee Report. *Allergy* **59,** 469–478 (2004).
4. Braman, S. S. The global burden of asthma. *Chest* **130,** 4S–12S (2006).
5. Accordini, S. *et al.* The Cost of Persistent Asthma in Europe: An International Population-Based Study in Adults. *Int. Arch. Allergy Immunol.* **160,** 93–101 (2013).
6. Agostinis, F. *et al.* The safety of sublingual immunotherapy with one or multiple pollen allergens in children. *Allergy* **63,** 1637–1639 (2008).
7. Bateman, E. D. *et al.* Global strategy for asthma management and prevention: GINA executive summary. *Eur. Respir. J.* **31,** 143–178 (2008).
8. Kim, Y.-M., Kim, Y.-S., Jeon, S. G. & Kim, Y.-K. Immunopathogenesis of Allergic Asthma: More Than the Th2 Hypothesis. *Allergy Asthma Immunol. Res.* **5,** 189–196 (2013).
9. Anderson, G. P. Endotyping asthma: new insights into key pathogenic mechanisms in a complex, heterogeneous disease. *Lancet Lond. Engl.* **372,** 1107–1119 (2008).
10. Lötvall, J. *et al.* Asthma endotypes: a new approach to classification of disease entities within the asthma syndrome. *J. Allergy Clin. Immunol.* **127,** 355–360 (2011).
11. Wenzel, S. E. Asthma phenotypes: the evolution from clinical to molecular approaches. *Nat. Med.* **18,** 716–725 (2012).

12. Passalacqua, G. & Ciprandi, G. Allergy and the lung. *Clin. Exp. Immunol.* **153,** 12–16 (2008).
13. Salazar, F. & Ghaemmaghami, A. M. Allergen Recognition by Innate Immune Cells: Critical Role of Dendritic and Epithelial Cells. *Front. Immunol.* **4,** (2013).
14. Karp, C. L. Guilt by intimate association: What makes an allergen an allergen? *J. Allergy Clin. Immunol.* **125,** 955–962 (2010).
15. Paul, W. E. & Zhu, J. How are TH2-type immune responses initiated and amplified? *Nat. Rev. Immunol.* **10,** 225–235 (2010).
16. Woodfolk, J. A., Commins, S. P., Schuyler, A. J., Erwin, E. A. & Platts-Mills, T. A. E. Allergens, sources, particles, and molecules: Why do we make IgE responses? *Allergol. Int.* **64,** 295–303 (2015).
17. Galli, S. J., Tsai, M. & Piliponsky, A. M. The development of allergic inflammation. *Nature* **454,** 445–454 (2008).
18. Trinchieri, G., Pflanz, S. & Kastelein, R. A. The IL-12 family of heterodimeric cytokines: new players in the regulation of T cell responses. *Immunity* **19,** 641–644 (2003).
19. Lighvani, A. A. *et al.* T-bet is rapidly induced by interferon-gamma in lymphoid and myeloid cells. *Proc. Natl. Acad. Sci. U. S. A.* **98,** 15137–15142 (2001).
20. Kraft, S. & Kinet, J.-P. New developments in FcepsilonRI regulation, function and inhibition. *Nat. Rev. Immunol.* **7,** 365–378 (2007).
21. Galli, S. J. *et al.* Mast cells as 'tunable' effector and immunoregulatory cells: recent advances. *Annu. Rev. Immunol.* **23,** 749–786 (2005).
22. Doherty, T. & Broide, D. Cytokines and growth factors in airway remodeling in asthma. *Curr. Opin. Immunol.* **19,** 676–680 (2007).
23. Arock, M. Mast cell differentiation: still open questions? *Blood* **127,** 373–374 (2016).
24. DeBruin, E. J. *et al.* Mast cells in human health and disease. *Methods Mol. Biol. Clifton NJ* **1220,** 93–119 (2015).

25. Amin, K. The role of mast cells in allergic inflammation. *Respir. Med.* **106,** 9–14 (2012).
26. Galli, S. J., Grimbaldeston, M. & Tsai, M. Immunomodulatory mast cells: negative, as well as positive, regulators of innate and acquired immunity. *Nat. Rev. Immunol.* **8,** 478–486 (2008).
27. Galli, S. J. *et al.* Approaches for analyzing the roles of mast cells and their proteases in vivo. *Adv. Immunol.* **126,** 45–127 (2015).
28. Brightling, C. E. *et al.* Mast-cell infiltration of airway smooth muscle in asthma. *N. Engl. J. Med.* **346,** 1699–1705 (2002).
29. Mathias, C. B. *et al.* IgE influences the number and function of mature mast cells, but not progenitor recruitment in allergic pulmonary inflammation. *J. Immunol. Baltim. Md 1950* **182,** 2416–2424 (2009).
30. Abonia, J. P. *et al.* Alpha-4 integrins and VCAM-1, but not MAdCAM-1, are essential for recruitment of mast cell progenitors to the inflamed lung. *Blood* **108,** 1588–1594 (2006).
31. Anand, P., Singh, B., Jaggi, A. S. & Singh, N. Mast cells: an expanding pathophysiological role from allergy to other disorders. *Naunyn. Schmiedebergs Arch. Pharmacol.* **385,** 657–670 (2012).
32. Moon, T. C. *et al.* Advances in mast cell biology: new understanding of heterogeneity and function. *Mucosal Immunol.* **3,** 111–128 (2009).
33. Iwasaki, A. & Medzhitov, R. Toll-like receptor control of the adaptive immune responses. *Nat. Immunol.* **5,** 987–995 (2004).
34. Bax, H. J., Keeble, A. H. & Gould, H. J. Cytokinergic IgE Action in Mast Cell Activation. *Front. Immunol.* **3,** (2012).
35. Caughey, G. H. Mast cell tryptases and chymases in inflammation and host defense. *Immunol. Rev.* **217,** 141–154 (2007).
36. Pejler, G., Abrink, M., Ringvall, M. & Wernersson, S. Mast cell proteases. *Adv. Immunol.* **95,** 167–255 (2007).

37. Hart, P. H. Regulation of the inflammatory response in asthma by mast cell products. *Immunol. Cell Biol.* **79,** 149–153 (2001).

38. Bradding, P., Walls, A. F. & Holgate, S. T. The role of the mast cell in the pathophysiology of asthma. *J. Allergy Clin. Immunol.* **117,** 1277–1284 (2006).

39. Pejler, G., Knight, S. D., Henningsson, F. & Wernersson, S. Novel insights into the biological function of mast cell carboxypeptidase A. *Trends Immunol.* **30,** 401–408 (2009).

40. Fajt, M. L. *et al.* Prostaglandin D2 pathway upregulation: Relation to asthma severity, control, and TH2 inflammation. *J. Allergy Clin. Immunol.* **131,** 1504–1512 (2013).

41. Bischoff, S. C. & Krämer, S. Human mast cells, bacteria, and intestinal immunity. *Immunol. Rev.* **217,** 329–337 (2007).

42. Pelaia, G. *et al.* Cellular Mechanisms Underlying Eosinophilic and Neutrophilic Airway Inflammation in Asthma. *Mediators Inflamm.* **2015,** (2015).

43. Possa, S. S., Leick, E. A., Prado, C. M., Martins, M. A. & Tibério, I. F. L. C. Eosinophilic Inflammation in Allergic Asthma. *Front. Pharmacol.* **4,** (2013).

44. Erle, D. J. & Sheppard, D. The cell biology of asthma. *J Cell Biol* **205,** 621–631 (2014).

45. Zosky, G. R. & Sly, P. D. Animal models of asthma. *Clin. Exp. Allergy* **37,** 973–988 (2007).

46. Nials, A. T. & Uddin, S. Mouse models of allergic asthma: acute and chronic allergen challenge. *Dis. Model. Mech.* **1,** 213–220 (2008).

47. Reddy, A. T., Lakshmi, S. P. & Reddy, R. C. Murine model of allergen induced asthma. *J. Vis. Exp. JoVE* e3771 (2012). doi:10.3791/3771

48. Irvin, C. G. & Bates, J. H. Measuring the lung function in the mouse: the challenge of size. *Respir. Res.* **4,** 4 (2003).

49. Bates, J. H. T., Rincon, M. & Irvin, C. G. Animal models of asthma. *Am. J. Physiol. - Lung Cell. Mol. Physiol.* **297,** L401–L410 (2009).

50. Takeda, K. *et al.* Development of Eosinophilic Airway Inflammation and Airway Hyperresponsiveness in Mast Cell–deficient Mice. *J. Exp. Med.* **186,** 449–454 (1997).

51. Williams, C. M. & Galli, S. J. Mast cells can amplify airway reactivity and features of chronic inflammation in an asthma model in mice. *J. Exp. Med.* **192,** 455–462 (2000).

52. Lei, Y., Gregory, J. A., Nilsson, G. P. & Adner, M. Insights into mast cell functions in asthma using mouse models. *Pulm. Pharmacol. Ther.* **26,** 532–539 (2013).

53. Oka, T., Kalesnikoff, J., Starkl, P., Tsai, M. & Galli, S. J. Evidence questioning cromolyn's effectiveness and selectivity as a 'mast cell stabilizer' in mice. *Lab. Investig. J. Tech. Methods Pathol.* **92,** 1472–1482 (2012).

54. Reber, L. L., Marichal, T. & Galli, S. J. New models for analyzing mast cell functions in vivo. *Trends Immunol.* **33,** 613–625 (2012).

55. Galli, S. J. & Kitamura, Y. Genetically mast-cell-deficient W/Wv and Sl/Sld mice. Their value for the analysis of the roles of mast cells in biologic responses in vivo. *Am. J. Pathol.* **127,** 191–198 (1987).

56. Berrozpe, G. *et al.* The W(sh), W(57), and Ph Kit expression mutations define tissue-specific control elements located between -23 and -154 kb upstream of Kit. *Blood* **94,** 2658–2666 (1999).

57. Pejler, G., Rönnberg, E., Waern, I. & Wernersson, S. Mast cell proteases: multifaceted regulators of inflammatory disease. *Blood* **115,** 4981–4990 (2010).

58. Hellman, L. & Thorpe, M. Granule proteases of hematopoietic cells, a family of versatile inflammatory mediators - an update on their cleavage specificity, in vivo substrates, and evolution. *Biol. Chem.* **395,** 15–49 (2014).

59. Chandrasekharan, U. M., Sanker, S., Glynias, M. J., Karnik, S. S. & Husain, A. Angiotensin II-forming activity in a reconstructed ancestral chymase. *Science* **271,** 502–505 (1996).

60. Karlson, U., Pejler, G., Tomasini-Johansson, B. & Hellman, L. Extended substrate specificity of rat mast cell protease 5, a rodent alpha-chymase with elastase-like primary specificity. *J. Biol. Chem.* **278,** 39625–39631 (2003).

61. Pejler, G., Abrink, M. & Wernersson, S. Serglycin proteoglycan: regulating the storage and activities of hematopoietic proteases. *BioFactors Oxf. Engl.* **35,** 61–68 (2009).

62. Abrink, M., Grujic, M. & Pejler, G. Serglycin is essential for maturation of mast cell secretory granule. *J. Biol. Chem.* **279,** 40897–40905 (2004).

63. Forsberg, E. *et al.* Abnormal mast cells in mice deficient in a heparin-synthesizing enzyme. *Nature* **400,** 773–776 (1999).

64. Pemberton, A. D. *et al.* Purification and characterization of mouse mast cell proteinase-2 and the differential expression and release of mouse mast cell proteinase-1 and -2 in vivo. *Clin. Exp. Allergy J. Br. Soc. Allergy Clin. Immunol.* **33,** 1005–1012 (2003).

65. Andersson, M. K., Karlson, U. & Hellman, L. The extended cleavage specificity of the rodent beta-chymases rMCP-1 and mMCP-4 reveal major functional similarities to the human mast cell chymase. *Mol. Immunol.* **45,** 766–775 (2008).

66. Tchougounova, E., Pejler, G. & Abrink, M. The chymase, mouse mast cell protease 4, constitutes the major chymotrypsin-like activity in peritoneum and ear tissue. A role for mouse mast cell protease 4 in thrombin regulation and fibronectin turnover. *J. Exp. Med.* **198,** 423–431 (2003).

67. Magnusson, S. E., Pejler, G., Kleinau, S. & Abrink, M. Mast cell chymase contributes to the antibody response and the severity of autoimmune arthritis. *FASEB J. Off. Publ. Fed. Am. Soc. Exp. Biol.* **23,** 875–882 (2009).

68. Sun, J. *et al.* Critical role of mast cell chymase in mouse abdominal aortic aneurysm formation. *Circulation* **120,** 973–982 (2009).

69. Lin, L. *et al.* Dual targets for mouse mast cell protease-4 in mediating tissue damage in experimental bullous pemphigoid. *J. Biol. Chem.* **286,** 37358–37367 (2011).

70. Beghdadi, W. *et al.* Mast cell chymase protects against renal fibrosis in murine unilateral ureteral obstruction. *Kidney Int.* **84,** 317–326 (2013).

71. Hendrix, S. *et al.* Mast cells protect from post-traumatic brain inflammation by the mast cell-specific chymase mouse mast cell protease-4. *FASEB J. Off. Publ. Fed. Am. Soc. Exp. Biol.* **27,** 920–929 (2013).

72. Nelissen, S. *et al.* Mast cells protect from post-traumatic spinal cord damage in mice by degrading inflammation-associated cytokines via mouse mast cell protease 4. *Neurobiol. Dis.* **62,** 260–272 (2014).

73. Piliponsky, A. M. *et al.* The chymase mouse mast cell protease 4 degrades TNF, limits inflammation, and promotes survival in a model of sepsis. *Am. J. Pathol.* **181,** 875–886 (2012).

74. Akahoshi, M. *et al.* Mast cell chymase reduces the toxicity of Gila monster venom, scorpion venom, and vasoactive intestinal polypeptide in mice. *J. Clin. Invest.* **121,** 4180–4191 (2011).

75. Tchougounova, E. *et al.* A key role for mast cell chymase in the activation of pro-matrix metalloprotease-9 and pro-matrix metalloprotease-2. *J. Biol. Chem.* **280,** 9291–9296 (2005).

76. Waern, I. *et al.* Mouse mast cell protease 4 is the major chymase in murine airways and has a protective role in allergic airway inflammation. *J. Immunol. Baltim. Md 1950* **183,** 6369–6376 (2009).

77. Waern, I., Lundequist, A., Pejler, G. & Wernersson, S. Mast cell chymase modulates IL-33 levels and controls allergic sensitization in dust-mite induced airway inflammation. *Mucosal Immunol.* **6,** 911–920 (2013).

78. Andersson, M. K., Enoksson, M., Gallwitz, M. & Hellman, L. The extended substrate specificity of the human mast cell chymase reveals a serine protease with well-defined substrate recognition profile. *Int. Immunol.* **21,** 95–104 (2009).

79. Saarinen, J., Kalkkinen, N., Welgus, H. G. & Kovanen, P. T. Activation of human interstitial procollagenase through direct cleavage of the Leu83-Thr84 bond by mast cell chymase. *J. Biol. Chem.* **269,** 18134–18140 (1994).

80. Reilly, C. F., Tewksbury, D. A., Schechter, N. M. & Travis, J. Rapid conversion of angiotensin I to angiotensin II by neutrophil and mast cell proteinases. *J. Biol. Chem.* **257,** 8619–8622 (1982).

81. Urata, H., Kinoshita, A., Misono, K. S., Bumpus, F. M. & Husain, A. Identification of a highly specific chymase as the major angiotensin II-forming enzyme in the human heart. *J. Biol. Chem.* **265,** 22348–22357 (1990).

82. Tani, K. *et al.* Chymase is a potent chemoattractant for human monocytes and neutrophils. *J. Leukoc. Biol.* **67,** 585–589 (2000).

83. Groschwitz, K. R., Wu, D., Osterfeld, H., Ahrens, R. & Hogan, S. P. Chymase-mediated intestinal epithelial permeability is regulated by a protease-activating receptor/matrix metalloproteinase-2-dependent mechanism. *Am. J. Physiol. Gastrointest. Liver Physiol.* **304,** G479-489 (2013).

84. Reuter, S., Stassen, M. & Taube, C. Mast Cells in Allergic Asthma and Beyond. *Yonsei Med. J.* **51,** 797–807 (2010).

85. Bradding, P. *et al.* Interleukin-4, -5, and -6 and tumor necrosis factor-alpha in normal and asthmatic airways: evidence for the human mast cell as a source of these cytokines. *Am. J. Respir. Cell Mol. Biol.* **10,** 471–480 (1994).

86. Carroll, N. G., Mutavdzic, S. & James, A. L. Increased mast cells and neutrophils in submucosal mucous glands and mucus plugging in patients with asthma. *Thorax* **57,** 677–682 (2002).

87. Kasper, B., Thole, H. H., Patterson, S. D. & Welte, K. Cytosolic proteins from neutrophilic granulocytes: a comparison between patients with severe chronic neutropenia and healthy donors. *Electrophoresis* **18,** 142–149 (1997).

88. The Cathelicidin LL-37 Activates Human Mast Cells and Is Degraded by Mast Cell Tryptase: Counter-Regulation by CXCL4 | The Journal of Immunology. Available at: http://www.jimmunol.org/content/183/4/2223.long. (Accessed: 21st March 2017)

89. Orinska, Z. *et al.* TLR3-induced activation of mast cells modulates CD8+ T-cell recruitment. *Blood* **106,** 978–987 (2005).

90. Cozens, A. L. *et al.* CFTR expression and chloride secretion in polarized immortal human bronchial epithelial cells. *Am. J. Respir. Cell Mol. Biol.* **10,** 38–47 (1994).

91. Ludwig, A., Schiemann, F., Mentlein, R., Lindner, B. & Brandt, E. Dipeptidyl peptidase IV (CD26) on T cells cleaves the CXC chemokine CXCL11 (I-TAC) and abolishes the stimulating but not the desensitizing potential of the chemokine. *J. Leukoc. Biol.* **72,** 183–191 (2002).

92. Yu, M. *et al.* Mast cells can promote the development of multiple features of chronic asthma in mice. *J. Clin. Invest.* **116,** 1633–1641 (2006).

93. O'Byrne, P. M., Gauvreau, G. M. & Brannan, J. D. Provoked models of asthma: what have we learnt? *Clin. Exp. Allergy J. Br. Soc. Allergy Clin. Immunol.* **39,** 181–192 (2009).

94. Tung, J. W. *et al.* Modern Flow Cytometry: A Practical Approach. *Clin. Lab. Med.* **27,** 453–v (2007).

95. Mattfeldt, T., Mall, G., Gharehbaghi, H. & Möller, P. Estimation of surface area and length with the orientator. *J. Microsc.* **159,** 301–317 (1990).

96. Hsia, C. C. W., Hyde, D. M., Ochs, M. & Weibel, E. R. An Official Research Policy Statement of the American Thoracic Society/European Respiratory Society: Standards for Quantitative Assessment of Lung Structure. *Am. J. Respir. Crit. Care Med.* **181,** 394–418 (2010).

97. Sridharan, G. & Shankar, A. A. Toluidine blue: A review of its chemistry and clinical utility. *J. Oral Maxillofac. Pathol. JOMFP* **16,** 251–255 (2012).

98. Fajt, M. L. & Wenzel, S. E. Mast cells, their subtypes, and relation to asthma phenotypes. *Ann. Am. Thorac. Soc.* **10 Suppl,** S158-164 (2013).

99. Balzar, S. *et al.* Mast Cell Phenotype, Location, and Activation in Severe Asthma. *Am. J. Respir. Crit. Care Med.* **183,** 299–309 (2011).

100. Bentley, A. M. *et al.* Prednisolone treatment in asthma. Reduction in the numbers of eosinophils, T cells, tryptase-only positive mast cells, and modulation of IL-4, IL-5, and interferon-gamma cytokine gene expression within the bronchial mucosa. *Am. J. Respir. Crit. Care Med.* **153,** 551–556 (1996).

101. He, S. & Walls, A. F. Human mast cell chymase induces the accumulation of neutrophils, eosinophils and other inflammatory cells in vivo. *Br. J. Pharmacol.* **125,** 1491–1500 (1998).

102. Waern, I. *et al.* Mast cells limit extracellular levels of IL-13 via a serglycin proteoglycan-serine protease axis. *Biol. Chem.* **393,** 1555–1567 (2012).

103. Schuijs, M. J., Willart, M. A., Hammad, H. & Lambrecht, B. N. Cytokine targets in airway inflammation. *Curr. Opin. Pharmacol.* **13,** 351–361 (2013).

104. Venkayya, R. *et al.* The Th2 lymphocyte products IL-4 and IL-13 rapidly induce airway hyperresponsiveness through direct effects on resident airway cells. *Am. J. Respir. Cell Mol. Biol.* **26,** 202–208 (2002).

105. Rincon, M. & Irvin, C. G. Role of IL-6 in asthma and other inflammatory pulmonary diseases. *Int. J. Biol. Sci.* **8,** 1281–1290 (2012).

106. Doe, C. *et al.* Expression of the T helper 17-associated cytokines IL-17A and IL-17F in asthma and COPD. *Chest* **138,** 1140–1147 (2010).

107. Alcorn, J. F., Crowe, C. R. & Kolls, J. K. TH17 cells in asthma and COPD. *Annu. Rev. Physiol.* **72,** 495–516 (2010).

108. Hawrylowicz, C. M. & O'Garra, A. Potential role of interleukin-10-secreting regulatory T cells in allergy and asthma. *Nat. Rev. Immunol.* **5,** 271–283 (2005).

109. Lloyd, C. M. & Hawrylowicz, C. M. Regulatory T Cells in Asthma. *Immunity* **31,** 438–449 (2009).

110. Zhu, W. & Gilmour, M. I. Comparison of allergic lung disease in three mouse strains after systemic or mucosal sensitization with ovalbumin antigen. *Immunogenetics* **61,** 199–207 (2009).

111. De Vooght, V. *et al.* Choice of mouse strain influences the outcome in a mouse model of chemical-induced asthma. *PloS One* **5,** e12581 (2010).

112. Gueders, M. M. *et al.* Mouse models of asthma: a comparison between C57BL/6 and BALB/c strains regarding bronchial responsiveness, inflammation, and cytokine production. *Inflamm. Res. Off. J. Eur. Histamine Res. Soc. Al* **58,** 845–854 (2009).

113. Yu, M. *et al.* Identification of an IFN-γ/mast cell axis in a mouse model of chronic asthma. *J. Clin. Invest.* **121,** 3133–3143 (2011).

114. Mizutani, H., Schechter, N., Lazarus, G., Black, R. A. & Kupper, T. S. Rapid and specific conversion of precursor interleukin 1 beta (IL-1 beta) to an active IL-1 species by human mast cell chymase. *J. Exp. Med.* **174,** 821–825 (1991).

115. Omoto, Y. *et al.* Human mast cell chymase cleaves pro-IL-18 and generates a novel and biologically active IL-18 fragment. *J. Immunol. Baltim. Md 1950* **177,** 8315–8319 (2006).

116. Longley, B. J. *et al.* Chymase cleavage of stem cell factor yields a bioactive, soluble product. *Proc. Natl. Acad. Sci. U. S. A.* **94,** 9017–9021 (1997).

117. Guillabert, A. *et al.* Role of neutrophil proteinase 3 and mast cell chymase in chemerin proteolytic regulation. *J. Leukoc. Biol.* **84,** 1530–1538 (2008).

118. Gela, A. *et al.* Eotaxin-3 (CCL26) exerts innate host defense activities that are modulated by mast cell proteases. *Allergy* **70,** 161–170 (2015).

119. Roy, A. *et al.* Mast cell chymase degrades the alarmins heat shock protein 70, biglycan, HMGB1, and interleukin-33 (IL-33) and limits danger-induced inflammation. *J. Biol. Chem.* **289,** 237–250 (2014).

120. Lefrançais, E. *et al.* Central domain of IL-33 is cleaved by mast cell proteases for potent activation of group-2 innate lymphoid cells. *Proc. Natl. Acad. Sci. U. S. A.* **111,** 15502–15507 (2014).

121. Fu, Z. *et al.* Highly Selective Cleavage of Cytokines and Chemokines by the Human Mast Cell Chymase and Neutrophil Cathepsin G. *J. Immunol. Baltim. Md 1950* **198,** 1474–1483 (2017).

122. Lazaar, A. L. *et al.* Mast Cell Chymase Modifies Cell-Matrix Interactions and Inhibits Mitogen-Induced Proliferation of Human Airway Smooth Muscle Cells. *J. Immunol.* **169,** 1014–1020 (2002).

123. Rothenberg, M. E. & Hogan, S. P. The eosinophil. *Annu. Rev. Immunol.* **24,** 147–174 (2006).

124. Menzies-Gow, A. *et al.* Anti-IL-5 (mepolizumab) therapy induces bone marrow eosinophil maturational arrest and decreases eosinophil progenitors in the bronchial mucosa of atopic asthmatics. *J. Allergy Clin. Immunol.* **111,** 714–719 (2003).

125. Takatsu, K. & Nakajima, H. IL-5 and eosinophilia. *Curr. Opin. Immunol.* **20,** 288–294 (2008).

126. Grimbaldeston, M. A. *et al.* Mast Cell-Deficient W-sash c-kit Mutant KitW-sh/W-sh Mice as a Model for Investigating Mast Cell Biology in Vivo. *Am. J. Pathol.* **167,** 835–848 (2005).

127. Korkmaz, B., Moreau, T. & Gauthier, F. Neutrophil elastase, proteinase 3 and cathepsin G: physicochemical properties, activity and physiopathological functions. *Biochimie* **90,** 227–242 (2008).

128. Korkmaz, B., Horwitz, M. S., Jenne, D. E. & Gauthier, F. Neutrophil elastase, proteinase 3, and cathepsin G as therapeutic targets in human diseases. *Pharmacol. Rev.* **62,** 726–759 (2010).

129. Eisenbarth, S. C. Use and limitations of alum-based models of allergy. *Clin. Exp. Allergy* **38,** 1572–1575 (2008).

130. Brewer, J. M. *et al.* Aluminium hydroxide adjuvant initiates strong antigen-specific Th2 responses in the absence of IL-4- or IL-13-mediated signaling. *J. Immunol. Baltim. Md 1950* **163,** 6448–6454 (1999).

131. Kool, M. *et al.* Alum adjuvant boosts adaptive immunity by inducing uric acid and activating inflammatory dendritic cells. *J. Exp. Med.* **205,** 869–882 (2008).

132. Lambrecht, B. N., Kool, M., Willart, M. A. M. & Hammad, H. Mechanism of action of clinically approved adjuvants. *Curr. Opin. Immunol.* **21,** 23–29 (2009).

133. Lambrecht, B. N., Kool, M., Willart, M. A. M. & Hammad, H. Mechanism of action of clinically approved adjuvants. *Curr. Opin. Immunol.* **21,** 23–29 (2009).

134. Nakae, S. *et al.* TNF can contribute to multiple features of ovalbumin-induced allergic inflammation of the airways in mice. *J. Allergy Clin. Immunol.* **119,** 680–686 (2007).

135. Conrad, M. L. *et al.* Comparison of adjuvant and adjuvant-free murine experimental asthma models. *Clin. Exp. Allergy J. Br. Soc. Allergy Clin. Immunol.* **39,** 1246–1254 (2009).

136. Berend, N., Salome, C. M. & King, G. G. Mechanisms of airway hyperresponsiveness in asthma. *Respirol. Carlton Vic* **13,** 624–631 (2008).

137. He, S.-H. & Zheng, J. Stimulation of mucin secretion from human bronchial epithelial cells by mast cell chymase. *Acta Pharmacol. Sin.* **25,** 827–832 (2004).

138. Fahy, J. V., Kim, K. W., Liu, J. & Boushey, H. A. Prominent neutrophilic inflammation in sputum from subjects with asthma exacerbation. *J. Allergy Clin. Immunol.* **95,** 843–852 (1995).

139. Jatakanon, A. *et al.* Neutrophilic inflammation in severe persistent asthma. *Am. J. Respir. Crit. Care Med.* **160,** 1532–1539 (1999).

140. Foley, S. C. & Hamid, Q. Images in allergy and immunology: neutrophils in asthma. *J. Allergy Clin. Immunol.* **119,** 1282–1286 (2007).

141. Schiemann, F. *et al.* Mast cells and neutrophils proteolytically activate chemokine precursor CTAP-III and are subject to counterregulation by PF-4 through inhibition of chymase and cathepsin G. *Blood* **107,** 2234–2242 (2006).

142. Kanoh, S., Tanabe, T. & Rubin, B. K. IL-13-induced MUC5AC production and goblet cell differentiation is steroid resistant in human airway cells. *Clin. Exp. Allergy* **41,** 1747–1756 (2011).

143. Rubin, B. K. Secretion properties, clearance, and therapy in airway disease. *Transl. Respir. Med.* **2,** (2014).

144. Kumar, R. K. & Foster, P. S. Murine model of chronic human asthma. *Immunol. Cell Biol.* **79,** 141–144 (2001).

145. Blyth, D. I., Pedrick, M. S., Savage, T. J., Hessel, E. M. & Fattah, D. Lung inflammation and epithelial changes in a murine model of atopic asthma. *Am. J. Respir. Cell Mol. Biol.* **14,** 425–438 (1996).

146. Lee, J. J. *et al.* Interleukin-5 Expression in the Lung Epithelium of Transgenic Mice Leads to Pulmonary Changes Pathognomonic of Asthma. *J. Exp. Med.* **185,** 2143–2156 (1997).

147. Mojtabavi, N., Dekan, G., Stingl, G. & Epstein, M. M. Long-lived Th2 memory in experimental allergic asthma. *J. Immunol. Baltim. Md 1950* **169,** 4788–4796 (2002).

148. Becker, M. *et al.* Genetic variation determines mast cell functions in experimental asthma. *J. Immunol. Baltim. Md 1950* **186,** 7225–7231 (2011).

149. Chai, O. H., Han, E.-H., Lee, H.-K. & Song, C. H. Mast cells play a key role in Th2 cytokine-dependent asthma model through production of adhesion molecules by liberation of TNF-α. *Exp. Mol. Med.* **43,** 35–43 (2011).

150. Reuter, S. *et al.* Mast cell-derived tumour necrosis factor is essential for allergic airway disease. *Eur. Respir. J.* **31,** 773–782 (2008).

151. da Silva, E. Z. M., Jamur, M. C. & Oliver, C. Mast Cell Function. *J. Histochem. Cytochem.* **62,** 698–738 (2014).

152. Fang, K. C., Raymond, W. W., Lazarus, S. C. & Caughey, G. H. Dog mastocytoma cells secrete a 92-kD gelatinase activated extracellularly by mast cell chymase. *J. Clin. Invest.* **97,** 1589–1596 (1996).

153. Leckie, M. J. *et al.* Sputum T lymphocytes in asthma, COPD and healthy subjects have the phenotype of activated intraepithelial T cells (CD69+ CD103+). *Thorax* **58,** 23–29 (2003).

154. Robinson, D. S. *et al.* Predominant TH2-like bronchoalveolar T-lymphocyte population in atopic asthma. *N. Engl. J. Med.* **326,** 298–304 (1992).

155. Kurowska-Stolarska, M. *et al.* IL-33 amplifies the polarization of alternatively activated macrophages that contribute to airway inflammation. *J. Immunol. Baltim. Md 1950* **183,** 6469–6477 (2009).

156. Prasse, A. *et al.* IL-10-producing monocytes differentiate to alternatively activated macrophages and are increased in atopic patients. *J. Allergy Clin. Immunol.* **119,** 464–471 (2007).

157. Nocker, R. E. *et al.* Influx of neutrophils into the airway lumen at 4 h after segmental allergen challenge in asthma. *Int. Arch. Allergy Immunol.* **119,** 45–53 (1999).

158. Ordoñez, C. L., Shaughnessy, T. E., Matthay, M. A. & Fahy, J. V. Increased neutrophil numbers and IL-8 levels in airway secretions in acute severe asthma: Clinical and biologic significance. *Am. J. Respir. Crit. Care Med.* **161,** 1185–1190 (2000).

159. Green, R. H. *et al.* Analysis of induced sputum in adults with asthma: identification of subgroup with isolated sputum neutrophilia and poor response to inhaled corticosteroids. *Thorax* **57,** 875–879 (2002).

160. Nakagome, K., Matsushita, S. & Nagata, M. Neutrophilic inflammation in severe asthma. *Int. Arch. Allergy Immunol.* **158 Suppl 1,** 96–102 (2012).

161. Norzila, M. Z., Fakes, K., Henry, R. L., Simpson, J. & Gibson, P. G. Interleukin-8 secretion and neutrophil recruitment accompanies induced sputum eosinophil activation in children with acute asthma. *Am. J. Respir. Crit. Care Med.* **161,** 769–774 (2000).

162. Ferguson, A. C., Whitelaw, M. & Brown, H. Correlation of bronchial eosinophil and mast cell activation with bronchial hyperresponsiveness in children with asthma. *J. Allergy Clin. Immunol.* **90,** 609–613 (1992).

163. Murdoch, J. R. & Lloyd, C. M. Resolution of allergic airway inflammation and airway hyperreactivity is mediated by IL-17-producing {gamma}{delta}T cells. *Am. J. Respir. Crit. Care Med.* **182,** 464–476 (2010).

164. Wilson, A. M. The role of antihistamines in asthma management. *Treat. Respir. Med.* **5,** 149–158 (2006).

165. Nelson, H. S. Prospects for antihistamines in the treatment of asthma. *J. Allergy Clin. Immunol.* **112,** S96-100 (2003).

166. Kuna, P., Bjermer, L. & Tornling, G. Two Phase II randomized trials on the CRTh2 antagonist AZD1981 in adults with asthma. *Drug Des. Devel. Ther.* **10,** 2759–2770 (2016).

167. Barnes, P. J. New drugs for asthma. *Semin. Respir. Crit. Care Med.* **33,** 685–694 (2012).

168. Hall, I. P. *et al.* Efficacy of BI 671800, an oral CRTH2 antagonist, in poorly controlled asthma as sole controller and in the presence of inhaled corticosteroid treatment. *Pulm. Pharmacol. Ther.* **32,** 37–44 (2015).

Appendix

Media, buffers and Solutions

Distilled water used for the following solutions was prepared with an ultra-ion-exchange membrane filtration system (Milli-Q Reagent Water System, Millipore, Eschborn, Germany).

Cell culture media	**Composition**
Human lung mast cell medium	Stem Pro-34 SFM + 2,6% Supplement (StemPro-nutrient supplement) + 1% L-Glutamine + 1% Penicillin/Streptomycin + 0,1µg/ml human SCF
Human lung mast cell stimulation medium	RPMI 1640 Ø phenol red (2 g/l $NaHCO_3$) + 1,39 NaCL + 20mM HEPES + 1% L-Glutamine + 1% Penicillin/Streptomycin + 0,5% Supplement + 0,1µg/ml human SCF
Human epithelial cell line medium (16HBE14o-cell line)	DMEM (high glucose, 2mM L-Glutamin) + 10% FCS
Mouse BMMC complete medium	Iscove's modified Dulbecco medium + 10% FCS + 1% Penicillin/Streptomycin + 1% L-Glutamine + 1% Vitamins + 1 mM sodium pyruvate + 1 % nonessential amino acids + 0,05 mM ß-Mercaptoethanol + 10 ng/ml m-SCF + 5 ng/ml m-IL-3
Mouse lung cell medium (restimulation assay)	RPMI 1640 phenol red (10 mM HEPES) + 10% FCS + 1% L-Glutamine + 1% Penicillin/Streptomycin + 0,05 mM ß-Mercaptoethanol + 1 mM Sodium pyruvate

Buffer	**Composition**
Dulbecco's PBS (D-PBS) Ø CaMg	2,7 mM KCl 140 mM NaCl 1,5 mM KH_2PO_4 10 mM Na_2HPO_4 pH 7,4
D-PBS Ø CaMg/0,1% BSA (restimulation assay)	D-PBS Ø CaMg + 0,1% BSA
D-PBS Ø CaMg/0,5% BSA (PMN/MC isolation)	D-PBS Ø CaMg + 0,5% BSA
Lysis buffer	155 mM NH_4Cl 10 mM $KHCO_3$ 0,1 mM EDTA
Mast cell buffer	136 mM NaCL 5,5 mM Glucose 12 mM HEPES 0,27 mM KCl 0,38 mM Na_3PO_4 0,1% BSA
Phosphate buffer (chemotaxis)	0,1 M Na_2HPO_4x 2 H_2O pH 7,0
Blocking buffer (chemotaxis)	0,1 M $NaHCO_3$ 0,1 M Na_2CO_3 1% BSA pH 9,0
Myloperoxidase substrate buffer (chemotaxis)	33 mM $C_6H_8O_7$ pH 4,1
Washing buffer (restimulation assay)	RPMI 1640 mit 10 mM HEPES + 0,1% BSA
Digestion buffer (restimulation assay)	Washing buffer + 0,5 mg/ml Collagenase D + 1 ng/ml murine GM-CSF + 0,5 mg/ml DNase I

Cell culture media	Composition
Chymase substrate buffer	600 mM Tris 3 M NaCl pH 8,0
FACS staining buffer	D-PBS Ø CaMg + 0,1% BSA
FACS fixation buffer	D-PBS Ø CaMg + 4%PFA

Solution	Composition
Myeloperoxidase substrate solution (chemotaxis)	50 µL TMB-Substrate/mL Substrate buffer
ß-Hexosamindase substrate solution	1,36 mg substrate /ml substrate buffer
ß-Hexosamindase stop solution	0,217 M Glycine 0,216 M NaCl pH 10,45
Chymase substrate solution	91 µl substrate per 1,3 ml substrate buffer
Trypan blue solution	0,9% NaCl 0,5% Trypan blue in distilled water
Toluidine blue solution	0,2% Toluidine blue in 1M HCl

List of Tables and Figures